Analytical modeling to evaluate the effect of cross phase modulation on WDM optical Networks

By

Ragavendra Anantha padmanabhan

B.E (Electronics and Communication Engineering), Madras University, India, 2004

Submitted to the Department of Electrical Engineering and Computer Science and the faculty of the Graduate School of the University of Kansas in partial fulfillment of the requirements for the degree of Master of Science

Thesis Committee

_____

Dr. Rongqing Hui (Chair)

_____

Dr. Christopher Allen

_____

Dr. Victor Frost

Date of Thesis Defense: 08/25/06

The Thesis Committee for Ragavendra Anantha padmanabhan certifies that this is the approved version of the following thesis

Analytical modeling to evaluate the effect of cross phase modulation on WDM optical Networks

Thesis Committee

_____

Dr. Rongqing Hui (Chair)

_____

Dr. Christopher Allen

_____

Dr. Victor Frost

Date Approved: _____

ACKNOWLEDGEMENTS

The mediocre teacher tells. The good teacher explains. The superior teacher demonstrates. The great teacher inspires.

-William Arthur Ward

I would like to sincerely thank my thesis advisor and project supervisor, Professor Hui for his invaluable guidance throughout my thesis work. As the above quote states, I consider my advisor as a great teacher who inspires. His ideas, encouragement, affable nature, kindness, and support were greatly helpful. Even with his busy schedule being the program director at NSF, he spent considerable amount of his time helping me through the different phases of my thesis. As a fresh graduate with no research experience, I learnt a lot from his association. I sincerely thank him for giving me an opportunity to work under his able guidance. His timely advice, excellent directions and motivation has helped me complete my thesis.

I would also like to thank Dr. Allen and Dr. Frost for accepting to be on the committee and for their valuable suggestions. In regard to the thesis, taking the course on multi-wavelength optical networks by Dr. Frost helped me understand the basics of optical networks. I thoroughly enjoyed the course and the final project gave me a good insight into WDM networks.

I wish to thank my Mother, who has always been by my side, motivating me, giving me strength to accomplish, and encouraging me to achieve my goals. I would also like to thank my sister and brother in law for their motivation and support throughout my Masters. I feel indebted to them for their help. I wish to thank my friends who helped me in proofreading the document.

Finally, I wish to thank the supreme power of GOD for his grace, for instilling me with the knowledge and confidence to achieve my goals. With HIS blessings, I strongly believe that I will have an excellent career.

ABSTRACT

In the modern world of technology, data rates up to 40 Gb/s are becoming a reality and the bandwidth hungry applications such as teleconferencing, telemedicine, IPTV have already begun to make their presence in the commercial market. These bandwidth hungry applications attract the need for optical communications in which the fibers can theoretically provide infinite bandwidth. In order to satisfy such needs, one of the solutions that can be put into effect is the concept of DWDM (Dense Wavelength Division Multiplexing) which involves transmitting multiple wavelengths spaced very close to each other and thereby providing higher bandwidth efficiency. In case of DWDM, the wavelength channels are very close to each other in the order of 0.4 nm or lower. As a result of closely spaced wavelengths, there will be crosstalk and other detrimental effects. This provides the underlying concept for this thesis, which is developing an analytical model for evaluating the optical system performance. In case of DWDM, the signal power of one wavelength phase modulates the other closely traveling wavelength channel. This phase modulation can then be converted into time jitter through a chromatic dispersion of the fiber which reduces the performance of the optical system. The information carrying capacity of the fiber diminishes to a greater extent in case of higher powers. For higher data rates, higher powers are required and the system is more susceptive to this crosstalk effect. An analytical model is developed to evaluate the nonlinear time jitter introduced by cross phase modulation and the results are compared with numerical simulations using VPI simulation tool. They agree reasonably well.

TABLE OF CONTENTS

LIST OF FIGURES

LIST OF TABLES

1. INTRODUCTION

Ever since the olden days, there has always been a need to communicate. This need paved the way to the invention of technologies which allow people to communicate over large distances. Along with this need, the need for sending more data at higher rates became inevitable. The invention of electrical communications made these needs feasible. In electrical systems, the information is superimposed onto a carrier in the sending side. The receiving side extracts the needed information from the carrier. The amount of information carried directly relates to the frequency range of the carrier and thus sending more information implies increasing the carrier frequency which in turn increases the available bandwidth. So to achieve higher bandwidth, higher frequencies or shorter wavelengths are employed. The term wavelength brings optical communication into limelight through which huge amount of information at very high data rates, such as 40 Gb/s, can be achieved.

1.1 The fiber optic systems

The bit-rate-distance product BL (in which B is the bit rate and L is the repeater spacing), determines the figure of merit for the communication systems. Even though huge transmission rates up to 100 Mb/s were achieved, the problem of repeater spacing was disturbing. The limitations due to repeater spacing were solved with the invention of Lasers and optical fibers. In spite of this, the fibers suffered a huge loss factor up to 1000 dB/Km. It was then found that the loss could be brought down to 20 dB/Km in the wavelength region of 1 μm [1]. Thus the combination of the laser

sources and the availability of low-loss fiber made the world of optical communication possible and attractive.

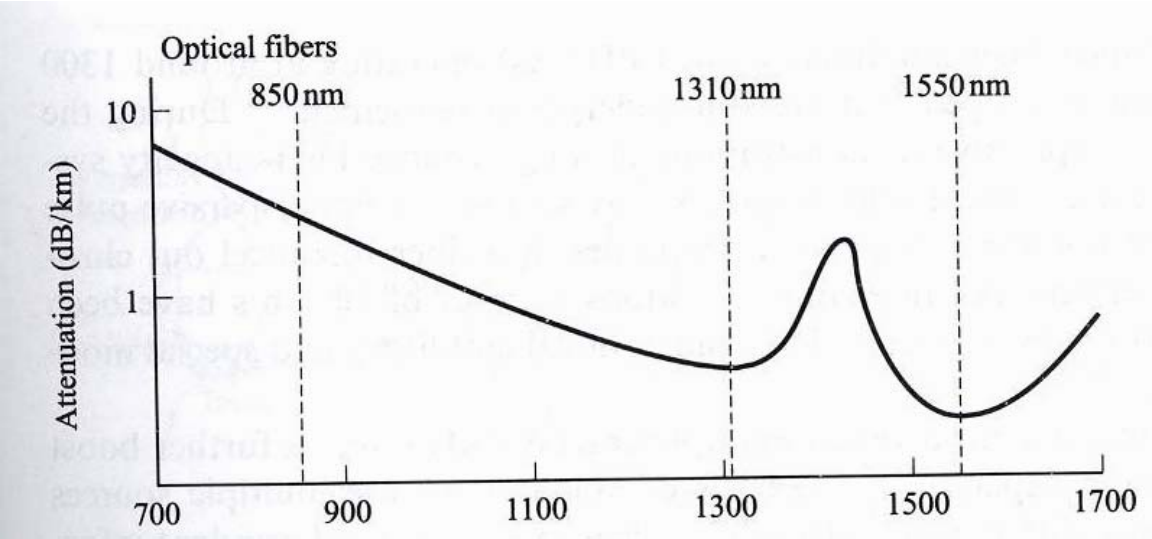

Figure 1.1 Operating regions of optical fiber [Ref 2]

The three main operating regions of the optical fibers are shown in figure 1.1. The first generation optical fibers operated at 850 nm, used GaAs based optical sources, silicon photodetectors, and multimode fibers. But their capacity was limited due to intermodal dispersion and fiber loss. Their capacity ranged from 45 to 140 Mb/s with repeater spacing of 10 Km. The lower-loss, lower-dispersion window of 1300 nm were used in long-haul telephone links with long distance repeater less transmission. The bit rates achieved were 2.5 Gb/s with repeater spacing of 40 Km. In case of LAN, both single mode and multimode fibers are used which provide capacity up to 10 to 100 Mb/s over 500 m to tens of Kilometers [2]. The lowest attenuation was provided by the fiber operating at 1550 nm but it had large signal dispersion. This was solved by the dispersion-shifted fibers. So for high-capacity long distance links and under sea transmission links, this operating wavelength was much suited [3]. The

transmission rate achieved is 10 Gb/s. Moreover, the optical amplifiers played an important role to boost the capacity. EDFA (Erbium Doped Fiber Amplifier) is widely used at 1550 nm.

1.2 World of Multiplexing

To further enhance and explore the advantages of the high capacity provided by optical communication systems, multiplexing came into being which consists of combining multiple numbers of wavelengths onto the same fiber in the region of 1300-1600 nm spectrum. With the invention of lasers with extremely narrow line widths, more channels can be multiplexed onto the same fiber which provides the basis for DWDM (Dense Wavelength Division Multiplexing). The main components of the DWDM system are the multiplexer at the transmitting end and the demultiplexer at the receiving end. The multiplexer combines the different wavelengths and they are separated back at the receiving end with a demultiplexer. The challenge involved is that the multiplexer should be able to combine the wavelengths along a low-loss path. The demultiplexer should have a narrow spectral width to avoid any spurious signals.

1.3 Waveforms used for communication

The most popular optical bit streams are NRZ and RZ formats. NRZ format is Non-Return-to-Zero, in which “1”s are represented by one level and “0”s are represented by the other level. The pulse remains on throughout the bit slot and the amplitude never drops to zero. Pulse width has a direct relation with this representation. Clock

recovery is usually more difficult with NRZ coding because loss of timing would occur if there are long strings of the same amplitude level. This can be overcome by the use of block codes and scrambling. NRZ uses the full bit duration while transmission. Since the pulse width has a direct relationship with the representation, it may lead to bit-pattern-dependent effects if the optical pulse spreads during transmission [4]. Also NRZ uses smaller signal bandwidth.

RZ format has attracted a lot of attention to satisfy the needs of higher data rates. In this format, the "1" bit is shorter than the bit interval, the amplitude returns to zero and typically occupying 50% of the bit slot and the "0" bit always stays at amplitude level "0". A long string of "0" can cause de-synchronization. This can be overcome by using a bi-phase or optical Manchester code. Twice the bandwidth of NRZ coding is required due to the usage of half the bit duration for data transmission resulting in increased capacity.

1.4 Simulation tools

There are commercially available simulation softwares which have all the required optical components to completely simulate a real optical system. One such software is the VPI Transmission design suite, which has comprehensive libraries, physical models of optical components, and GUI for the users to simulate them. Various components include optical fiber links, amplifiers, transmitters, multiplexers, laser sources, switches and cross-connects. Some of the network architectures include DWDM, optical TDM and fiber based CATV systems. The VPI optical network

simulation layer (ONSL) controls the data exchange between the design suite and other simulation tools such as Python, MATLAB, and C. There are lots of visualization tools available that display the waveforms through a digital scope or through a spectrum analyzer. The Eye diagrams that are very important in determining the information carrying capacity of the optical systems can be displayed through scopes.

The layered simulation technology makes it possible to work independently at the component, link, and transport-network layers and can be analyzed at a particular layer. Results at each level can be passed on to the other levels making the lower layers transparent to the higher layers. Each component has its own parameters which can be easily configured and stored in a file for future use. The VPIcomponentMaker^{TM} Active photonics is an integrated design environment for active photonic circuits and advanced semiconductor lasers [5]. VPIcomponentMaker™ Optical Amplifiers provide stable, efficient algorithms for multi-band, multi-stage, hybrid, Raman, doped amplifiers. VPItransmissionMaker™WDM can be used to design advanced systems including novel modulation schemes, PMD compensation, Raman amplification, partial regeneration, adaptive dispersion compensation, optical channel monitoring and power flattering [5]. VPItransmissionMaker™Cable Access allows the benefits and limitations of fiber in access systems to be explored in detail [5]. These various

simulation tools efficiently simulate a real optical system which is very useful in analyzing in optical performance of systems.

1.5 Purpose of thesis

In the modern 10 - 40 Gb/s optical networks, due to the tight spacing of wavelengths, there is a high possibility of the optical signal in one wavelength affecting the amplitude and phase of the signal in a closely traveling wavelength. This limits the performance of the optical system and this effect hugely depends on the modulation format used. When high optical powers are launched into an optical fiber, the wavelength channel carrying this power will phase modulate the neighboring channel due to the direct dependence of the non-linear refractive index of the fiber. This optical phase modulation broadens the optical spectrum of the channel. If the fiber has chromatic dispersion, different frequency components travel in different speed, and therefore, this nonlinear phase modulation will be converted into a time jitter at the end of the fiber. This is a major performance delimiting factor in DWDM systems especially for RZ optical signal where the pulse width is narrow. To analyze performance of the WDM optical network, two approaches were followed in this thesis. The first one is the analytical modeling approach which is simple and faster to analyze the performance. MATLAB is used to implement the analytical model. The other method is by numerical simulation with the VPI software which almost replicates a real system. To verify the analytical system, a comparison is made with the VPI software and the results are discussed under the results section of this thesis. Since RZ waveforms are popular in modern high speed long distance optical

communication systems and they are more susceptive to time jitter due to their short pulse width, emphasis is also given to RZ waveform.

1.6 Importance of this work

This thesis finds its application in the case of RWA (Routing and wavelength assignment algorithm) in PPO (Plug and play optical nodes). A network can be opaque in which there is a need for optical-electrical-optical (OEO) conversion at each and every node. This will increase the cost since large number of regenerators will be needed to achieve this OEO conversion. To overcome these limitations, translucent networks are employed which has this OEO conversion only at certain nodes. Ultimately, a network that is transparent, and has no OEO conversion is required which will not have the electronic bottleneck in current networks [17]. This transparent network will have greater scalability since the signal is in optical form throughout the network. Since optical signal quality degrades along the fiber length; impairments are incurred due to non ideal components. Due to this, linear and non linear effects are added on the optical signal throughout the network. This results in higher bit error rate at the output of the fiber. Thus in these kinds of networks, there must be a method to know these impairments and the characteristics of the physical links. Linear effects such as PMD (Polarization mode dispersion), GVD (Group Velocity Dispersion), and crosstalk are independent of the signal optical power levels. On the other hand, non linear effects such as FWM, SPM, XPM affects the signal quality when signal optical power is high enough and these effects become more and more important for high data rate long distance systems which require high signal

optical power. Thus the RWA algorithms must be aware of the physical impairments while setting up a route from the source to destination. An analytical model must be developed to efficiently model these impairments. The RWA must, along with the help of the model, reject the lower signal quality links and should chose higher quality links. This can only be possible if the model developed is fast enough to characterize the physical path so that the output can be used by the RWA to set up an efficient route. Even though the path parameters are known prior, since the link quality changes due to the live traffic load, the model must run each time when the RWA wants to find a better path through the network. Numerical simulation software available in the market such as VPI will efficiently model the impairments but it is not fast enough to calculate the impairments. Since RWA needs to set up the path immediately to reduce network delays, the analytical model developed in this thesis can be used to calculate the impairments fast enough so that the routing decisions can be made efficiently.

2. FIBER CHARACTERISTICS, LOSSES AND NON-LINEAR EFFECTS

2.1 Overview:

The fundamental component that makes the optical communication possible is the optical fiber. The phenomenon which guides the light along the optical fiber is the total internal reflection. It is an optical phenomenon which occurs when the incident light is completely reflected. Critical angle is the angle above which the total internal reflection occurs. In case of materials with different refractive indices, light will be reflected and refracted at the boundary surface. This will occur only from higher refractive index to a lower refractive index such as light passing from glass to air. This phenomenon forms the basis of optical communication through fibers.

An optical fiber is a dielectric waveguide, it is cylindrical, and guides the light parallel to the axis. The cylindrical structure is dielectric with a radius "a" and refractive index of "n_1". This is the called the *core* of the fiber and the layer that encompasses this structure is called the *cladding*. Cladding has a refractive index "n_2" which is lesser than "n_1". This helps in providing mechanical strength and helps reducing scattering losses. It also prevents the core from surface contamination. Cladding doesn't take part in light propagation.

2.2 Types of fibers

Fibers can be classified according to the core's material composition. If the refractive index of the core is uniform and changes abruptly at the cladding boundary, then it is called as Step-index fiber. If the refractive index changes at each radial distance, then it is called as Graded-index fiber. These fibers can be divided into Single mode and multi mode fibers. Single mode fibers operate in only one mode of propagation. Multimode fibers can support hundreds of modes. Both laser diodes and light emitting diodes (LED) can be used as light wave sources in fiber-optical communication systems. When compared to Laser diodes, LEDs are less expensive, less complex and have a longer lifetime, however, their optical powers are typically small and spectral linewidths are much wider than that of laser diodes. In Multimode fibers different modes travel in different speed, which is commonly referred to as intermodal dispersion, giving room to pulse spreading. In signle mode fibers, different signal frequency components travel in different speed within the fundamental mode and this result in chromatic dispersion. Since the effect of chromatic dispersion is proportional the spectral linewidth of the source, laser diodes are often used in high-speed optical systems because of their narrow spectral linewidth.

2.3 Fiber Losses

For efficient recovery of the received signal, the signal to noise ratio at the receiver must be considerably high. Fiber losses will affect the received power eventually reducing the signal power at the receiver. Hence optical fibers suffered heavy loss and

degradation over long distances. To overcome these losses, optical amplifiers were invented which significantly boosted the power in the spans in between the source and receiver. However, optical amplifiers introduce amplified spontaneous emission (ASE) noises which are proportional to the amount of optical amplifications they provide, low loss in optical fibers is still a critical requirement in long distance optical systems to efficiently recover the signal at the receiver.

Attenuation Coefficient is a fiber-loss parameter which is expressed in the units of dB/Km. The optical power traveling inside the fiber changes along the length and is governed by Beer's law:

$$dP/dz = - \alpha P, \tag{2.1}$$

where "α" is the attenuation constant in Neper. If P_{in} and P_{out} are the power at the input and output of the fiber and L is the length of the fiber, then the power at the output is,

$$P_{out} = P_{in} \exp(- \alpha L) \tag{2.2}$$

In terms of dB/Km, α can be expressed as,

$$\alpha \text{ (dB/Km)} = - \frac{10}{L} \log_{10} \left(\frac{P_{out}}{P_{in}} \right) \sim 4.343 \ \alpha \tag{2.3}$$

For short wavelengths, the loss may exceed 5 dB/Km and makes it unsuitable for long distance transmission [4]. These losses are mainly due to material absorption and Rayleigh scattering. Material absorption is the phenomenon exhibited by silica fibers. The intrinsic absorption is caused by fused silica and extrinsic absorption is caused by

impurities in silica. The other contributing factor is the Rayleigh scattering which is caused by the density fluctuations in the fiber. These fluctuations change the refractive index on a smaller scale. Light scattering in such medium is called Rayleigh scattering [6]. The intrinsic loss of silica fibers due to this scattering is expressed as,

$$\alpha_R = C / \lambda^4 \tag{2.4}$$

Where C is a constant in the range of 0.7 – 0.9 (dB/Km)-μm^4 and depends on the fiber core. This constitutes the scattering loss to be 0.12 – 0.16 (dB/Km) at λ = 1.55 μm [4].

2.3.1 Chromatic Dispersion

In multi-mode fibers, intermodal dispersion is the dominant contributor of signal waveform distortion. Although intermodal dispersion is eliminated in single mode fibers, different frequency component of optical signal carried by the fundamental mode still travel in slightly different speed giving rise to a wavelength-dependent group delay. As group delay depends on wavelength, different amount of time is taken for the different spectral components to reach a certain distance. Due to this effect the optical signal with a certain spectral width spreads with time when it travels through the fiber. This pulse spreading is important and needs to be determined. The following equation gives the value for pulse spreading.

$$D = -\frac{2\pi c}{\lambda^2}\beta_2 \tag{2.5}$$

where D is the dispersion parameter, c, the light velocity, λ, the wavelength and β_2 is the GVD (Group Velocity Dispersion) parameter. It is measured in ps/nm/km. Dispersion can also be measured by adding the material and waveguide dispersion together unless a very precise value is needed. Thus material dispersion and waveguide dispersion can be calculated separately and summing up these values will give the dispersion value.

2.4 Fiber Nonlinearities

The non-linear effects of the fibers play a detrimental role in the light propagation. Nonlinear Kerr effect is the dependence of refractive index of the fiber on the power that is propagating through it. This effect is responsible for SPM, XPM and FWM. The other two important effects are stimulated Brillouin scattering (SBS) and stimulated Raman scattering (SRS).

2.4.1 Self Phase modulation

In fibers, the refractive index always has some dependence on the optical intensity which is the optical power per effective area. This relation can be given as,

$$n = n_0 + n_2 I = n_0 + n_2 \frac{P}{A_{eff}} \tag{2.6}$$

where n_0 is the ordinary refractive index , n_2 is the non-linear refractive index co-efficient, A_{eff} is the effective core area, and P is the power of the optical signal. This non-linearity is called as Kerr nonlinearity. This produces Kerr effect in which the propagating signal is phase modulated by the carrier. This leads to a phenomenon called Self-phase modulation that converts power fluctuations into phase fluctuations in the same wave [8].

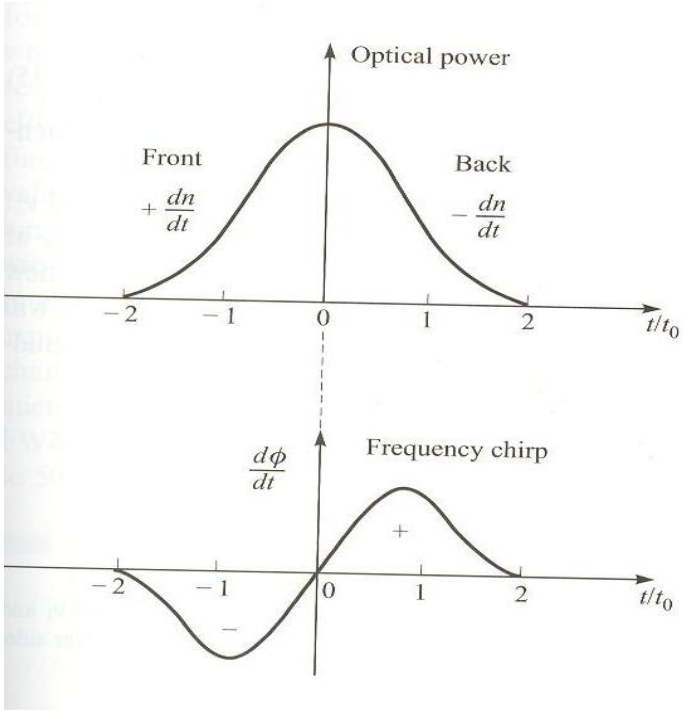

Figure 2.1 Frequency chirping effect [Ref 2]

In a material in which the refractive index depends on the intensity of the signal, and as this time varying signal intensity propagates along the fiber, it will produce time varying refractive index. This produces higher refractive index at the peak of the pulse when compared to the edges of the pulse. This produces a time varying phase

change $d\theta / dt$. Due to this change, the frequency of the optical signal undergoes a frequency shift from its initial value. This effect is known as frequency chirping, in which different parts of the pulse undergo different phase change [2]. The rising edge experiences a shift towards the higher frequency and the trailing edge experiences a shift towards the lower frequency. Since this effect depends heavily on the signal intensity, SPM has more effect on high intensity signal pulses. In case of fibers which have the GVD effects, the pulse broadens which leads to difficulty in the receiver side to decode the signal. When the chromatic dispersion is negative, the edges of frequencies which experienced higher shifts tend to move away from the centre of the pulse. The edges of frequencies which experienced lower shifts tend to move away from the centre in the opposite direction. Thus this GVD affected pulse will be broadened at the end of the fiber. The chirping worsens due to this effect. Thus SPM can worsen the performance of the optical system in case of long haul transmission.

2.4.2 Cross phase modulation

As with equation (2.6), the refractive index of the fiber depends on the time varying signal intensity and this result in time varying refractive index. This also leads to an effect called Cross phase modulation (XPM). XPM has more pronounced effect in case of WDM systems in which more optical channels are transmitted simultaneously. In case of XPM, the phase shift depends on the power of other channel. The total phase shift can be represented as [7],

$$\theta_j^{NL} = \gamma L_{eff}(P_j + 2\sum_{m \neq j} P_m) \tag{2.7}$$

where θ_j^{NL} is the non-linear phase shift for the j^{th} channel, $M = \frac{N^2}{2}(N-1)$ varies from 1 to 5 W^{-1}/Km, L_{eff} is the effective length of the fiber, P_j and P_m are the power for the channels *i* and *j*. On the right-hand-side of equation (2.7), the first term represents effect of SPM and the second term represents that of XPM. The factor of 2 in equation (2.7) implies that XPM is twice as effective as SPM for the same amount of power [7]. The phase shift which is directly created by XPM at the end of the fiber depends on the bit patterns and powers of the neighboring channels. The effect of XPM also depends on the wavelength separation between the signal channel and the neighboring channel. If the channels are separated widely, then the XPM effects are relatively weak because the two bit streams walk-off from each other quickly. In case of the DWDM systems, the channel wavelength separation is very narrow which leads to strong XPM effect. Since XPM results in a inter channel crosstalk, its effect, to some extent, also depends on the bit pattern of the two channels. This will be shown in later sections.

To analyze the effect of XPM and SPM, the nonlinear Schrödinger equation can be used which is represented as [7],

$$\frac{\partial A}{\partial z} + \frac{i\beta_2}{2}\frac{\partial^2 A}{\partial t^2} = -\frac{\alpha}{2}A + i\gamma |A|^2 A \tag{2.8}$$

The equation (2.8) neglects the third-order dispersion and the term α is added for fiber losses.

By increasing the effective area, nonlinearities can be reduced. A_{eff} is about 80 μm^2 for standard fibers and is 50 μm^2 for dispersion shifted fibers [3].

2.4.3 Four wave mixing

This is a phenomenon that occurs in case of DWDM systems in which the wavelength channel spacing is very close to each other. This effect is generated by the third order distortion that creates third order harmonics. These cross products interfere with the original wavelength and causes mixing. In fact these spurious signals fall right on the original wavelength which results in difficulty in filtering them out. In case of 3 channel system, there will be 9 cross products and 3 of the cross products will be on the original wavelength. This is caused by the channel spacing and fiber dispersion. If the channel spacing is too close, then FWM occurs. If the dispersion is lesser, then FWM is higher since dispersion is inversely proportional to mixing efficiency. In the figure 2.2, we see that the cross product lies right on the original signal which poses problem when filtering.

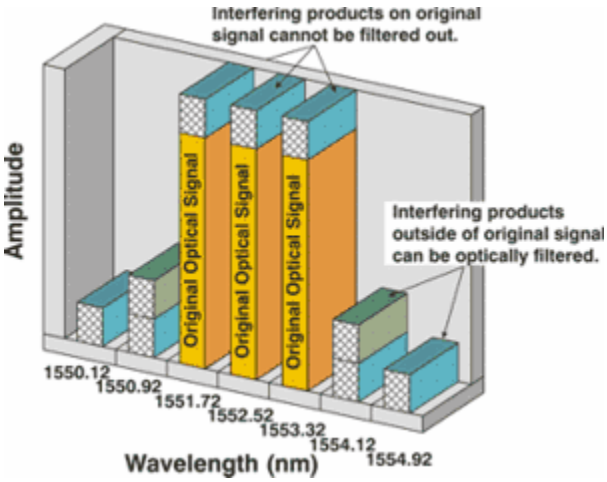

Figure 2.2 Four wave mixing [Ref 20]

In general, for N wavelengths there will be M cross products which is given by [2],

$$M = \frac{N^2}{2}(N-1) \tag{2.9}$$

2.4.4 Stimulated Brillouin Scattering

SBS falls under the category of inelastic scattering in which the frequency of the scattered light is shifted downward [4]. This results in the loss of the transmitted power along the fiber. At low power levels, this effect will become negligible. SBS sets a threshold on the transmitted power, above which considerable amount of power is reflected. This back reflection will make the light to reverse direction and travel towards the source. This usually happens at the connector interfaces where there is a change in the refractive index. As the power level increases, more light is backscattered since the level would have crossed the SBS threshold. The parameters which decide the threshold are the wavelength and the line width of the transmitter.

Lower line width experiences lesser SBS and the increase in the spectral width of the source will reduce SBS. In case of bit streams with shorter pulse width, no SBS will occur [4]. The value of the threshold depends on the RZ and NRZ waveforms which are used to modulate the source. It is typically 5 mW and can be increased to 10 mW by increasing the bandwidth of the carrier greater than 200 MHz by phase modulation [4].

2.4.5 Stimulated Raman Scattering

SRS occurs when the pump power increases beyond the threshold, however with SRS it can happen in either direction, forward and backward. The molecular oscillations set in at the beat frequency and the amplitude of the scattering increases with the oscillations. The equations that govern the feedback process are [7],

$$\frac{dI_p}{dz} = -g_R I_P I_S - \alpha_P I_P \tag{2.10}$$

$$\frac{dI_S}{dz} = g_R I_P I_S - \alpha_S I_S \tag{2.11}$$

Where g_R is the SRS gain. I_P and I_S are intensities of Pump and stokes field.

In case of the threshold power, the P_{th} is given by,

$$P_{th} = 16\alpha(\pi w^2)/g_R \tag{2.12}$$

where πw^2 is the effective area of the fiber core and w is the spot size.

Even though there are some detrimental effects posed by these two effects, SBS and SRS can also be used in a positive way. Since both deal with transferring energy to the signal from a pump, they can be used to amplify the optical signal. Raman gain is also used in compensating losses in the fiber transmission.

Comparison between SBS and SRS

Property	SBS	SRS
Direction of scatter	Only in backward direction	In both forward and backward direction
Frequency shift	About 10 GHz	About 13 THz
Spectrum width	Narrow width	Broad spectrum width

Table 2.1 Comparison of SBS and SRS properties

2.5 Eye Diagrams

In digital transmission systems, eye diagrams are very useful in qualitatively measuring the signal either at input or at the output. Eye diagram is a measure of signal waveform distortion including timing jitter and skew. This presents the user with a display very similar to an oscilloscope. Eye diagrams are very much useful in evaluating the performance of the digital systems. The undistorted eye diagram looks nearly square in shape. The eye opening will be wide open. But with signal impairments such as timing jitter and poor synchronization, the eye diagram becomes distorted and the size of the eye opening reduces both horizontally and vertically.

Thus both phase and amplitude distortion will make the opening lesser than the original.

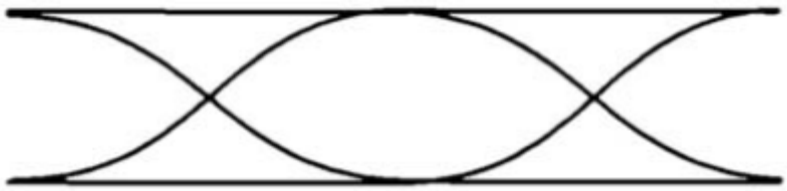

Figure 2.3 Eye diagram of an undistorted optical signal at the output [Ref 20]

In figure 2.3, we can see the undistorted eye with no signal impairments.

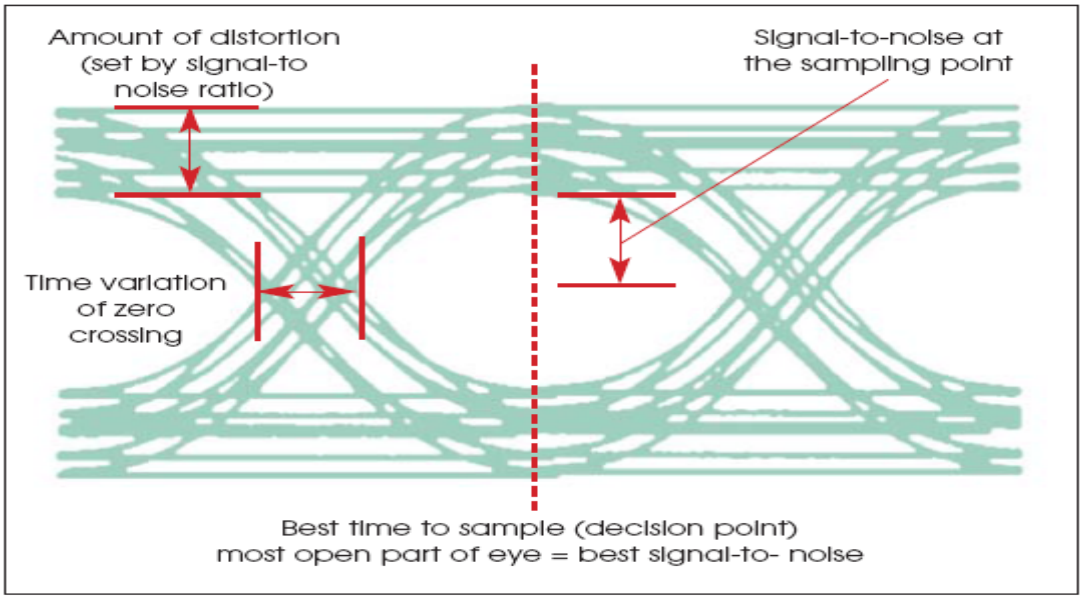

Figure 2.4 Impairments in the received eye diagram [Ref 20]

From the figure 2.4 we can see that the amplitude distortion and timing jitter considerably affect the eye shape which implies that the performance is degraded at the output. This provides the user with the magnitude of distortions.

3. ANALYTICAL MODELING

3.1 XPM induced waveform distortions

The impairments caused by the cross phase modulation in high bit rate DWDM systems will affect the performance of these systems to a greater extent. To evaluate the optical system performance under the influence of XPM, an analytical model is derived which is faster, simple and as accurate as possible. The roots of this model lie in the derivation of the analytical time jitter formula. Previous analytical studies involved analyzing only the intensity modulation generated at the end of the fiber. Also the effects were analyzed only for the NRZ modulation format. This thesis provides a simple and efficient way to model the cross phase modulation involving both intensity distortion and time jitter in a WDM optical system.

In ref. [9], a generalized method is developed to calculate the XPM induced field distortions in multispan WDM systems. This method does not involve the split-step Fourier transform. The XPM-induced optical phase modulation and the resulted signal power fluctuations are calculated and the accuracy of the model is checked with numerical simulation. A five span system with each span length accounting to 100 Km is considered. Dispersion of 17 ps/nm-km is used and a dispersion compensation of -102 ps/nm-km is used. Launch powers used were in the order of 3 dBm with 10 Gb/s NRZ modulated waveform. Furthermore, the paper did not compare the results with delays between the pump and probe channel's bit patterns.

Although the delays impose only minor problems, the effect of bit shifts must be considered to simulate an optical system to improve the accuracy of the results. Our model also considers delays between the data patterns which efficiently simulates the effects of bit shifts in the real system. Our model implements the split step Fourier transform method to implement the effect of SPM and dispersion which is implemented by the VPI simulation tool to efficiently model an optical system. Thus a fair comparison can be made with VPI and our analytical model. Also [9] cannot be compared with a simulation tool such as VPI since it does not involve the split step Fourier transform. [9] considered only the optical phase modulation and the resulting intensity crosstalk for all modulation formats but did not calculate the time jitter at the output of the fiber. Our model considers both intensity crosstalk and timing jitter distortions for both the modulation formats.

In [14], spectral characteristics of XPM in multispan IM-DD (Intensity Modulation Direct-Detection) optical systems are investigated both experimentally and theoretically. An analytical model was developed to determine the effects of XPM theoretically. Only intensity modulated systems are considered and the experiments verify the intensity fluctuations in an IM-DD system. Higher launch powers in the order of 11.5 dBm were used. The waveform used for the modulation is NRZ format. This work considers only the IM-DD and PM-IM systems mechanisms. The phase modulation created by XPM is converted into intensity modulation due to chromatic dispersion and thus only the effect of intensity crosstalk is considered and the effect

of timing jitter is not included in this work. Our model considers RZ modulation formats where [14] do not consider them. Also [14] do not consider the delay between the probe and the pump channel which is implemented in our model.

Due to the limitations in [9] and [14], in which they were not able to calculate the effect of timing jitter due to XPM, our analytical model efficiently considers both intensity and timing jitter due to XPM in both the modulation formats. Thus our model can be used to calculate both the effects of XPM.

We consider a WDM system with a SMF (Single Mode Fiber). The probe channel at the input of the fiber is a CW (Continuous Wave), and its intensity and phase modulation created by the power carried by the pump channel on another wavelength are analyzed. The phase variation of the probe channel *i* induced by Kerr interaction with pump channel *k* along the infinitesimal distance from z to z + dz is given in Fourier space by [9],

$$d\theta_i(z,\omega) = -2\gamma_i P_k(z,\omega)dz \tag{3.1}$$

where γ_i is the non-linear coefficient. The power of the pump channel $P_k(z,\omega)$ can be expressed as $P_k(z,\omega) = P_k(0,\omega).\cos(q_k z).\exp(-\alpha z - i\omega z / v_{g,k})$ with the assumption made by the small signal analysis in [10]. Here $q_k = -\beta_{2,k}\omega^2/2$ with $\beta_{2,k}$ accounting for dispersion, α as the attenuation coefficient, and $v_{g,k}$ denoting the group velocity. This infinitesimal phase fluctuation created at fiber section dz will propagate to the

end of the fiber of length L. Due to chromatic dispersion of the fiber this small phase modulation will evolve into an intensity fluctuation through PM-IM (Phase modulation to Intensity modulation) conversion and also a phase delay will happen through a PM-PM (Phase modulation to Phase modulation) conversion [10],

$$dP_{XPM,i}(z,\omega) = -2P_i(z)\exp\left[\left(-\alpha - i\omega / v_{g,i}\right)(L-z)\right].\sin\left[q_i(L-z)\right]d\theta_i(z,\omega) \quad (3.2)$$

$$d\theta_{XPM,i}(z,\omega) = \exp\left[\left(-\alpha - i\omega / v_{g,i}\right)(L-z)\right].\cos\left[q_i(L-z)\right]d\theta_i(z,\omega) \quad (3.3)$$

(3.2) denotes the power fluctuations and (3.3) denotes the phase fluctuations at the end of the fiber due to the pump - probe interaction at z.

Here the attenuation and propagation delay of the channel *i* is given by $\exp[(-\alpha - i\omega / v_{g,i})(L-z)]$ $P_i(z)$ and $P_i(z)$ is the average power of the channel *i* at a distance *z* from the beginning of the fiber [9].

Since the major focus of this work is to derive analytical equations to calculate XPM-induced time jitter, in our analytical modeling, only the phase fluctuation in equation (3.3) is considered.

3.2 Concept of Walk off length

Prior to discussing about modeling in depth, it is important to understand the Schrödinger equation. Solving Schrödinger equation will present an exact solution

only numerically. This involves the dispersion and non-linear effects of the fiber. According to [11], the non-linear interaction is exclusive only at the first walk off length in the beginning of each fiber span. Only dispersion has the effect of transforming the phase into intensity distortions and the non-linear effects are negligible after the first walk off length. Walk off length introduces the intensity changes due to the change in the relative alignments of the interacting channels. This relative change accounts for the small time difference between the pulses, Δt which characterizes this intensity changes. This is given by [11]

$$L_{wo} \approx \Delta t / (D\Delta\lambda) \tag{3.4}$$

where D is the chromatic dispersion and $\Delta\lambda$ is the wavelength separation between the channels in nm. For RZ and NRZ signals, Δt is the pulse duration for RZ and for NRZ it is the edge duration of the falling and rising edges. Thus walk off length is directly proportional to the intensity changes and inversely proportional to the product of dispersion and wavelength spacing.

When the channel spacing is very large, the walk off length becomes shorter than the effective length of the fiber and is insignificant. In case of very small wavelength separation, walk off length becomes large enough in comparison to the effective length of the fiber. In this case, the XPM distortions are governed by the fiber losses and the walk off length becomes independent of wavelength spacing. In case of comparable lengths of the fiber and the walk off length, XPM distortions are related to both walk off and fiber attenuation [11]. Thus when the separation is lesser than ~

0.4 nm for a fiber with dispersion coefficient of 17 ps/nm-km, the walk off length is high enough so that its effect can be neglected. In case of higher separation, the signals are well separated in the frequency domain which means that the effect of the walk off length is insignificant. In case of fibers with relatively lower dispersion, in the range of 2-5 ps/nm-km, the inverse dependence on the wavelength separation is achieved only at the higher values of $\Delta\lambda$ since the dispersion is smaller.

Cross phase modulation is very much dependent on chromatic dispersion. It plays an important role in converting the phase distortion into both intensity distortion and time jitter. It also affects the system in the walk off lengths. Per span compensation can be introduced which will eliminate the dispersion induced XPM effects in these fibers but it will reduce the advantage of using these fibers in case of linear transmission. Also the dependence of the XPM on optical intensities exhibit a linear relation [13] which makes possible the analysis of impairments caused by high power channels, which is the main objective of this thesis.

3.3 Phase noise to Intensity noise conversion

In a WDM optical system which operates at the wavelength of 1550 nm, the standard single mode fibers experience significant dispersion which limits the performance of optical systems. Dispersion converts the phase modulation into intensity modulation at the output of the fiber. Therefore the factors which cause this conversion must be studied. A detailed analysis has been given by [10] which introduces a conversion

matrix which describes the input and output relations of the corresponding phase and intensity modulation.

Let $S_{in}(t)$ be the optical power input and $\phi_{in}(t)$ be the phase of the input signal. Then a conversion matrix is defined using [10]

$$\begin{pmatrix} \dfrac{\Delta S_{out}(j\omega)}{2\langle s\rangle} \\ \phi_{out}(j\omega) \end{pmatrix} = \begin{pmatrix} \cos(\omega^2 F) & -\sin(\omega^2 F) \\ \sin(\omega^2 F) & \cos(\omega^2 F) \end{pmatrix} \begin{pmatrix} \dfrac{\Delta S_{in}(j\omega)}{2\langle s\rangle} \\ \phi_{in}(j\omega) \end{pmatrix} \tag{3.7}$$

where $\Delta S_{out}(j\omega)$ and $\Delta S_{in}(j\omega)$ are the input and output intensities. $\phi_{out}(j\omega)$ and $\phi_{in}(j\omega)$ are the output and input phase of the signal channel. F accounts for the dispersion parameter. This conversion matrix provides relations for both PM-IM and PM-PM conversions.

The transfer function can be obtained from the above matrix. To calculate the intensity and phase modulation at either end of the fiber, we also need the correlation between them which can be deduced from the knowledge of the transmitter used in the system.

By using this conversion matrix, signal impairments due to the channels propagating along the dispersive fiber can be analyzed. The conversion of frequency to phase modulation occurs strongly if the attenuation parameter α is greater than 1 [10]. This matrix also considers the correlation between the phase and intensity modulation.

3.4 Intensity distortion caused by XPM

Before modeling the XPM induced impairments involving both time jitter and amplitude distortions in a system, we first describe the model that includes only intensity distortions. In Intensity Modulation – Direct Detection (IM-DD) systems, XPM crosstalk levels are highly dependent on fiber dispersion and wavelength channel spacing. Due to the high power in the pump channel, the probe channel experiences some phase modulation. Phase modulation alone does not account for system degradation. But due to chromatic dispersion, this phase modulation gets converted into intensity modulation [10]. This will seriously degrade the performance of the optical system. In case of the IM-DD system, the non linear Kerr effect along with the fiber chromatic dispersion gives rise to these performance impairments.

The assumption made in this thesis considers SPM and XPM as separate effects. In case of the dispersive fiber, dispersion and non linearity act together. In case of an infinitesimal length of the fiber, these effects can be assumed to act independently. After considering the effects due to XPM, the XPM induced intensity distortions can be represented as [14],

$$\Delta s_{jk}^{\ m}(\Omega, L_N) = 4\gamma_i p_j(L_N) p_k^{\ (m)}(\Omega,0) \exp\left[i\Omega \sum_{n=1}^{m-1} d_{jk}^{\ (n)} L^{(n)} \right] . \frac{\sin\left[\Omega^2 \sum_{n=m}^{N} \beta_2^{\ (n)} L^{(n)} / 2 \right]}{\alpha - i\Omega d_{jk}^{\ (i)}} . \exp(i\Omega L_N / v_j) \tag{3.5}$$

where $\Delta s_{jk}{}^{m}(\Omega, L_N)$ is the amplitude fluctuations at the end of N amplified spans which is created by the XPM-induced phase modulation at the m[th] span. L_N is the total length of the fiber. $p_k{}^{(m)}(\Omega,0)$ is the pump input power in the m[th] span, d_{jk} is the walk-off length between two channels in the m[th] span.

Equation 3.5 is used to calculate the intensity crosstalk due to the dispersion and nonlinearities.

3.4.1 Intensity distortions impact

In a system which uses NRZ (Non-Return-to-Zero) waveform, the probe signal at the output of the fiber which is distorted due to XPM, has a direct relation with the undistorted optical signal of the probe at the output. The XPM induced crosstalk from pump to probe is given by [14],

$$C_{jk}(t) = F^{-1}\left\{F\left[m_k(t)\right]\sqrt{\Delta p_{jk}(\Omega, L)}\sqrt{H_j(\Omega)}\right\} m_j(t) \tag{3.6}$$

where $m_j(t)$ is the normalized probe waveform at the output and $m_k(t)$ is the normalized pump waveform at the input. F^{-1} and F indicate the Fourier transform and inverse Fourier transforms. $H_j(\Omega)$ is the baseband filter transfer function of the system.

3.4.2 Cross phase modulation involving both timing and intensity distortions

The dispersive nature of the fiber causes impairments in the optical networks. Timing jitter is formed due to the phase distortions developed in the dispersive fiber. These phase distortions occur due to the non linear refractive index of the fiber. Since the power in a channel directly affects the refractive index of the fiber, when there are power variations along the length of the fiber, it changes the refractive index of the fiber. This index of refraction has a direct impact on the phase of the signal. Thus when there are time dependent variations in the fiber, phase variation is introduced in the optical signal. These optical phase variations is then converted into both intensity fluctuation and timing jitter at the output of the fiber through chromatic dispersion. This has a serious effect on the performance of the system. Intensity distortions and timing jitter are separate effects and they combine to produce more deleterious effects on the data transmission. The intensity distortion is due to the broadening of the upper rail corresponding to the transmission of “ones” and timing jitter is the broadening of edges of the eye corresponding to transition between “ones” and “Zeros” [16].

Due to the walk off effect, misalignment of the bit patterns occurs and this results in an optical frequency shift that is induced on the probe channel by the pump channel. Since the shift is induced by the misaligned edges, the shift at the rising edge is cancelled out by the one at the falling edge thereby giving nil shifts. In case of systems with optical amplifiers placed at equal intervals between the fiber spans, due to the power fluctuations different channels of asymmetric bit patterns collide with

each other and this net frequency shift depends on the channel spacing. At the end of the fiber this effects results in timing jitter since the magnitude depends on the bit pattern as well as on the channel wavelength [4]. Even for high dispersive fibers where the walk off happens more quickly at the edge, but due to the pseudo random nature of the bits, there might be a situation in which long "ones" are transmitted which will see the falling edge after a long time. By this time, the probe would have accumulated considerable timing jitter.

Timing jitter considerably degrades the performance of the optical systems and it draws a huge attention in case of high data rate DWDM systems. Thus to evaluate the performance of the optical systems, an analytical model is derived which involves the effect of both timing jitter and amplitude distortions.

Consider two channels, the pump channel *k* and the probe channel *i*. Due to the power in the pump channel, the phase of the probe channel varies along the length of the fiber. To evaluate the effect of this pump power, consider a standard SMF fiber of length L. Let *dz* be the small section of fiber for the analysis. Let *z'* be the portion of the fiber at a distance (z'-z).

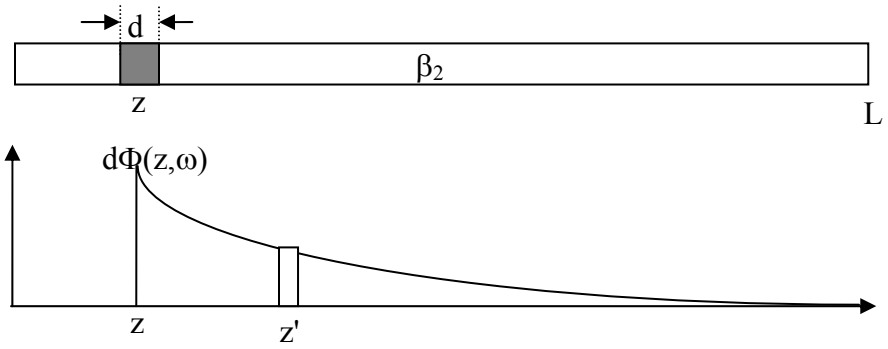

Figure 3.1 SMF fiber of length L with dz the small section of fiber under analysis

As a result of cross-phase modulation, the phase variation of the signal channel (*i*) due to the presence of pump channel (*k*) in a short fiber section *dz* at *z* is [9]:

$$d\Phi_i(z,\omega) = -2\gamma P_k(z,\omega)dz = -2\gamma P_k(0,\omega)\cos(q_k z)\exp(-\alpha z - j\omega z / v_k)dz \tag{3.8}$$

where α is the fiber attenuation, $P_k(0,\omega)$ is the power of the pump channel, q_k for envelope distortions, and v_k for group velocity of the pump channel.

This phase modulation created at *z* is subjected to change while propagating along the fiber. At the point *z'*, this phase modulation becomes:

$$d\Phi_i(L,z,\omega) = \exp\left[-\left(j\omega / v_i\right)(L-z)\right]\cos\left[q_i(L-z)\right]d\Phi_i(z,\omega) \tag{3.9}$$

Where $q_i = q_k = -\dfrac{\beta_2\omega^2}{2}$

Where β_2 accounts for dispersion.

The corresponding frequency variation is the derivative of the phase variation,

$$\begin{aligned} dF_i(L,z,\omega) &= \omega d\Phi_i(L,z,\omega) \\ &= \omega\exp\left[-\left(j\omega / v_i\right)(L-z)\right]\cos\left[q_i(L-z)\right]d\Phi_i(z,\omega) \end{aligned} \tag{3.10}$$

Or the equivalent wavelength variation is:

$$\begin{aligned} d\lambda_i(L,z,\omega) &= -\frac{\lambda_i^2}{c} dF_i(L,z,\omega) \\ &= -\frac{\lambda_i^2 \omega}{c} \exp\left[-\left(j\omega / v_i\right)(L-z)\right] \cos\left[q_i(L-z)\right] d\Phi_i(z,\omega) \end{aligned} \tag{3.11}$$

This frequency variation will be converted into a time jitter due to chromatic dispersion of the optical fiber (different frequency component travels at different speed).

Assume the fiber chromatic dispersion parameter is constant along the fiber and neglecting the 2nd order dispersion (β_2 is wavelength independent), then at the receiver (z = L) the time jitter created by this short fiber section is:

$$\begin{aligned} dt(z,\omega) &= \int_0^L d\lambda_i(L,z,\omega) D(L-z) dz \\ &= -\frac{\lambda_i^2 \omega d\Phi_i(z,\omega)}{c} \int_0^L \exp\left[-\left(j\omega / v_i\right)(L-z)\right] \cos\left[q_i(L-z)\right] \left[D(L-z)\right] dz \end{aligned} \tag{3.12}$$

Then, the total contribution of the time jitter for the entire fiber can be obtained by integration:

$$\Delta t_i(\omega) = \int dt_i(z,\omega) =$$

$$\frac{\lambda_i^2 \omega \cdot \gamma_i P_k(0,\omega)}{c} \int_0^L \cos(q_k z) \exp(-\alpha z - j\omega z / v_k) \begin{Bmatrix} \exp\left[\left(-j\omega / v_i\right)(L-z)\right] \\ \{\exp\left[\left(-jq_i\right)(L-z)\right] + \exp\left[\left(jq_i\right)(L-z)\right] \end{Bmatrix} D(L-z) dz$$

$$= \frac{\lambda_i^2 \omega \cdot \gamma_i P_k(0,\omega)}{c} \int_0^L \cos(q_k z) \exp(-\alpha z - j\omega z / v_k) \begin{Bmatrix} \exp\left[\left(-j\omega / v_i - jq_i\right)(L-z)\right] \\ +\exp\left[\left(-j\omega / v_i + jq_i\right)(L-z)\right] \end{Bmatrix} D(L-z) dz$$

$$= \frac{H}{2} * \int_0^L \exp(-\alpha - j\omega / v_k + jq_k)z + \exp(-\alpha - j\omega / v_k - jq_k)z \begin{Bmatrix} \exp\left[\left(-j\omega / v_i - jq_i\right)(L-z)\right] \\ +\exp\left[\left(-j\omega / v_i + jq_i\right)(L-z)\right] \end{Bmatrix} D(L-z)dz$$

Where H= $\frac{\lambda_i^2 \omega \cdot \gamma_i P_k(0,\omega)}{c}$

First integration term:

$$A(\omega) = 0.5 * \int_0^L \begin{Bmatrix} \exp(-\alpha - j\omega / v_k + jq_k)z \\ +\exp(-\alpha - j\omega / v_k - jq_k)z \end{Bmatrix} \{\exp[(-j\omega / v_i - jq_i)(L-z)]D(L-z)dz$$

That is,

$$A(\omega) = \frac{\exp(-j\omega / v_i - jq_i)L}{2} * \int_0^L D(L-z)\{\exp(-\alpha + j\omega d_{ik} + j2q_k)z\} + \{\exp(-\alpha + j\omega d_{ik})z\}dz$$

$$A(\omega) = \frac{\exp(-j\omega / v_i - jq_i)L}{2} \begin{Bmatrix} \int_0^L DL\{\exp(-\alpha + j\omega d_{ik} + j2q_k)z + \exp(-\alpha + j\omega d_{ik})z\} \\ -D\int_0^L z * \{\exp(-\alpha + j\omega d_{ik} + j2q_k)z.dz \\ -D\int_0^L z * \{\exp(-\alpha + j\omega d_{ik})z.dz \end{Bmatrix}$$

(3.13)

The First integration term becomes

$$\text{Term 1} = DL\left[\frac{\exp(-\alpha + j\omega d_{ik} + j2q_k)L - 1}{-\alpha + j\omega d_{ik} + j2q_k} + \frac{\exp(-\alpha + j\omega d_{ik})L - 1}{-\alpha + j\omega d_{ik}}\right]$$

The second term becomes

Term 2

=

$$\frac{L*\exp(-\alpha+j\omega d_{ik}+j2q_k)L}{-\alpha+j\omega d_{ik}+j2q_k}-\frac{1}{(-\alpha+j\omega d_{ik}+j2q_k)^2}\left[\exp(-\alpha+j\omega d_{ik}+j2q_k)L-1\right]$$

The third term becomes

$$\text{Term 3}=\frac{L*\exp(-\alpha+j\omega d_{ik})L}{-\alpha+j\omega d_{ik}}-\frac{1}{(-\alpha+j\omega d_{ik})^2}\left[\exp(-\alpha+j\omega d_{ik})L-1\right]$$

Thus $A(\omega)=$

$$\frac{\exp(-j\omega/v_i-jq_i)L*D}{2}*$$

$$\left\{\begin{array}{l} L\left[\dfrac{\exp(-\alpha+j\omega d_{ik}+j2q_k)L-1}{-\alpha+j\omega d_{ik}+j2q_k}+\dfrac{\exp(-\alpha+j\omega d_{ik})L-1}{-\alpha+j\omega d_{ik}}\right] \\ -\left[\dfrac{L*\exp(-\alpha+j\omega d_{ik}+j2q_k)L}{-\alpha+j\omega d_{ik}+j2q_k}-\dfrac{1}{(-\alpha+j\omega d_{ik}+j2q_k)^2}\left[\exp(-\alpha+j\omega d_{ik}+j2q_k)L-1\right]\right] \\ -\left[\dfrac{L*\exp(-\alpha+j\omega d_{ik})L}{-\alpha+j\omega d_{ik}}-\dfrac{1}{(-\alpha+j\omega d_{ik})^2}\left[\exp(-\alpha+j\omega d_{ik})L-1\right]\right] \end{array}\right\}$$

(3.14)

Similarly, for the second term,

$B(\omega)=$

$$\frac{\exp(-j\omega/v_i+jq_i)L*D}{2}\left\{\begin{array}{l} L\left[\dfrac{\exp(-\alpha+j\omega d_{ik})L-1}{-\alpha+j\omega d_{ik}}+\dfrac{\exp(-\alpha+j\omega d_{ik}-j2q_k)L-1}{-\alpha+j\omega d_{ik}-j2q_k}\right] \\ -\left[\dfrac{L*\exp(-\alpha+j\omega d_{ik}-j2q_k)L}{-\alpha+j\omega d_{ik}-j2q_k}-\dfrac{1}{(-\alpha+j\omega d_{ik}-j2q_k)^2}\left[\exp(-\alpha+j\omega d_{ik}-j2q_k)L-1\right]\right] \\ -\left[\dfrac{L*\exp(-\alpha+j\omega d_{ik})L}{-\alpha+j\omega d_{ik}}-\dfrac{1}{(-\alpha+j\omega d_{ik})^2}\left[\exp(-\alpha+j\omega d_{ik})L-1\right]\right] \end{array}\right\}$$

(3.15)

Then,

$$\Delta t_i(\omega) = \frac{\lambda_i^2 \omega D \cdot \gamma_i P_k(0,\omega)}{c}\{A(\omega) + B(\omega)\}$$

For Multi-span system, the n[th] span will see the Dispersion in the (n+1) spans. Thus in general, this can be written as,

$L_{y+1} = D_{y+1} = 0$; where y is the number of spans

$A_n =$

$$\frac{\exp(-j\omega/v_i - jq_i)L_n * D_n}{2}\left\{\begin{array}{l} L_n\left[\dfrac{\exp(-\alpha + j\omega d_{ik} + j2q_k)L_n - 1}{-\alpha + j\omega d_{ik} + j2q_k} + \dfrac{\exp(-\alpha + j\omega d_{ik})L_n - 1}{-\alpha + j\omega d_{ik}}\right] \\ -\left[\dfrac{L_n * \exp(-\alpha + j\omega d_{ik} + j2q_k)L_n}{-\alpha + j\omega d_{ik} + j2q_k} - \dfrac{1}{(-\alpha + j\omega d_{ik} + j2q_k)^2}\left[\exp(-\alpha + j\omega d_{ik} + j2q_k)L_n - 1\right]\right] \\ -\left[\dfrac{L_n * \exp(-\alpha + j\omega d_{ik})L_n}{-\alpha + j\omega d_{ik}} - \dfrac{1}{(-\alpha + j\omega d_{ik})^2}\left[\exp(-\alpha + j\omega d_{ik})L_n - 1\right]\right] \end{array}\right\}$$

$$+ \sum_{x=n+1}^{y} D_i L_i * \left[\frac{\exp(-\alpha + j\omega d_{ik} + j2q_k)L_n - 1}{-\alpha + j\omega d_{ik} + j2q_k} + \frac{\exp(-\alpha + j\omega d_{ik})L_n - 1}{-\alpha + j\omega d_{ik}}\right] \quad (3.16)$$

B_n =

$$\frac{\exp(-j\omega/v_i + jq_i)L_n * D_n}{2}\left\{\begin{array}{l} L_n\left[\frac{\exp(-\alpha + j\omega d_{ik})L_n - 1}{-\alpha + j\omega d_{ik}} + \frac{\exp(-\alpha + j\omega d_{ik} - j2q_k)L_n - 1}{-\alpha + j\omega d_{ik} - j2q_k}\right] \\ -\left[\frac{L_n * \exp(-\alpha + j\omega d_{ik} - j2q_k)L_n}{-\alpha + j\omega d_{ik} - j2q_k} - \frac{1}{(-\alpha + j\omega d_{ik} - j2q_k)^2}\left[\exp(-\alpha + j\omega d_{ik} - j2q_k)L_n - 1\right]\right] \\ -\left[\frac{L_n * \exp(-\alpha + j\omega d_{ik})L_n}{-\alpha + j\omega d_{ik}} - \frac{1}{(-\alpha + j\omega d_{ik})^2}\left[\exp(-\alpha + j\omega d_{ik})L_n - 1\right]\right] \end{array}\right\}$$

$$+ \sum_{x=n+1}^{y} D_i L_i * \left[\frac{\exp(-\alpha + j\omega d_{ik})L_n - 1}{-\alpha + j\omega d_{ik}} + \frac{\exp(-\alpha + j\omega d_{ik} - j2q_k)L_n - 1}{-\alpha + j\omega d_{ik} - j2q_k}\right] \qquad (3.17)$$

$$\text{Time Jitter} = \sum_{n=1}^{N} \frac{\lambda_i^2 \omega^n \gamma_i P_k{}^n(0,\omega)}{c}\left[\mathrm{A_n} + B_n\right] \qquad (3.18)$$

Where ‘N’ is the total number of spans.

3.4 Simulation Models

To verify the analytical model we have developed, we can use the VPI Inc numerical simulation software and compare the results with the analytical model. VPI model gives us almost the exact physical realization of a system. This provides the manufacturers, system designers, and system testers to upgrade the existing network and it also allows users to build an entirely new network from scratch. One such model is built from scratch to analyze the effect of the cross phase modulation in WDM systems. VPI provides the users with laser diodes, filters, modulators and all the components which are essential to build an optical network. VPI also provides

users to analyze the signal diagrams at various parts of the simulation and allows users to obtain data points from the outputs and seemingly incorporate those outputs on other simulation software such as MATLAB. In this thesis, one such method of extracting the data from VPI and loading that onto MATLAB is done to get more precise analysis.

VPI permits users to save the configuration files for later use so that it is not necessary for the user to configure the component's parameters every time they want to simulate the network. VPI has the functionality of building our own component which will improve the model efficiently. One such component that was built in this thesis was the dispersion compensation module which consists of a fiber with dispersion compensation parameters. VPI has precise control over adjusting the parameters of the components. VPI has a built in mathematical model which includes all the fiber non-linearities, dispersion, FWM, Raman Effect, SPM, XPM, higher order non linearity effects, and even polarization analysis namely scalar and vector PMD, field analysis, split step parameters for split step Fourier transforms, attenuation, dispersion slope and also boundary values. To sum up, it can be said that VPI almost exactly simulates a real system and its behavior. Thus the thesis takes more credibility for the VPI software. There is however, one disadvantage in using this simulation system. VPI takes considerable amount of time to simulate the system. If the network consists of more number of spans and more parameters are assigned to the components, then the software becomes very slow in analyzing the effect. Even

on a Pentium 4 machine with 512 MB RAM, which is considered to be a relatively fast processor, VPI performs slower when it comes to multiple spans.

This becomes an inefficient solution in case of future dynamic DWDM systems in which the routing decision is made by the resources available in the wavelength path and also by the impairments in the wavelength channel. Quick decision has to be made to route through the path which has lesser impairments and more resources available. The model which VPI uses will not be efficient since a routing decision has to be made very quickly. Since VPI model takes a considerable amount of time to simulate multi-span systems, a model has to be developed which can efficiently help routing algorithms to make a decision with resources and impairments along the channel. One such analytical model is developed which is far more efficient in terms of making a quicker decision about the path to be chosen since it requires lesser time to analyze the effects and lets the routing algorithm to choose the path quicker.

This thesis presents an analytical model implemented in MATLAB which is fast in calculating the impairments even in multi-span systems. This analytical model is implemented in MATLAB for single span, multi-span systems with and without dispersion compensation. Results from both the simulation software are compared and the effects of cross phase modulation on optical systems are analyzed. These results are discussed under the results section.

3.4.1 Basic VPI model

To build a model, first the optical network design components have to be taken into consideration. Components such as the kind of fibers that should be used, whether it is a single span or multi span system, whether the system needs dispersion compensation module, the filters to be used, the modulators to be used, photo diodes to be used, modulation format to be used and the PRBS generators. Here a basic model is built with a single span. With the inclusion of multiple fiber spans and dispersion compensation modules, a multi span system can be built.

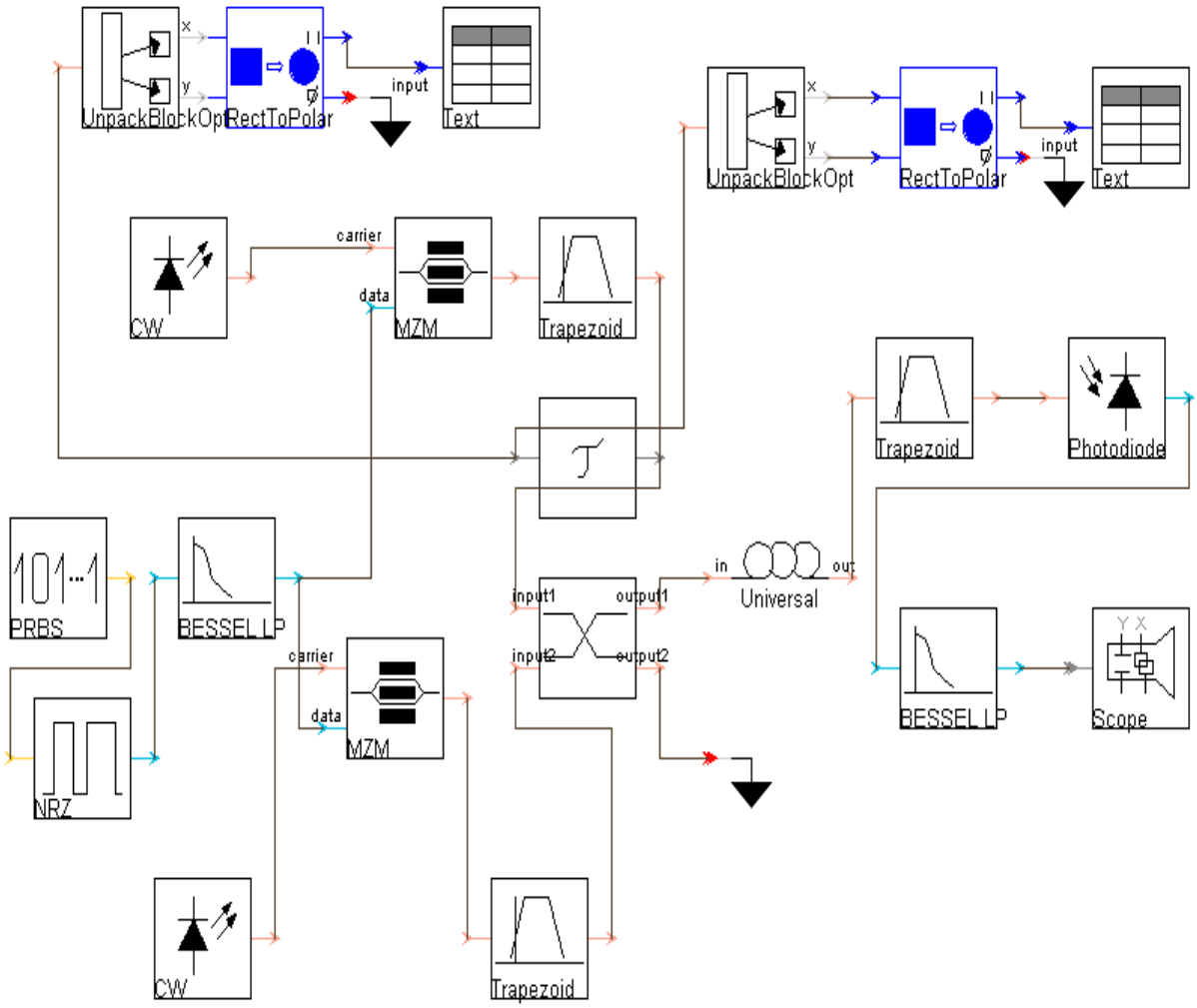

Figure 3.2 Block diagram of VPI software for single span NRZ modulated system

The figure 3.2 shows the block diagram for a NRZ modulated single span optical network system. This consists of the following components.

a. Transmitter section

b. Fiber section

c. Receiver section

a. Transmitter Section

The transmitter consists of the PRBS generator, which generates pseudo random bit sequences at the rate of 10 Gbps with $2^7 - 1$ bits. This bit sequence is fed to the NRZ Coder, which produces an electrical NRZ coded signal. Further more, this is fed into a low pass filter which has a bandwidth of 7.5 GHz for NRZ signals and 15 GHz for RZ signal since RZ signal requires twice the bandwidth of the NRZ format.

Two channels are used in this simulation. One is the pump signal which has higher power and which produces phase modulation of the neighboring channel. This pump channel operates at the frequency of 193.68 THz which is equivalent to 1549.6 nm wavelength channel. The line width of the channel is 10 MHz.

The neighboring channel is the probe channel (signal channel) which experiences the phase modulation and the time jitter at the output of the fiber due to the power in the pump channel. This channel operates at 193.6 THz which is equivalent to 1550.4 nm wavelength channel. Thus there is a separation of 0.8 nm between the two channels which are enough to produce the cross phase modulation and other non linear effects on the signal channel.

The modulator used here is the Mach-Zehnder modulator. It has two inputs, one for the laser diode and the other for the data from the channels. There are two Mach-Zehnder modulators used, one for pump channel and one for probe channel. It

converts the electrical signal into optical signal form. The output of the Mach-Zehnder modulator is shown below:

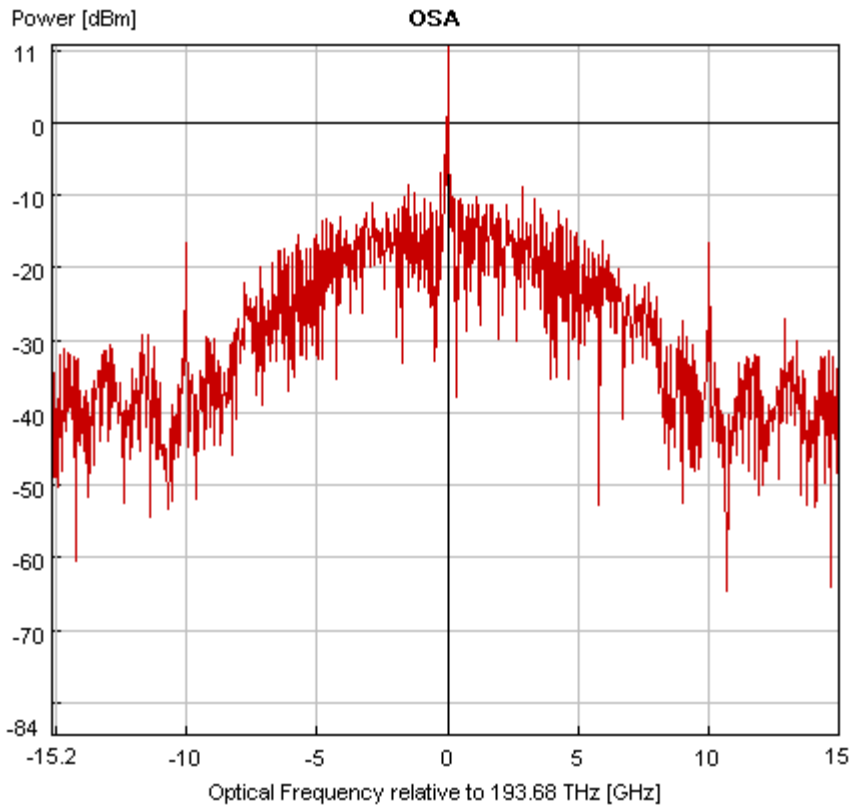

Figure 3.3 Optical waveform of NRZ modulated pump waveform

The trapezoidal filter that follows the modulator is a band pass filter with trapezoidal transfer function. It efficiently filters the sidebands of the pump and probe channel. The respective filters are centered at the probe and the pump channel frequencies. The pump channel experiences a delay in respect to the probe channel since in real time systems, the pump and probe channel bits are not always aligned. Thus a delay is introduced in the pump channel to simulate this effect.

The waveform from the output of the modulator is given to a text block which stores the NRZ modulated waveform in text form which can be used for other simulation software to perform data analysis. The Unpack Block Optical, converts optical block mode signal into native samples. This is fed into the rectangular to polar converter. It converts the complex number x + j y, for inputs "x" and "y", into magnitude and phase form. The phase output is in the range $-\pi$ to π. To make a fair comparison, the text data file from VPI model is extracted and used in MATLAB.

This setup is followed by an optical coupler for combining or splitting of optical signals. It can also be used as a physical signal splitter for signal check. The output of the coupler will have both the pump and the probe signal. An optical spectrum analyzer at the output of the fiber showing the two channels is shown below:

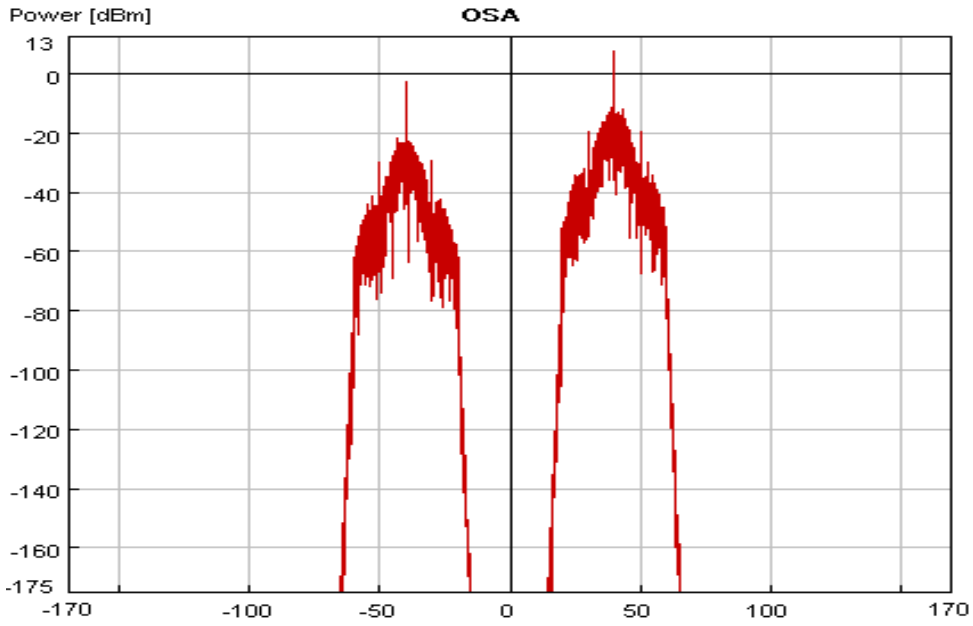

Figure 3.4 The output of the coupler which has both the pump and probe signal channels

b. Fiber Section

This waveform is fed into the fiber which is a standard single mode fiber. This is a simplified version of the universal fiber module for simulation of wideband nonlinear signal transmission in optical fibers. It takes into account the unidirectional signal flow, stimulated and spontaneous Raman scattering, Kerr nonlinearity and dispersion. In vectorial mode, it includes the PMD and polarization dependence of nonlinear effects.

The fiber can be of any length and the dispersion parameters are set accordingly. The fiber model in VPI gives numerous options with parameters associated with the fiber. The user can set the length, dispersion parameters, attenuation, dispersion slope, non-

linear index, core area of the fiber, SPM, XPM, FWM, split step parameters, and PMD options. The parameters will be adjusted according to the simulation.

At the output of the fiber, the probe signal would have undergone the XPM effects and the waveform at the output will be distorted. The following figure shows the signal of the received waveform after passing through the trapezoidal filter.

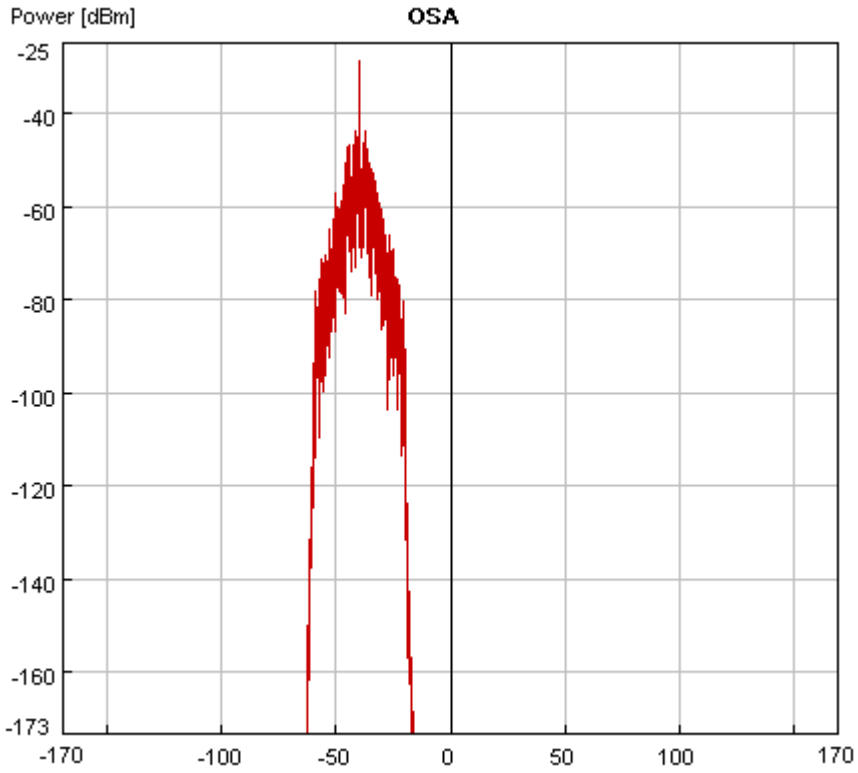

Figure 3.5 Signal waveform at the output of the trapezoidal filter

At the output of the trapezoidal filter, a Photo diode converts the optical signal into an electrical signal. This is a model of PIN and APD photodiodes. These can be simulated on the basis of predefined responsivity, avalanche multiplication, dark

current and noise. Alternatively, the voltage and temperature dependence is considered by using an equivalent RC circuit. Electric frequency response is not included and can be modeled by an external filter.

c. Receiver section:

An electrical low pass Bessel filter follows the APD. This has a cut-off frequency determined by the type of the waveform used for modulation. If it is a NRZ modulated waveform, then 7.5 GHz is used and if it is a RZ modulated waveform, 15 GHz is used since RZ requires twice the bandwidth of NRZ signals.

Finally at the output of the low pass filter, VPI provides a visualization tool called Scope. It is an optical or electrical oscilloscope with numerous data processing options, eye display and BER estimation features. It requires a preceding clock recovery module for BER estimation. In our case, we mostly go for the Eye diagram. A sample eye diagram is shown below in figure 3.6.

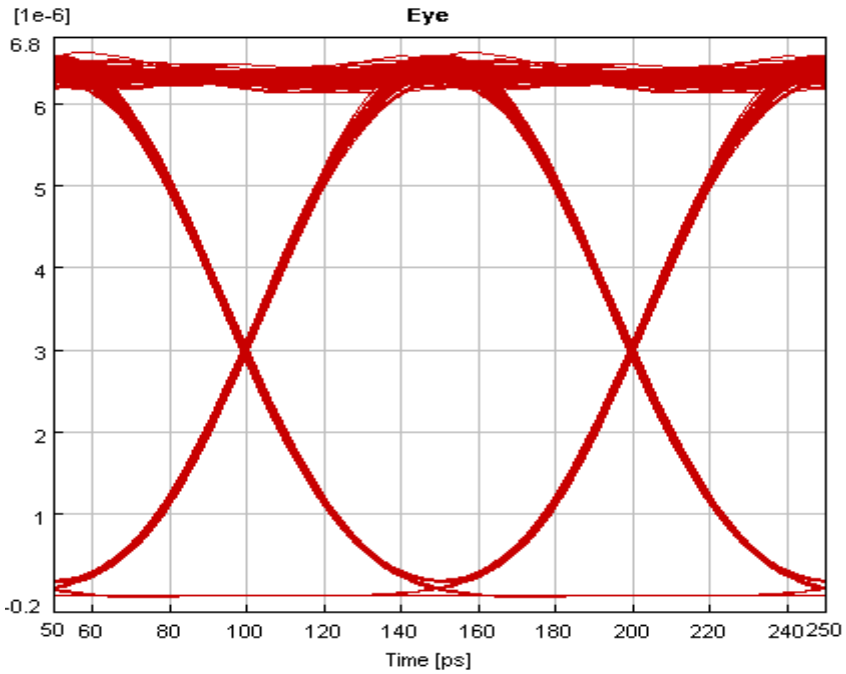

Figure 3.6 Eye diagram of a NRZ modulated waveform with no crosstalk

In figure 3.6, we can see that the eye opening is very wide and there is no cross talk in the eye since there is no time jitter at the edges of the eye. Thus eye diagrams can be used to effectively analyze the performance of an optical system. These eye diagrams play an important role in this thesis since all the effects are analyzed through the eye diagram display of the output signal waveform that has undergone all the impairments.

In case of a distorted eye diagram, the edges will have more time jitter and the eye opening will be small thus effectively reducing the system performance. Eye diagrams clearly depict the data handling capacity of a system. The more the eye is open, the more efficient the system. Performance degradation will directly affect the eye diagrams which in turn results in reduced eye opening and time jitter at the edges.

Till now, we have seen the eye diagrams for NRZ waveforms. Since this thesis concentrates also on RZ waveform, the following section explains about the RZ waveform characteristics.

3.4.2 RZ model

In case of the RZ waveform, it requires twice the bandwidth of NRZ waveform due to the pulse shape. The VPI simulation model remains the same except for replacing the NRZ block to RZ block and increasing the filter cut off frequency to 15 GHz.

The eye diagram of a typical RZ waveform without dispersion and crosstalk effects is shown below. The eye is wide open and the time jitter is negligible since the power of the pump is very less in the order of 1 to 4 mW. We can see that the eye shape is very different when compared to NRZ waveform.

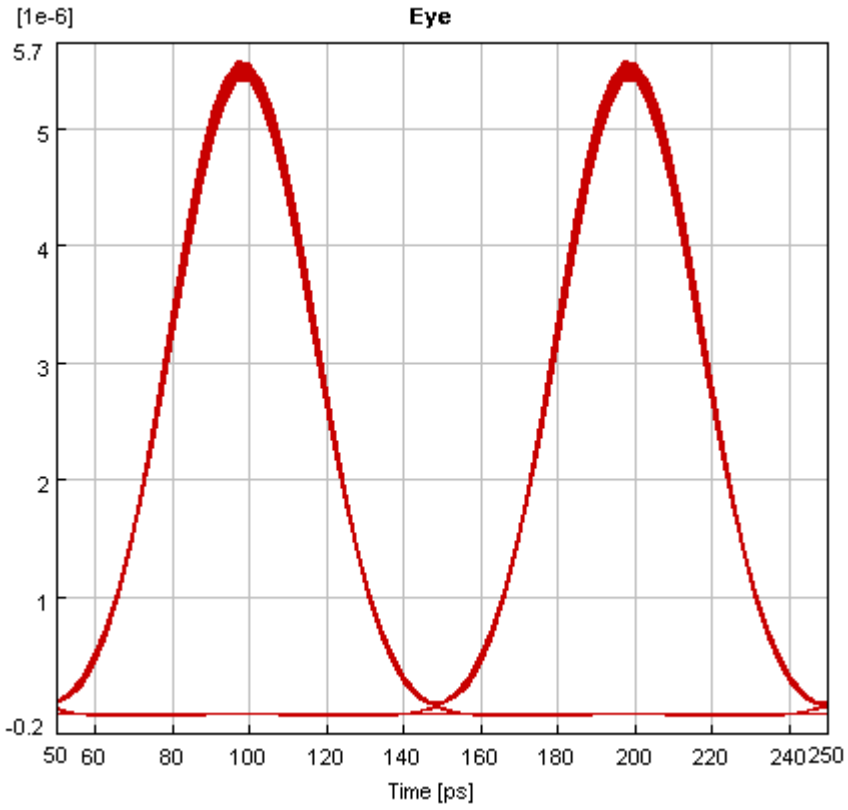

Figure 3.7 Typical eye diagram of a RZ waveform

3.4.3 Basic Analytical Model implemented in MATLAB

In case of the VPI model, to measure time jitter, it is not possible to set the probe channel to be CW and the pump channel to be modulated. Thus both the probe and the pump channel are modulated in case of VPI. Thus the output probe waveform will be affected by both chromatic dispersion and the SPM. To make a fair comparison, a program is developed in MATLAB to simulate this SPM and dispersion effect on the probe channel and then the time jitter and intensity fluctuations created by XPM are added onto it. This SPM and chromatic dispersion implementation on the probe

channel in MATLAB is based on split-step Fourier transform method. To simulate these effects, the following implementation is done in MATLAB

a. Transmitter section

b. XPM Modeling section

1. Creation of intensity modulation

2. Creation of time jitter

c. Fiber section

d. Receiver section

The following figure 3.8 shows the way in which the analytical model is implemented in MATLAB to calculate XPM.

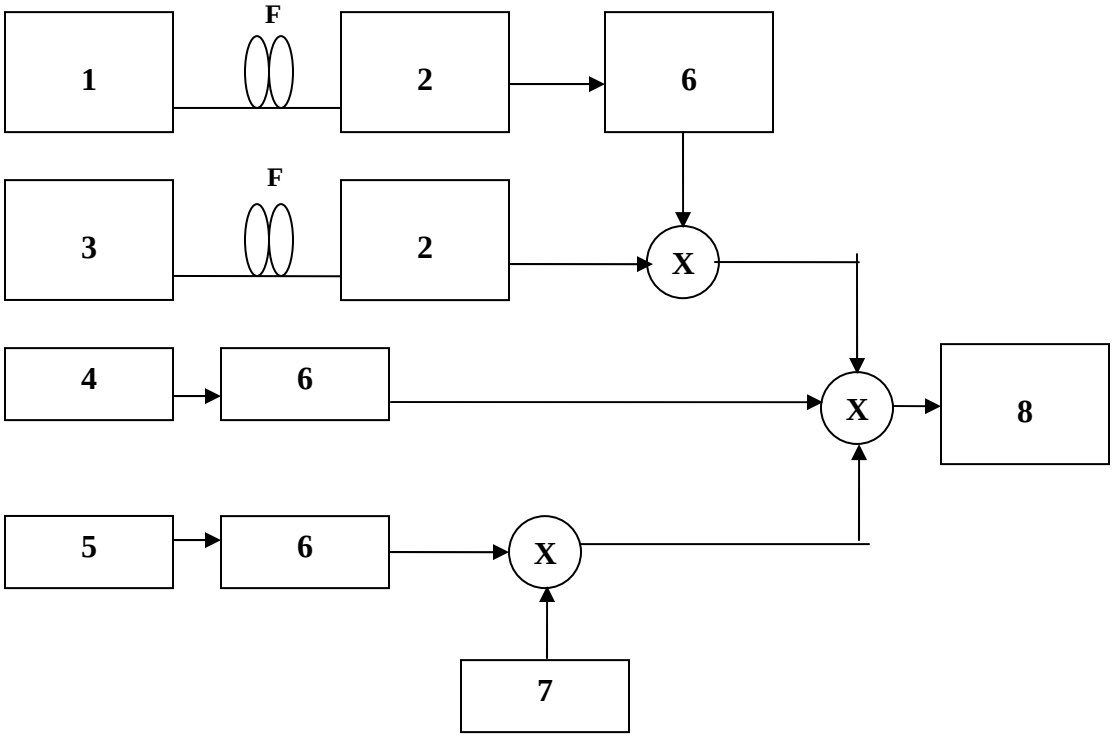

Figure 3.8 Block diagram for the Analytical model

The block diagram has the following components:

1. Intensity fluctuation transfer function

2. Bessel low pass filter

3. Time jitter transfer function

4. Pump channel at 1549.6 nm wavelength

5. Probe channel at 1550.4 nm wavelength

6. Normalization block

7. Dispersion and SPM effects

8. Eye diagram generation block

9. F – Fiber of corresponding length

a. Transmitter section

Transmitter section has a pump and a probe channel waveform derived from the text output of the VPI simulation. This is done to make accurate comparison between VPI and Matlab models. Given that when different waveforms are used, then an exact comparison cannot be made since both waveforms will have different delays and bit alignments. The waveforms received are normalized to "one" and then considered separately

The waveform taken from the input of the delay block at the VPI model serves as the unwavering probe waveform. The waveform taken from the output of the delay block of the VPI model serves as the shifted pump waveform. This shifting is necessary since no two waveforms can be perfectly aligned during transmission. Due to dispersion, the bit alignments always change along the length of the fiber. The figure below shows the pump NRZ waveform at the input of the fiber.

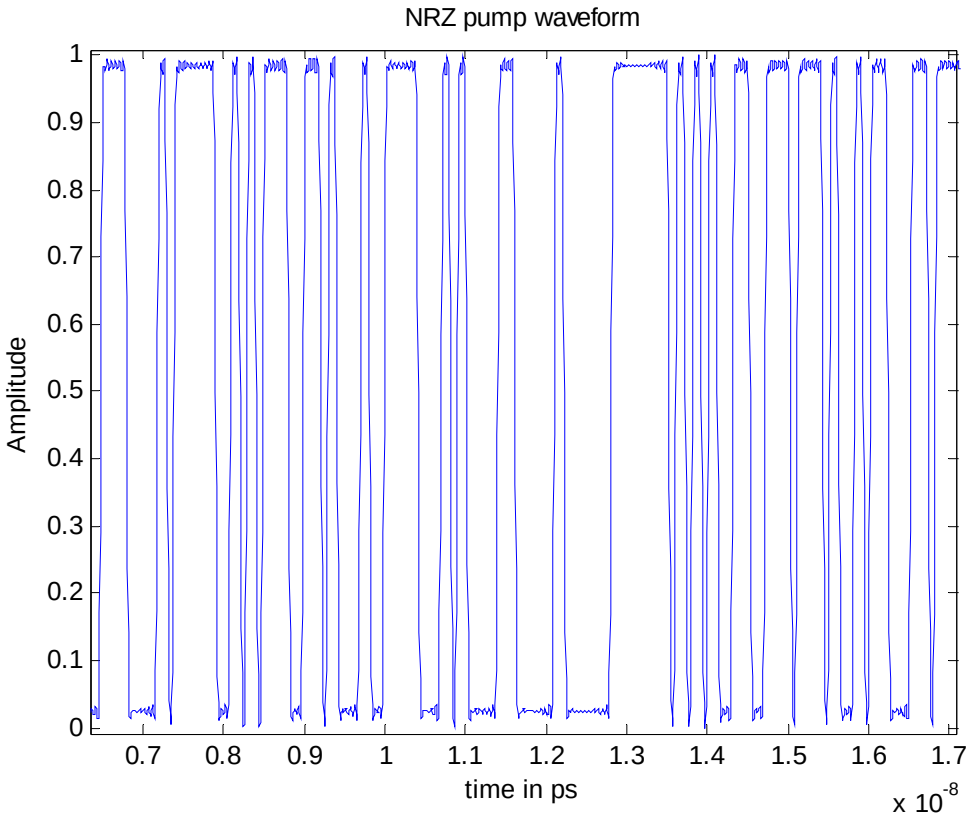

Figure 3.9 NRZ Pump waveform at the input of the fiber

The figure 3.9 shows the NRZ waveform for the pump channel. There are 128 bits of 100 ps bit width. This is generated at the rate of 10 Gbps. The pump channel is transmitted at 1549.6 nm and the probe channel at 1550.4 nm. The probe channel will be similar to the pump channel except for the delay.

To simulate the effect of Self phase modulation, the probe channel is considered separately and it is passed through the dispersion and self phase modulation transfer functions for the length of the fiber considered. If it is a dispersion compensated system, then the dispersion compensation is added to the fiber length. After the probe

passes through the dispersion and SPM effects, an eye diagram is generated which will be undistorted and having a wide eye opening. This is taken as the reference and this waveform is multiplied with the XPM effects to analyze how much the probe signal will be affected by the XPM and other nonlinearities. Since this thesis considers the effect of SPM to be less, the power for the probe signal is considered to be very less in the order of 1 to 4 mW. The figure below shows the undistorted clear eye. This waveform has undergone the dispersion and SPM effects.

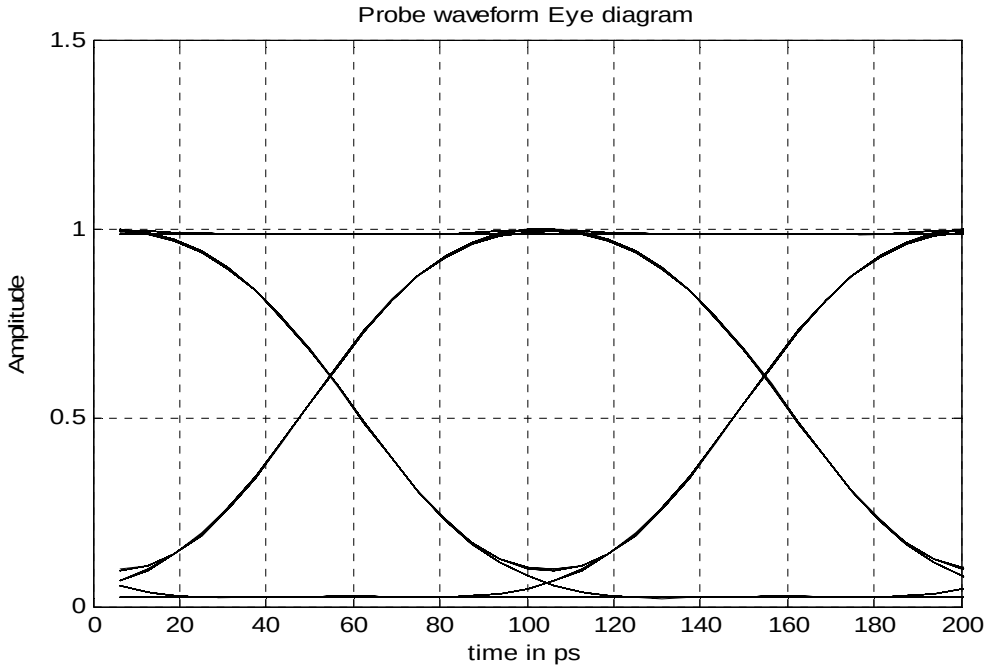

Figure 3.10 Eye diagram of the probe waveform after SPM and dispersion effects

In figure 3.10, we can see that the eye is clear and undistorted and this waveform will be used to multiply with the cross talk waveform calculated from the intensity and time jitter transfer functions which will create the effects of XPM and non-linear effects on the probe signal. The intensity and the time jitter are created in the fiber

which is finally imposed on the probe signal which will affect the data handling capacity of the optical system. The creation of intensity and time jitter is explained in the following section.

b. XPM modeling

The modeling section consists of two subsections namely the intensity and the time jitter effects. The intensity modulation is created by the analytical model described in section 3.3 and it is implemented in the MATLAB by developing a programming model.

b.1 Intensity modulation creation

Due to the pump channel, the probe channel is intensity modulated. The waveform created due to this intensity distortion is shown below. This intensity distortion occurs at the rails of the eye diagram. Thus a factor of “1” is added to the resulting intensity waveform. This is passed through a Bessel filter to filter the higher frequencies.

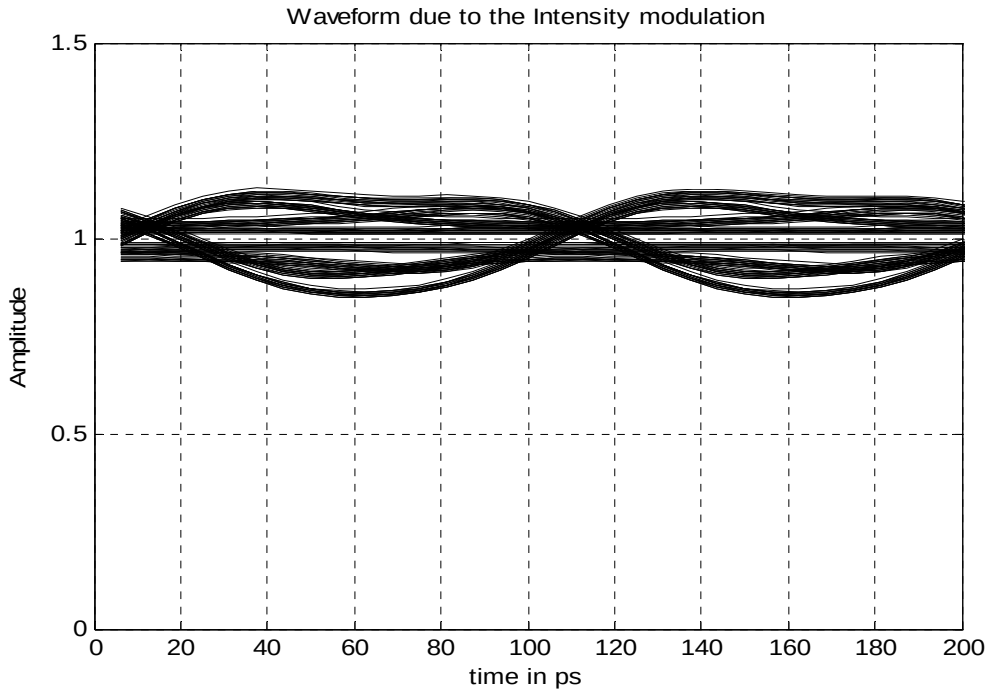

Figure 3.11 Intensity modulation due to XPM effect

b.2. Time jitter creation

Due to XPM considerable time jitter is accumulated along the length of the fiber. The time jitter is higher for higher pump channel powers and lower for lower pump channel powers. The difference in the probe and the pump bit alignments plays a major role in the accumulation of the crosstalk. If the edges are perfectly aligned, then it produces more time jitter and if they are not aligned exactly at the edges, then lesser time jitter is produced. The transfer function of the time jitter is shown below.

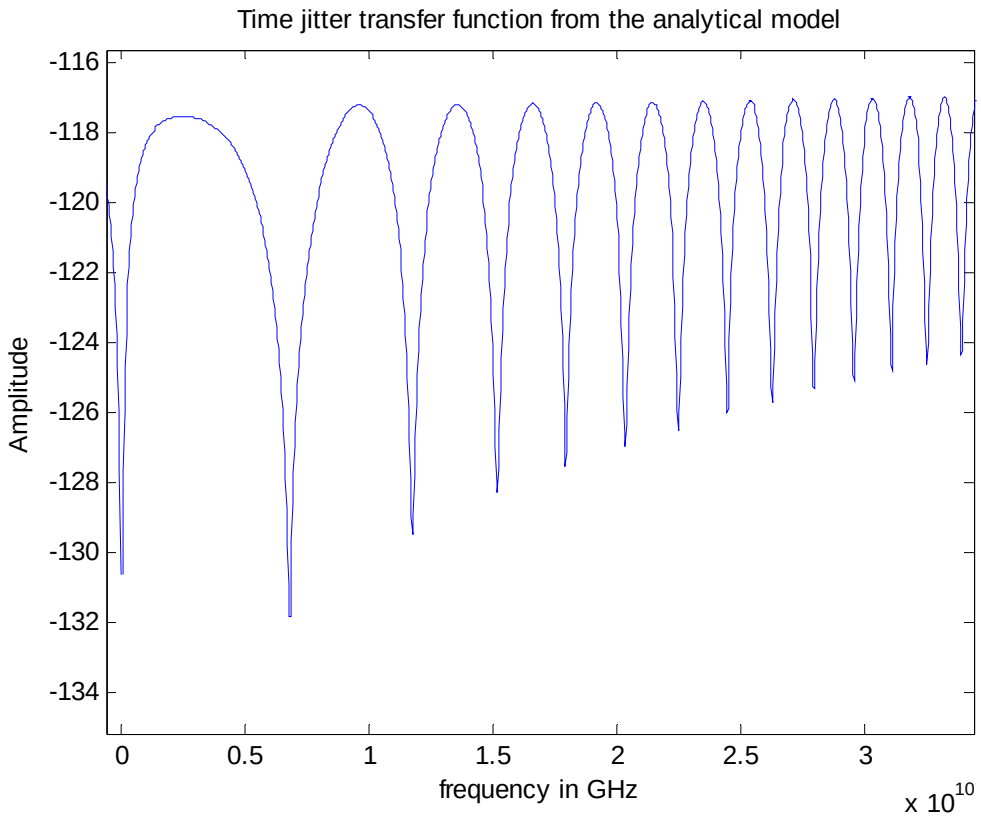

Figure 3.13 Transfer function of time jitter

The following figure shows the effect of the time jitter created in the fiber. The probe waveform is multiplied with the time jitter created and the resulting eye diagram is shown below.

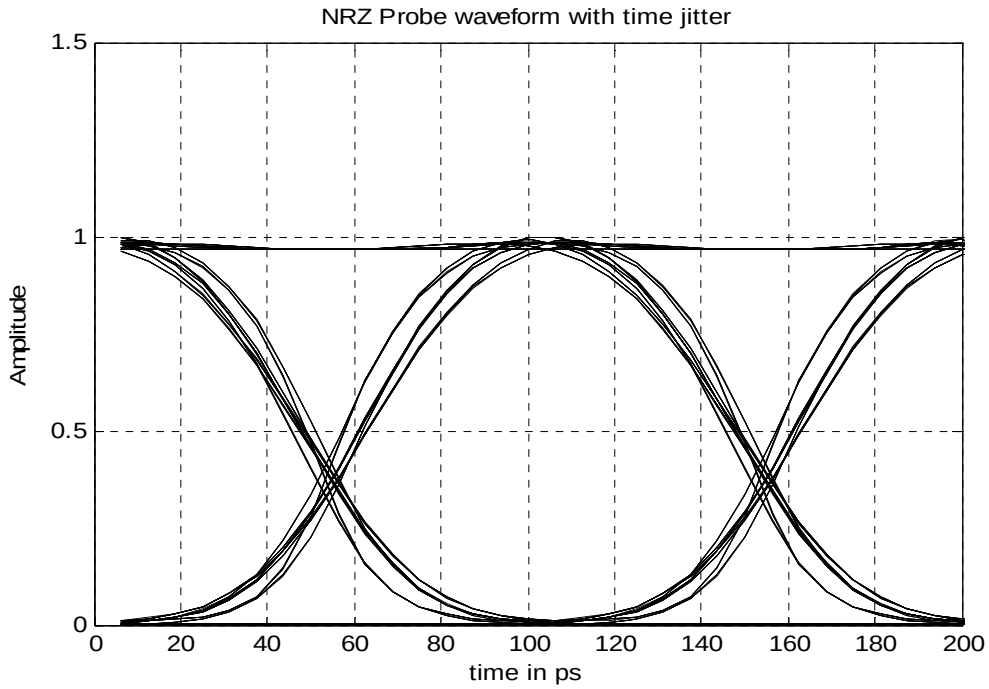

Figure 3.14 Probe waveform with time jitter alone

The above eye diagram is for a NRZ probe signal at the output of the fiber with 10 mW pump channel power. The eye diagram clearly shows the distortions at the edge of the eye.

c. Fiber section

The fiber section is simulated by developing a model which includes all the characteristics of a fiber such as length, dispersion, wavelength spacing, effective area, loss, dispersion slope etc. Both the intensity and time jitter transfer functions are passed through the fiber to generate the corresponding intensity fluctuations and time jitter impairments. The pump waveform is shifted and then multiplied with the intensity and time jitter transfer functions to generate the effect of the impairments.

Then this is passed through a Bessel low pass filter which will filter out all the high frequency components.

d. Receiver section

The receiver section in the MATLAB model consists of the multiplication of the time jitter and the intensity modulation onto the probe waveform. As we saw earlier, this will affect eye opening and decrease the data handling capacity of the system.

3.4.4 RZ waveform analysis

In RZ, time jitter plays more important role since the edges are more affected in this case. Thus analyzing RZ waveforms is a key to efficiently evaluate the effect of cross phase modulation. Figure 3.13 shows the typical Eye diagram of a RZ waveform without crosstalk and dispersion.

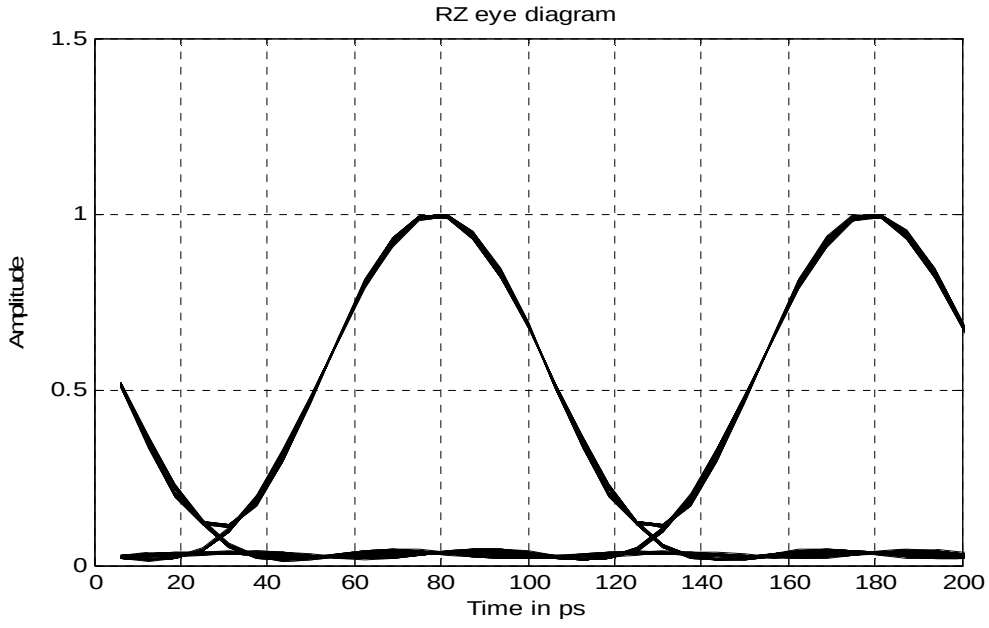

Figure 3.13 Eye diagram of a RZ waveform

3.5 Comparison criteria

Since the models for the simulation models are not exactly the same, to compare the results of both simulation models, a method has to be developed which gives us a fair comparison between the two simulations. It varies with span length, number of spans and amplifiers usage. The following figure explains the comparison method between the two simulation models.

MATLAB	**VPI**
NRZ modulation format 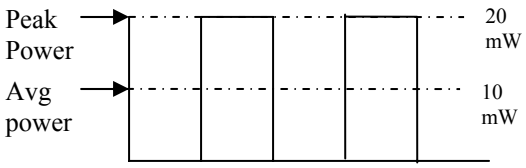 Average power = Peak power / 2	At the Laser diode input 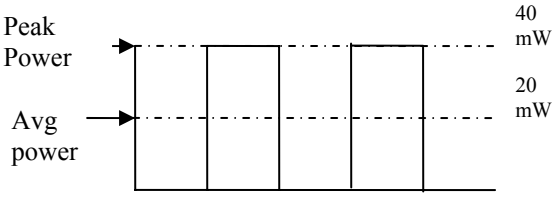 At the coupler output 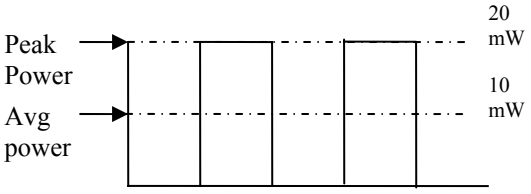 Average power at the coupler output = Peak power / 4

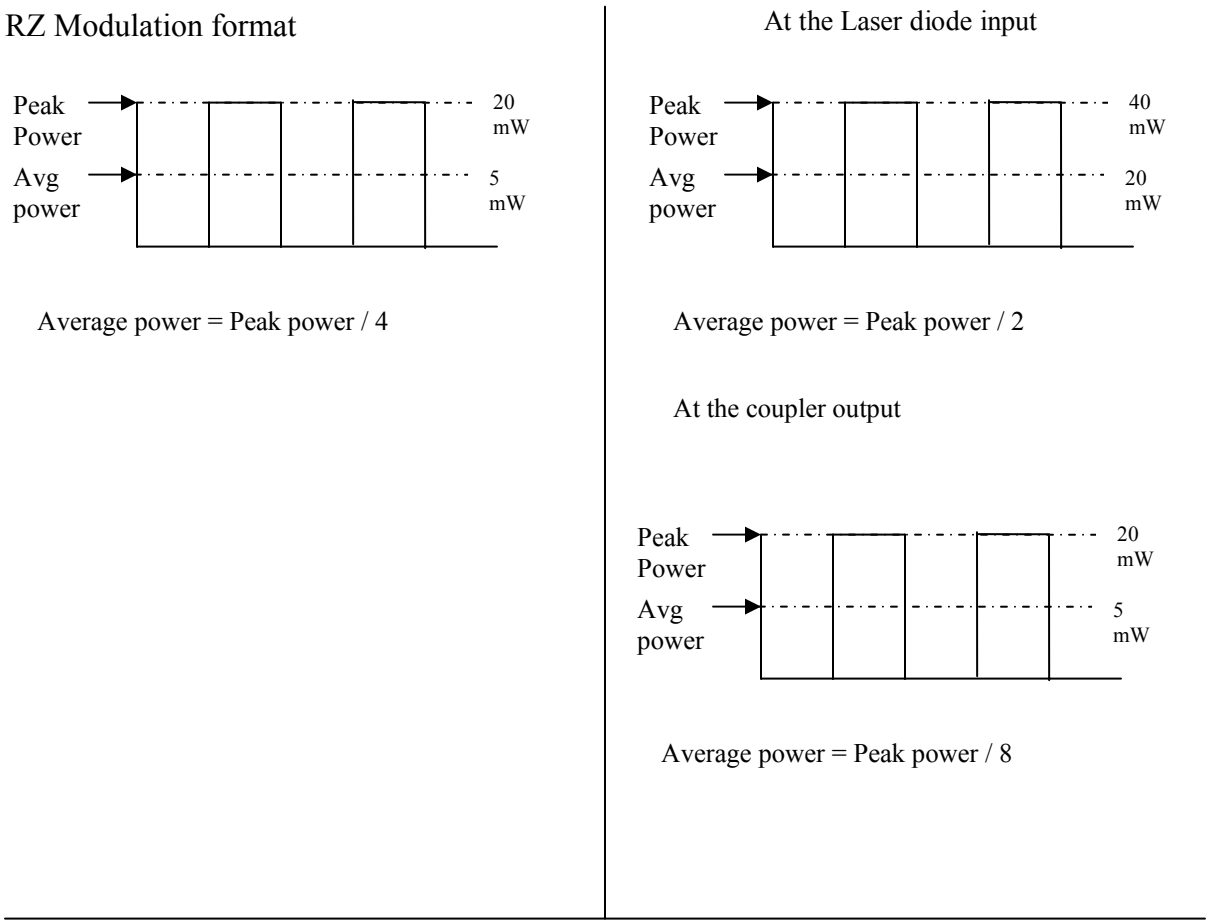

Figure 3.14 Comparison between MATLAB and VPI models

In figure 3.14, the comparison criteria for the two models under consideration are explained. In case of NRZ waveform, when we take the VPI model, for example, if the peak power at the laser diode is 40 mW, then the average power is 20 mW until the signal reaches the coupler. But once the signal passes through the coupler and combines with the probe signal, then due to the 3 dB difference with the coupler, the

peak power becomes 20 mW and average power becomes 10 mW. Thus when the peak power at the input of the laser diode is 40 mW, then the average power at the fiber is 10 mW. The average power is one fourth of the peak power at the laser diode. This average power is fed to the amplifiers that follow the first span.

In case of MATLAB with the same NRZ waveform, since there are no couplers or modulators, the average power is half of the peak power. To compare the two models for a particular power level, for example, if we want to test the system with 10 mW of pump power, then MATLAB must have 10 mW of peak power and VPI should have 20 mW of peak power.

In case of RZ waveform, due to the pulse duration, for VPI model, the average power at the output of the coupler is one eighth of the peak power at the laser diode input. This average power is fed to the amplifier spans at the following spans. In MATLAB, the average power is one fourth of the peak power and thus if we use 20 mW of peak power in MATLAB, then the average power is 5 mW and this power is used for the amplifiers at the VPI model. When we want to test a system with 20 mW of power, we need to multiply the MATLAB power by a factor of 2 which is 40 mW and this power is fed to the laser diode of the VPI model. The amplifiers used in this model are Black-Box Amplifier with wavelength dependent gain, based on data that can be measured from an actual device. The model accounts for the dependence of the gain and noise spectra on the degree of saturation induced by the input signals. The amplifier can be internally controlled to provide either constant gain or constant

output power. Measured amplifier characteristics are read from input files. The power input to the amplifiers is in dB unit.

Thus the comparison criteria is determined and used to analyze and compare the eye diagrams of both the VPI and MATLAB models. The following results section discusses the NRZ and RZ models in both VPI and MATLAB and a comparison is made at different power levels. Single span and multi span systems, dispersive and dispersion compensated systems are considered.

4. RESULTS

The result section is organized in the following order:

4.1 Transmission of single probe channel alone

4.2 Comparison with [16]

4.3 NRZ 1 span analysis and associated eye diagrams

4.4 NRZ 3 span analysis and associated eye diagrams

4.5 RZ 1 span analysis and associated eye diagrams

4.6 RZ 3 span analysis and associated eye diagrams

4.1 Transmission of single probe channel alone

This thesis considers the NRZ and RZ modulation formats involving two channels. The power in one channel affects the phase of the other channel and induces cross talk. If only one channel is transmitted, then it will not experience any cross talk since there is no neighboring channel to cause cross talk. This seldom happens in a WDM link since these links always carry multiple channels in the same link with narrow spacing between them. For simplicity and better understanding the worst effects of nonlinearities, first a single channel is considered. A launch power of 20 mW is used with 2.7 ps/nm-Km dispersion, with 100 Km fiber length and the following figure shows the eye diagram of the resulting channel after passing through the fiber and the nonlinearities. This eye diagram has only self phase modulation effects and there are no cross phase modulation effects in this eye.

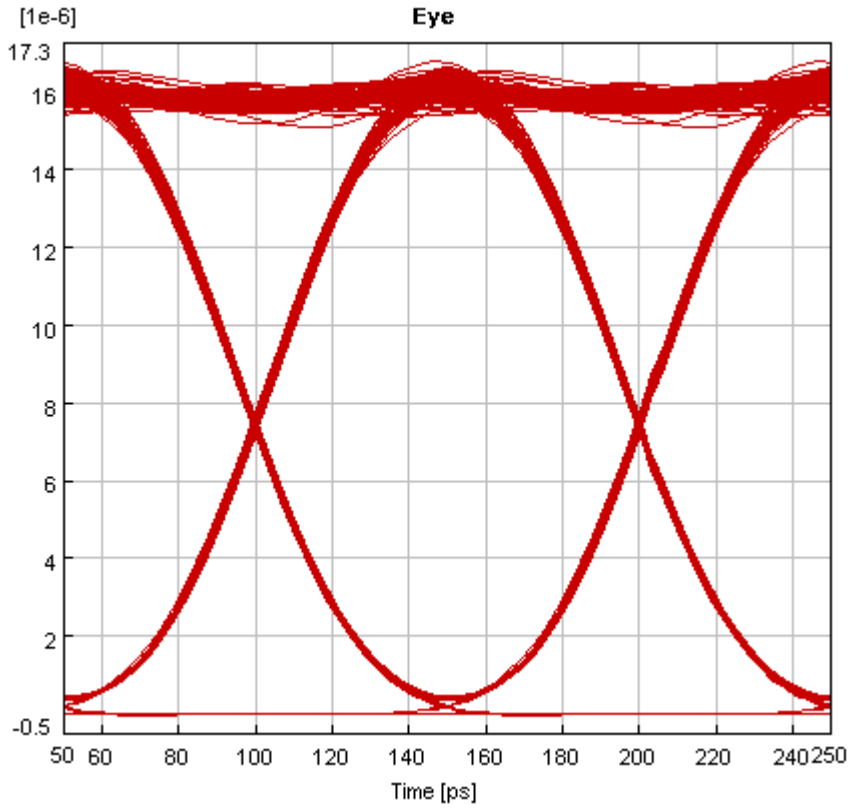

Figure 4.1 Eye diagram of a single channel NRZ waveform with no XPM

As we can see from figure 4.1, the eye is very clear and wide open which can efficiently recover the received bits. This eye is free of crosstalk interference. This eye has the effect of only dispersion and other nonlinearities. This still allows for efficient transmission due to the nature of eye opening. This is in concordance with [16] in which the author clearly explains that the transmission of single probe channel alone does not exhibit significant eye distortions.

The effects of XPM are added to this eye when the co-propagating pump channel induces phase modulation on the probe channel which is often the case under

consideration. The following sections discuss the addition of intensity and cross talk impairments and the associated eye diagram distortions.

4.2 Comparison with [16]

As discussed previously, WDM links always carry multiple channels together with narrow spacing which is the main cause of the cross phase modulation effects. This section focuses on comparing the VPI simulation model and the analytical model and finds a match between the two values. First a comparison is made between the previous work done by [16] and the model which is built using the analytical model developed in section 3.3.4 and the VPI simulation model. The VPI model used for this comparison is given below:

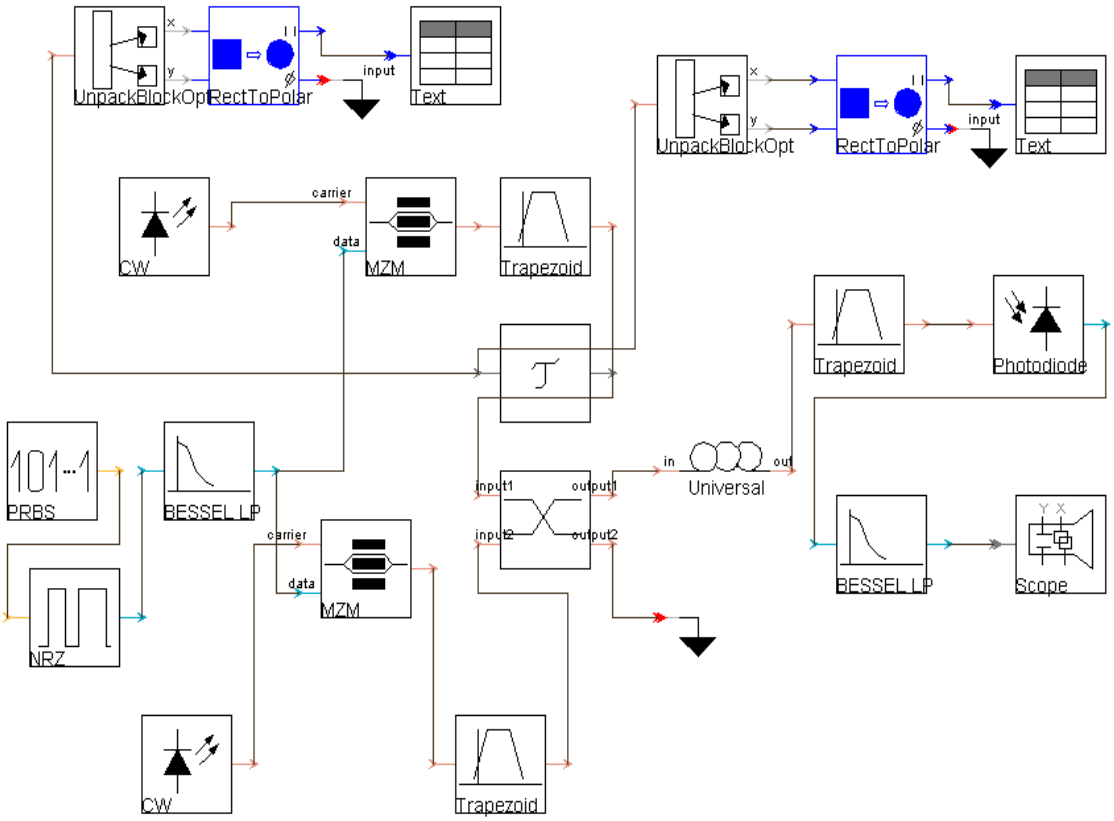

Figure 4.2 VPI model for comparison with the paper [16]

The explanation of various blocks in the VPI model was already discussed in section 3.4.1. The model for MATLAB can be obtained from section 3.4.3, except for the changes in the fiber parameters and the components used in the model.

In [16], the fiber parameters are as follows:

Parameter	Value
Launch power	5mW - 20 mW
Dispersion	2.7 ps/nm/Km
Fiber length	100 Km single span
Modulation format	NRZ waveform

Table 4.1Fiber parameters for the paper [16]

The same parameters were used with the analytical model and the comparison is made. But this comparison is made by taking into account the comparison criteria discussed in section 3.5. After comparing, the results were plotted out in the eye diagram format and the values are analyzed. According to [16], the horizontal eye closure is approximately ± 10 ps. With the analytical model using MATLAB, we arrived at 11.8 ps and with VPI model we arrived at 13 ps at a clock delay of 180 ps which is not very different from the value in [16]. The eye diagrams are also plotted for different clock delay values. The different delays are considered because two channels propagating in a WDM link will always have some delay in between each other. The channel walk off, the overlap between the data patterns is also taken into account. This walk off happens gradually with VPI and with analytical model, this walk off occurs at the output when the probe signal is multiplied with the crosstalk pump channel, which is due to the way the model was built. This also accounts for the difference in values between VPI and MATLAB simulations. The following diagram

shows the comparison between the VPI and analytical model for the values in [16]. Good agreement is seen with the eye diagrams.

The eye diagrams are generated for different power levels and delay values for VPI and analytical model built in MATLAB. Since lesser cross talk occurs at lower powers, eye diagrams at very lower powers will not have considerable distortions and thus analysis will be inefficient. So eye diagrams are generated only for powers at 5 mW, 10 mW, 15 mW, 20 mW.

4.2.1 Eye comparison for 5 mW of pump power

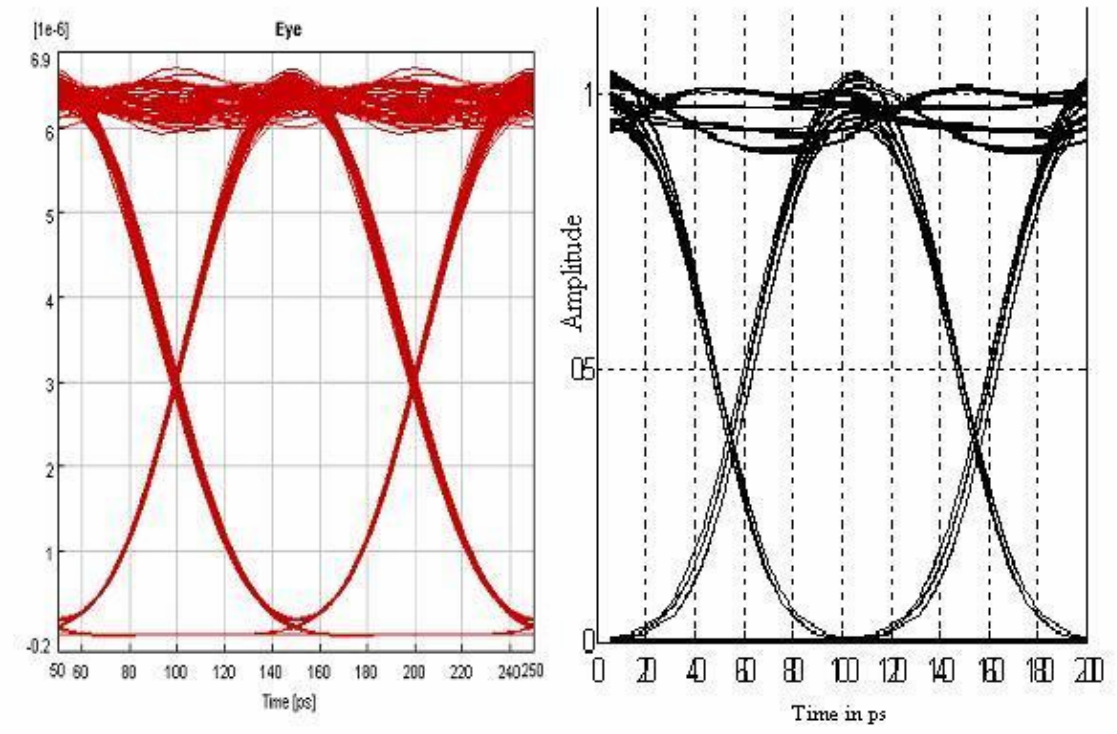

Figure 4.3 NRZ waveform Eye diagram for 5 mW of pump power

From figure 4.3, we can see that the effect of crosstalk is very less due to lower pump power of 5 mW. Thus efficient transmission can be achieved with this kind of pump power level. Also the eye diagrams from the VPI and analytical model match very well except for the cross point which is due to the filter characteristic. But the more important factor to consider is the time jitter due to XPM, which is measured at the edges of the eye. Intensity modulation is also evident which can be seen from the distortion in the railings of the eye. The time jitter values were 2 ps for the analytical model and 4.8 ps for VPI which are very less due to lower pump power.

4.2.2 Eye comparison for 10 mW of pump power

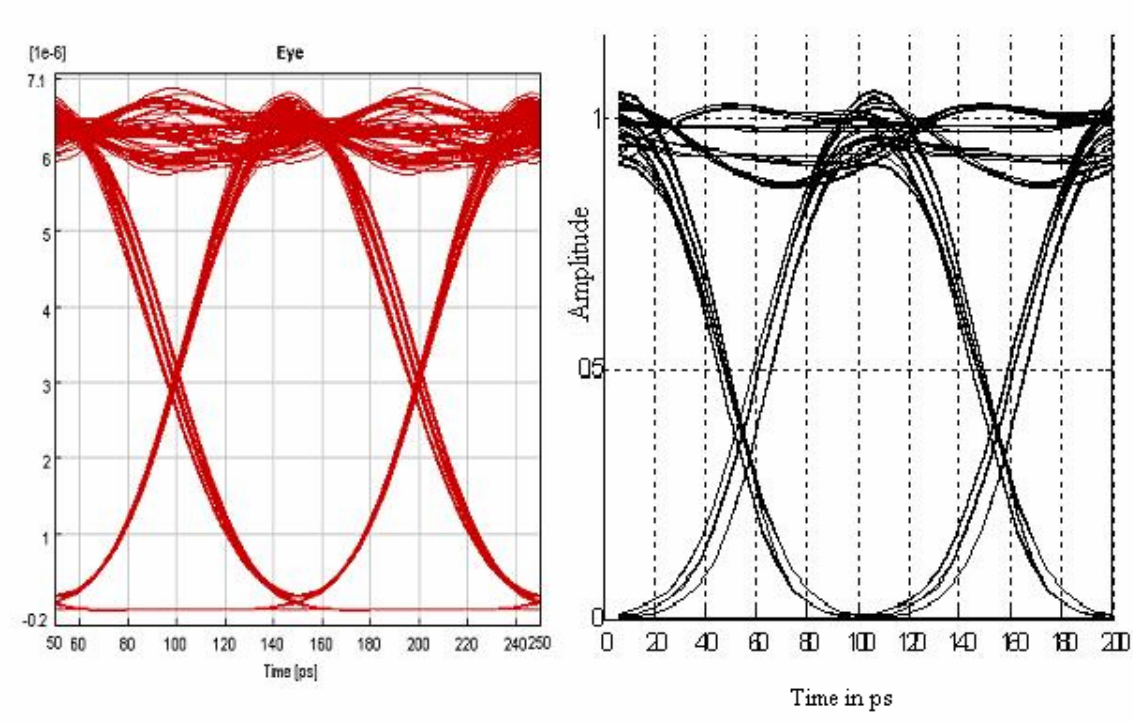

Figure 4.4 NRZ waveform Eye diagram for 10 mW of pump power

From figure 4.4, we can see that the time jitter has increased due to the higher pump crosstalk power. But the eye shape is retained. Time jitter values due to cross phase modulation are 4.6 ps for the analytical model and 7.9 ps for VPI.

4.2.3 Eye comparison for 15 mW of pump power

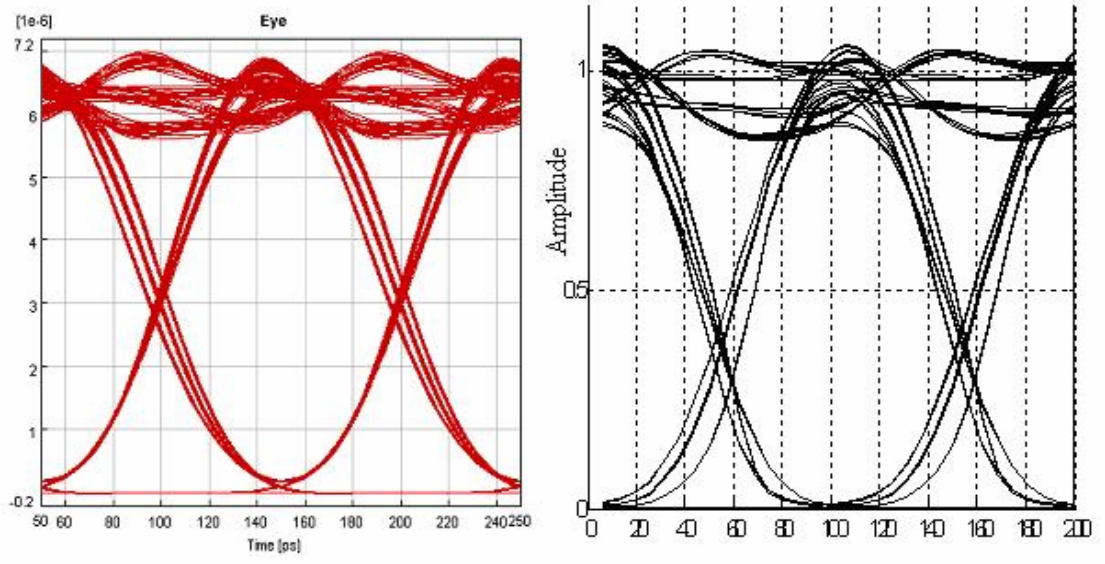

Figure 4.5 NRZ eye diagram for 15 mW of pump power

From figure 4.5, we can see that the time jitter has further increased and it is 7 ps for analytical model and 10.5 ps for VPI.

4.2.4 Eye comparison for 20 mW of pump power

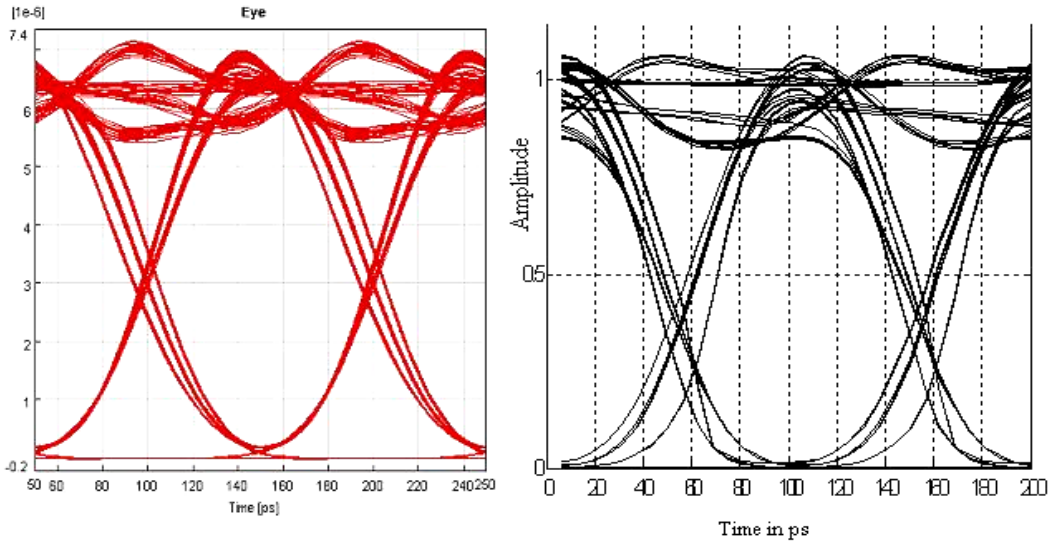

Figure 4.6 NRZ eye diagram for 20 mW of pump power

From figure 4.6, we can see that the time jitter has increased to 13.6 ps with VPI simulation and 10 ps with the analytical model. Thus at higher powers, the time jitter increases which results in inefficient transmission. Since this eye diagram includes both intensity distortions and cross phase modulation effects, the data handling capacity of the optical system will decrease.

4.2.5 VPI and analytical model comparison

The following figure shows the graph for the VPI and MATLAB time jitter values calculated in the range of ps.

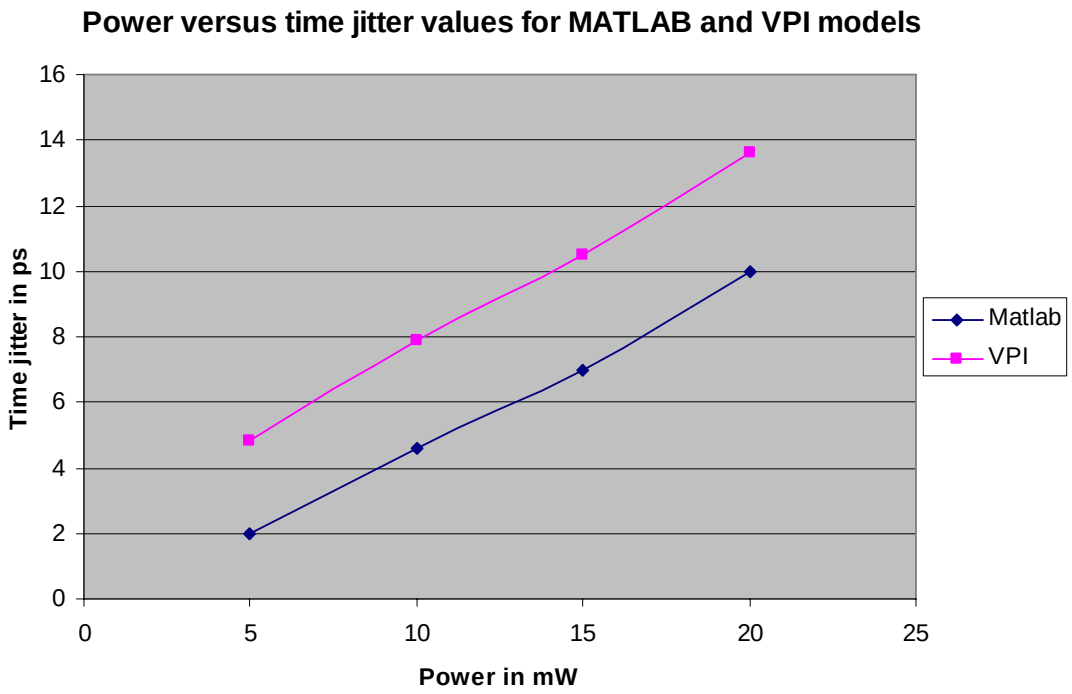

Figure 4.7 Power versus time jitter values for analytical and VPI models

From figure 4.7, we can see that the time jitter values have a difference of approximately 3 ps which is attributed towards the gradual walk-off in VPI. Since this gradual walk off is due to the delay seen between the data bit patterns of pump and probe channels, different delays will have different time jitter values.

Power in mW	MATLAB time jitter in ps	VPI time jitter in ps
5	2	4.8
10	4.6	7.9
15	7	10.5
20	10	13.6

Table 4.2 Time jitter values for analytical and VPI models

The table 4.2 shows the time jitter values for both VPI and MATLAB simulation values. We can see that both the values are close enough to each other and this will verify the analytical model developed in section 3.3.4. With this result, we can go on to other NRZ and RZ models. The same experiment is repeated for a different delay of 270 ps between the pump and the probe and the resulting eye diagrams and time jitter plots are explained.

4.2.6 VPI and analytical model comparison for 270 ps delay

The following graph is obtained for the VPI and analytical models with 270 ps delay between the pump and probe data patterns. We can see that the values match more closely when compared to 180 ps delay which is attributed towards the walk-off effect. The following table summarizes the time jitter values for both VPI and analytical simulations.

Power in mW	MATLAB time jitter in ps	VPI time jitter in ps
5	3.5	4.6
10	5.5	6.3
15	8	9.5
20	11.8	13

Table 4.3 Power versus time jitter values for 270 ps delay between pump and probe

The following figure plots the time jitter values of both analytical and VPI models as a function of power in mW.

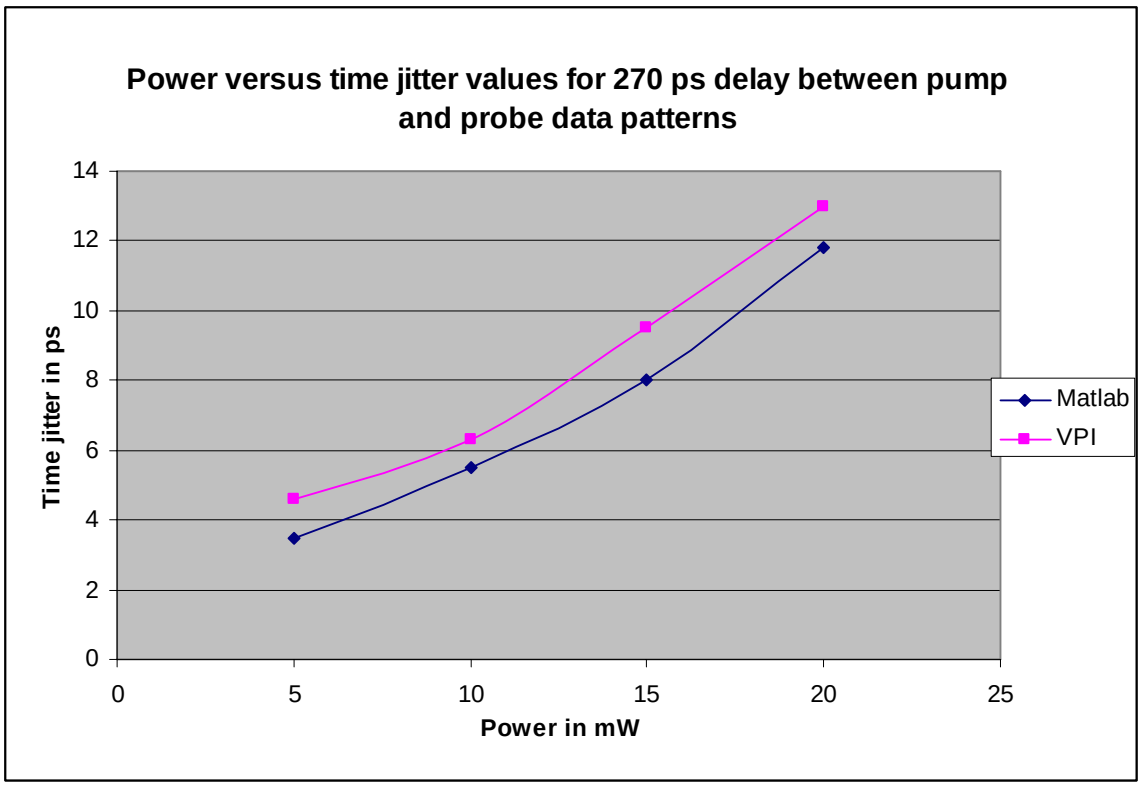

Figure 4.8 Power versus time jitter values for 270 ps delay between the pump and probe channels

In this figure 4.8, as previously explained in section 4.2.5, this change in values is attributed towards the gradual walk off effect in VPI. The following plot shows the variation of time jitter with respect to delay in bit patterns.

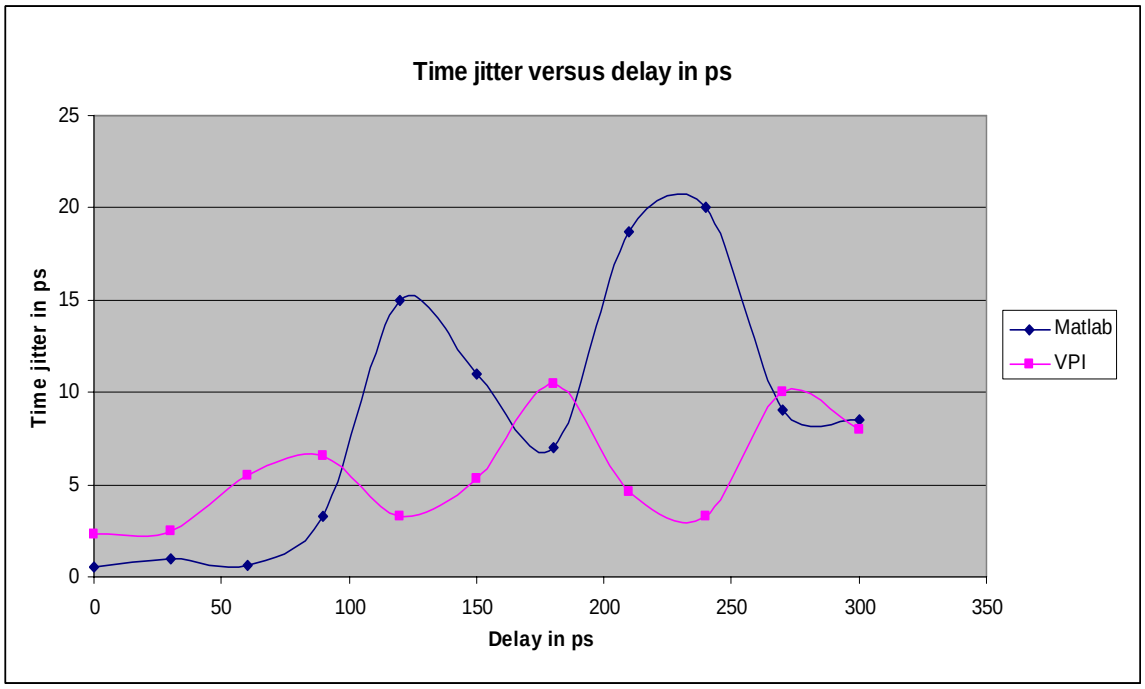

Figure 4.9 Delay versus time jitter plot

From figure 4.9, we can see that the time jitter has different values at different delay values. The gradual walk off effect in VPI has not been implemented in analytical model and is considered for future work. If the gradual walk off is implemented in the analytical model, then these two curves will be superimposed on each other and the time jitter values will always be approximately the same with VPI and analytical models.

4.3 NRZ single span analysis

With the comparison made between VPI and analytical models, we further investigate the NRZ single span model to evaluate the effect of cross phase modulation in WDM networks with NRZ modulation format and having a single span fiber. Since it is a

single span system, dispersion compensation need not be required. With no dispersion compensation, efficient transmission could still be achieved. The fiber parameters in this analysis differ from the one with [16] and they are tabulated below:

Parameter	Value
Launch power	5mW - 20 mW
Dispersion	17 ps/nm/Km
Fiber length	80 Km single span
Modulation format	NRZ waveform

Table 4.4 Parameters and their values for NRZ single span system

The VPI block diagram for the NRZ single span system is the same as the block diagram for section 4.2 with the exception of the changes in the fiber and component parameter values. The same analytical model is used to generate the time jitter values. The following sections compare the eye diagrams of both VPI and the analytical model built in MATLAB and a graph is plotted for the time jitter values as a function of power for different delay values. Even in this analysis, the same gradual walk off happens with VPI such that the time jitter values are different for different delay values.

4.3.1 Eye comparison for 5 mW of pump power

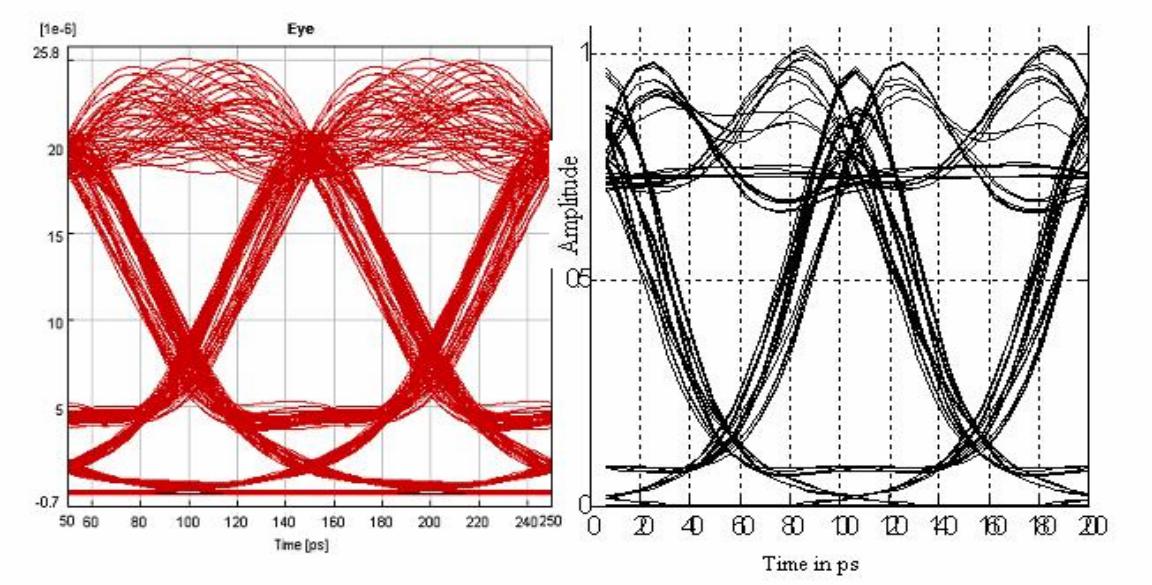

Figure 4.10 Eye diagram for NRZ single span model for 5 mW of pump power

From figure 4.10, we see that the time jitter for analytical model is 14 ps and for VPI, it is 17.3 ps. Since there is no dispersion compensation, the time jitter is higher for such small powers.

4.3.2 Eye comparison for 10 mW of power

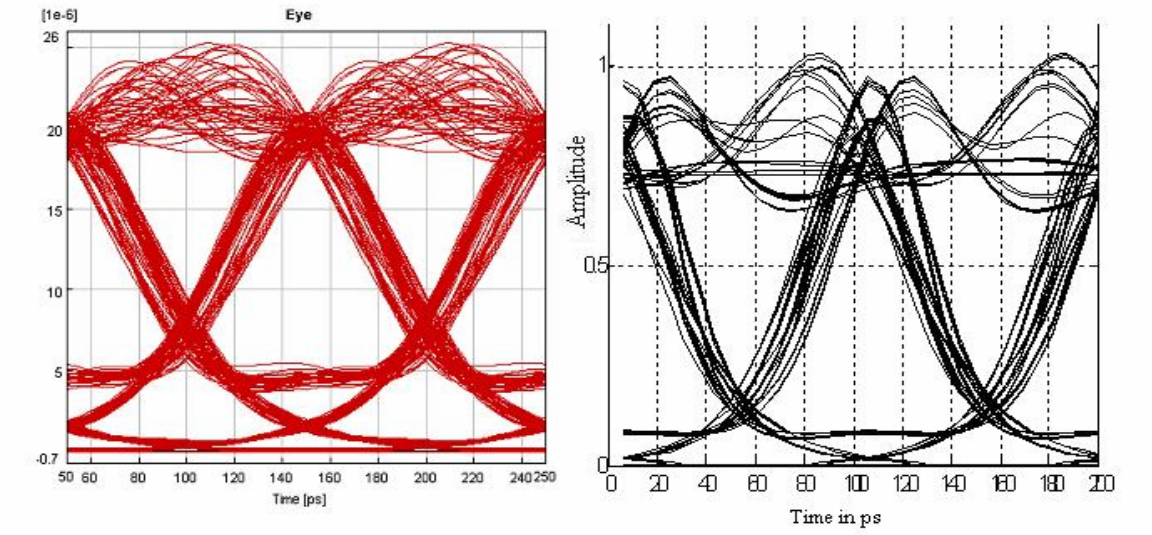

Figure 4.11 Eye diagram for NRZ single span model for 10 mW of pump power

From the above diagrams, the time jitter was found to be 16 ps for analytical model and 18 ps for VPI.

4.3.3 Eye comparison for 15 mW of power

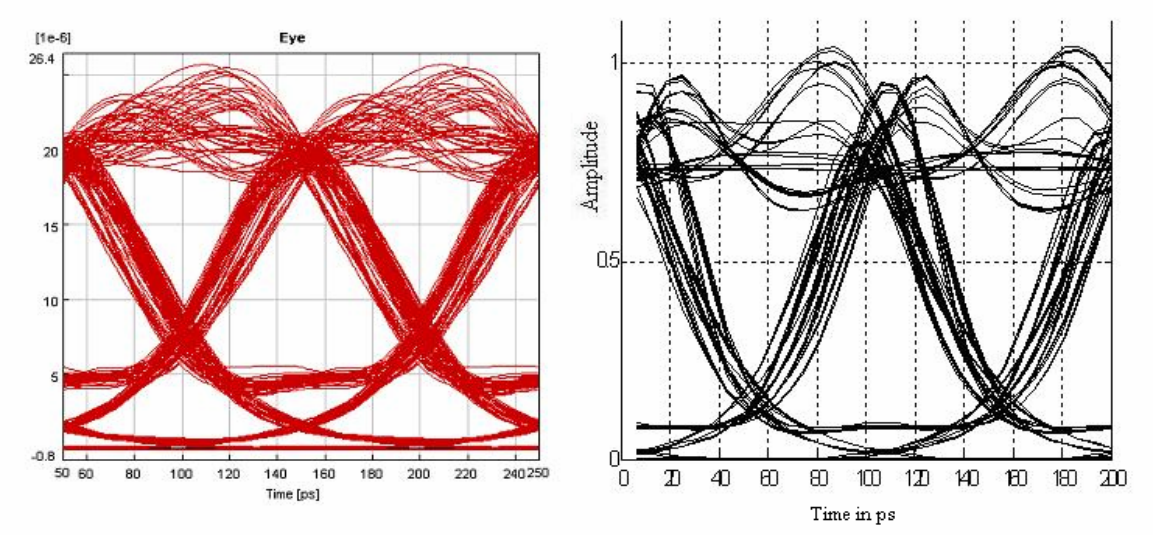

Figure 4.12 Eye diagram for NRZ single span model for 15 mW of pump power

From figure 4.12, we see that the time jitter is 18.2 ps for analytical model and 19.2 ps for VPI

4.3.4 Eye comparison for 20 mW of power

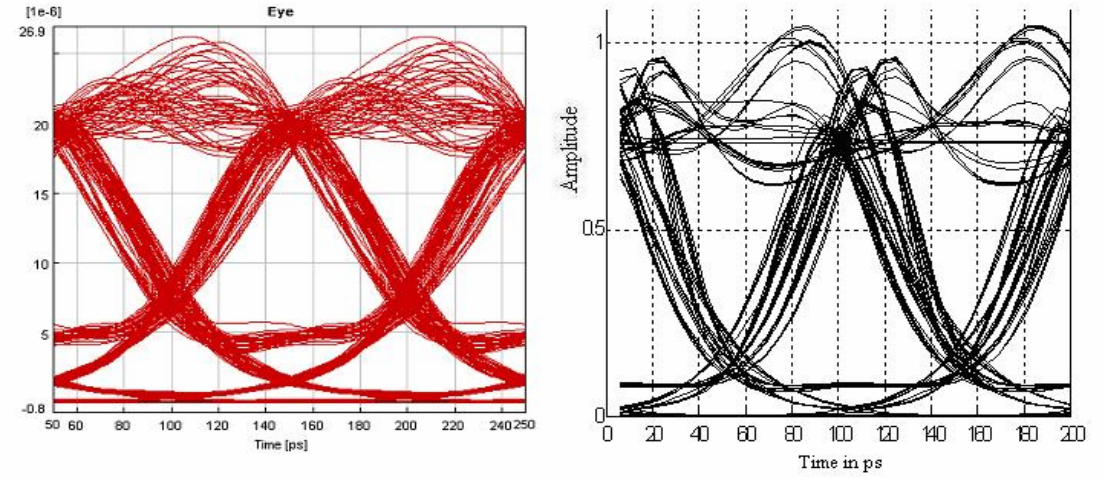

Figure 4.13 Eye diagram for NRZ single span model for 20 mW of pump power

From figure 4.13, we see that the time jitter is 19 ps for analytical model and 20 ps for VPI.

4.3.5 VPI and analytical model comparison

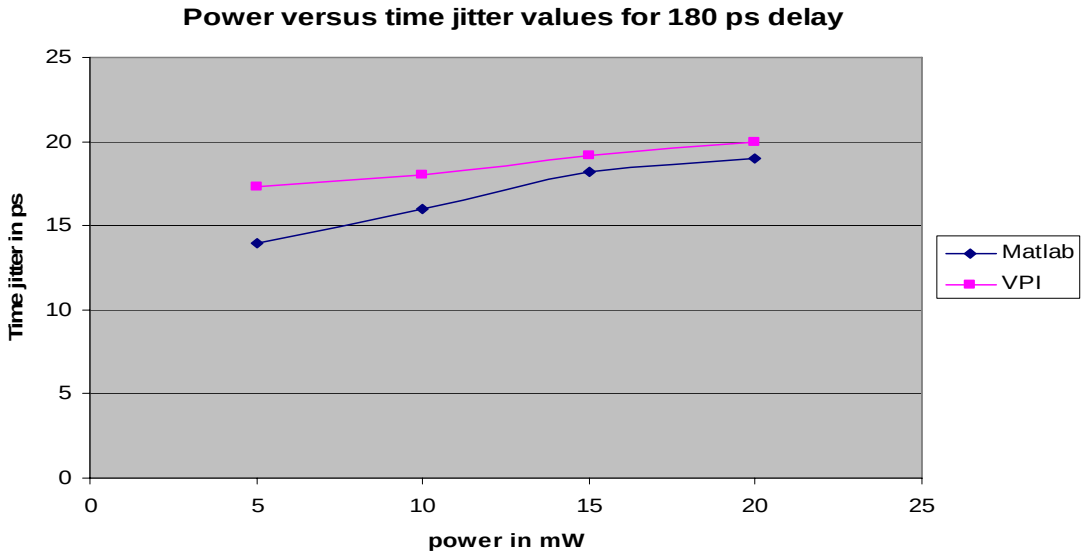

Figure 4.14, Power versus time jitter values for 180 ps delay between pump and probe data patterns

From figure 4.14, we see that the analytical model and VPI models has some difference in time jitter values which is attributed to the gradual walk off effect in VPI model.

Power in mW	MATLAB time jitter in ps	VPI time jitter in ps
5	14	17.3
10	16	18
15	18.2	19.2
20	19	20

Table 4.5 Time jitter values for analytical model and VPI for 180 ps delay between pump and probe data patterns

From table 4.5, we see the time jitter values with analytical model and VPI model for a delay of 180 ps between pump and probe data patterns.

4.4 NRZ 3 span analysis

In this section, the optical network with NRZ modulated waveforms in a three span system is analyzed. In case of a NRZ 3-span system, the basic setup is the same along with laser diodes, filters, modulators, and photo detectors. The number of spans would be 3, and amplifiers are required between the fiber spans to compensate for the signal degradation. Each amplifier is fed with the average power that is one-fourth the peak power at the laser diode. The amplifiers are placed at 80 Km, which is the length of a single span. The power of the pump channel is varied between 5mW to 20 mW and the resulting time jitter and intensity modulation is analyzed. This system also has dispersion compensation which is 80% of the total length of the fiber. Unlike the single span system, without dispersion compensation, the eye shape will be completely closed due to higher dispersion effects.

The following table shows the parameters used for this model.

Parameter	**Value**
Number of spans	3
Span length	80 Km
Dispersion	17 ps/km/nm
Amplifier power	1 to 10 dBm depending on the pump power input
Dispersion compensation	80%

Table 4.6 Parameters for 3 span NRZ modulated optical network

The block diagram for NRZ 3 span system is given below:

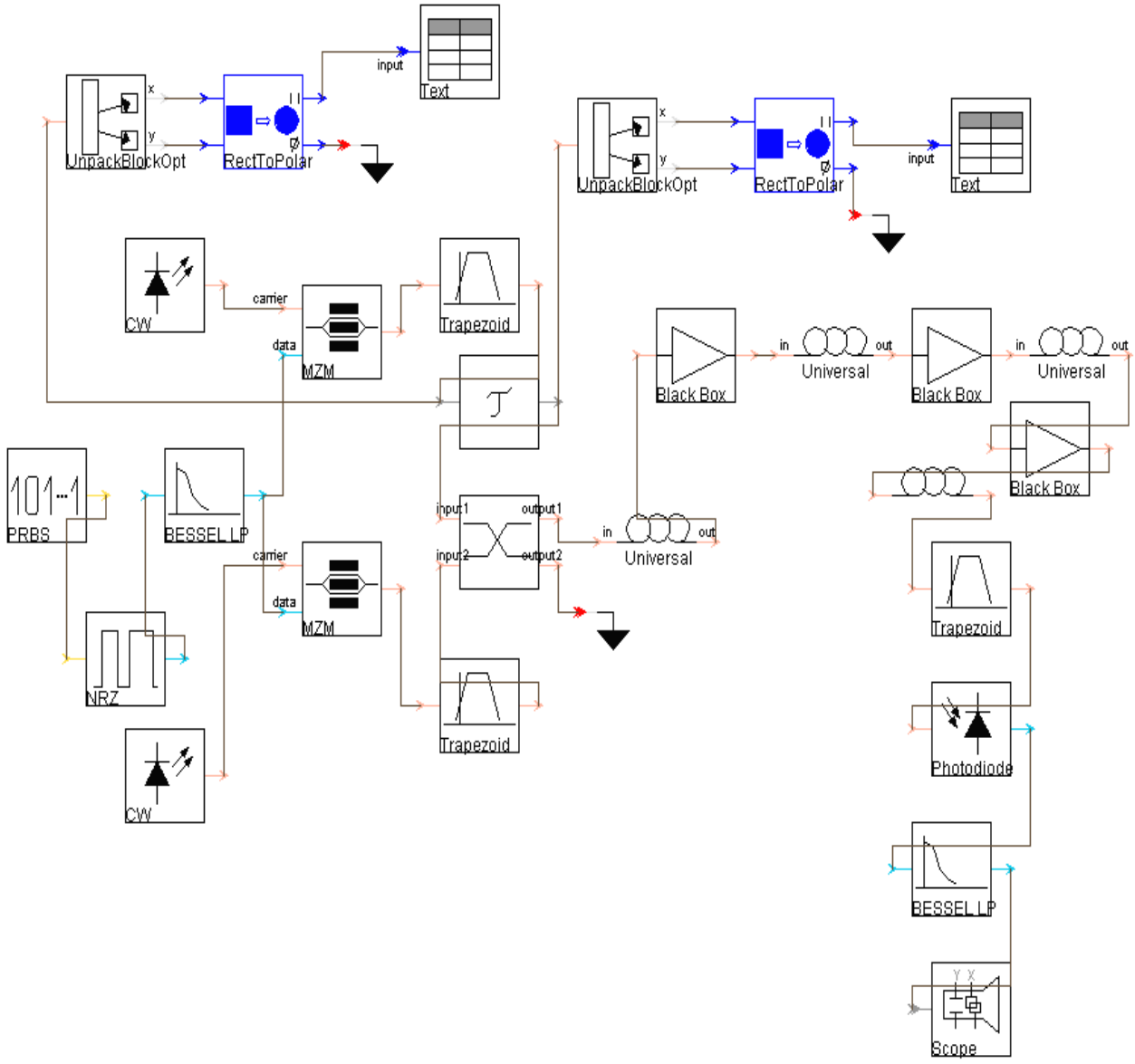

Figure 4.15 NRZ 3 span system VPI block diagram

In this figure 4.15, we can see that the amplifiers are placed at 80 Km length and the dispersion compensation is just in front of the receiver. The amplifier for the dispersion compensation fiber is fed with power as low as 0.1 mW so that it doesn't

affect the dispersion compensation mechanism. The pump power varied from 5 mW to 20 mW to see the changes in the intensity fluctuations and time jitter impairments. Also the delay block simulates different delays between the pump and the probe waveform.

4.4.1 Eye diagram comparison for 5 mW of pump power

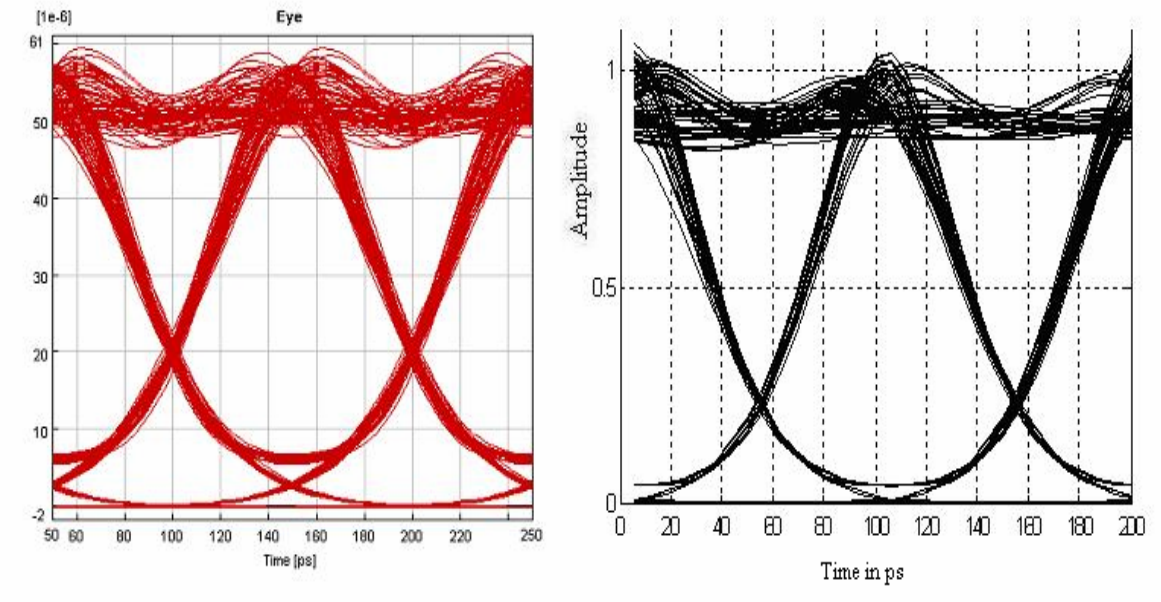

Figure 4.16 NRZ 3 span eye diagram for 5 mW of pump power

From figure 4.16, we see that the time jitter for analytical model is 6 ps and for VPI is 7 ps.

4.4.2 Eye diagram comparison for 10 mW of pump power

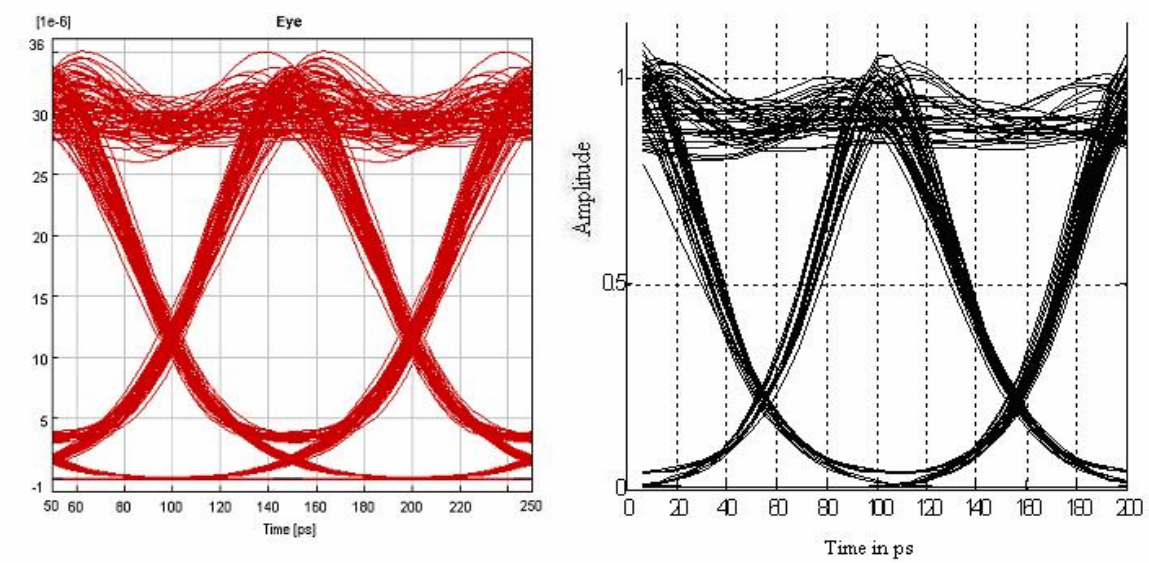

Figure 4.17 NRZ 3 span eye diagram for 10 mW of pump power

From figure 4.17, we see that the time jitter for analytical model is 9.1 ps and 10.4 ps for VPI.

4.4.3 Eye diagram comparison for 15 mW of pump power

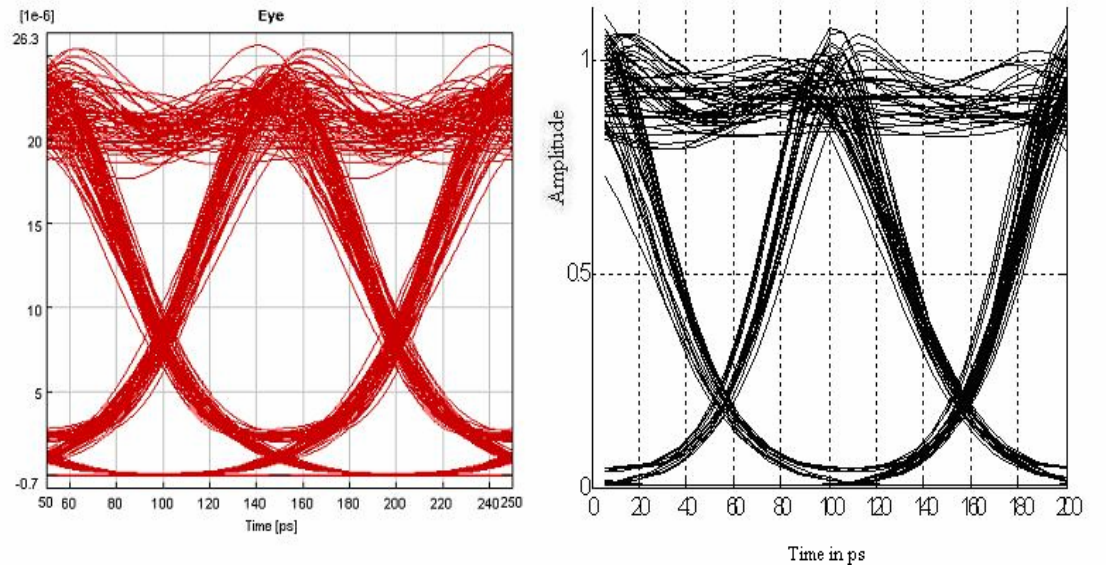

Figure 4.18 NRZ 3 span eye diagram for 15 mW of pump power

From figure 4.18, we see that the time jitter for analytical model is 12.8 ps and 14.6 ps for VPI.

4.4.4 Eye diagram comparison for 20 mW of pump power

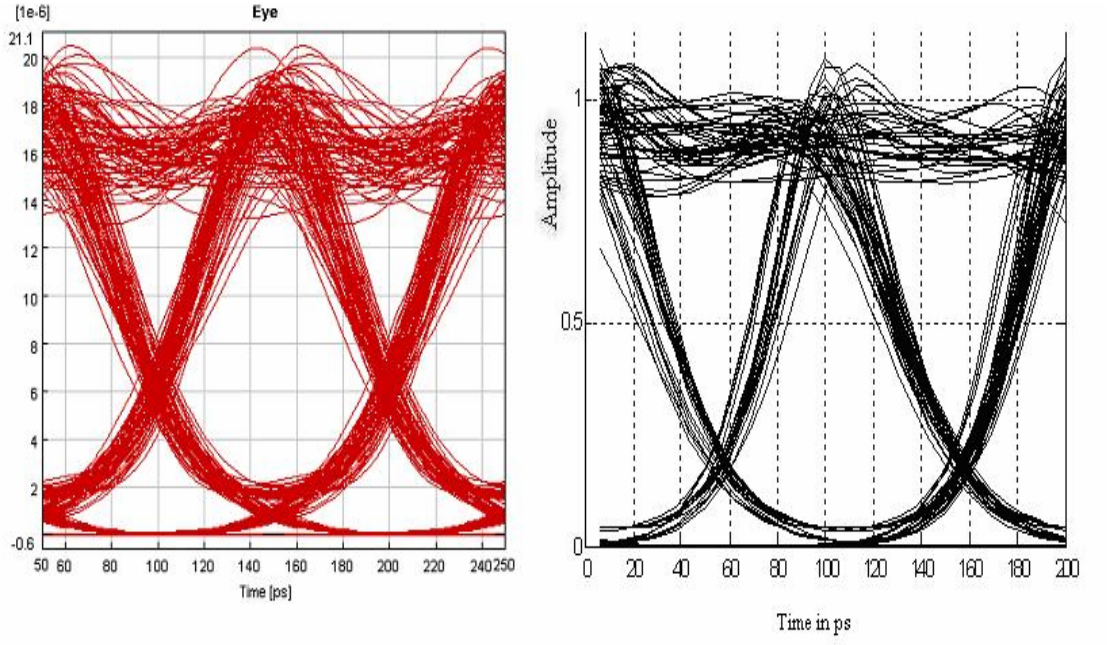

Figure 4.19 NRZ 3 span eye diagram for 15 mW of pump power

From figure 4.19, we see that the time jitter for analytical model is 16.5 ps and 19.5 ps for VPI.

4.4.5 VPI and analytical model comparison

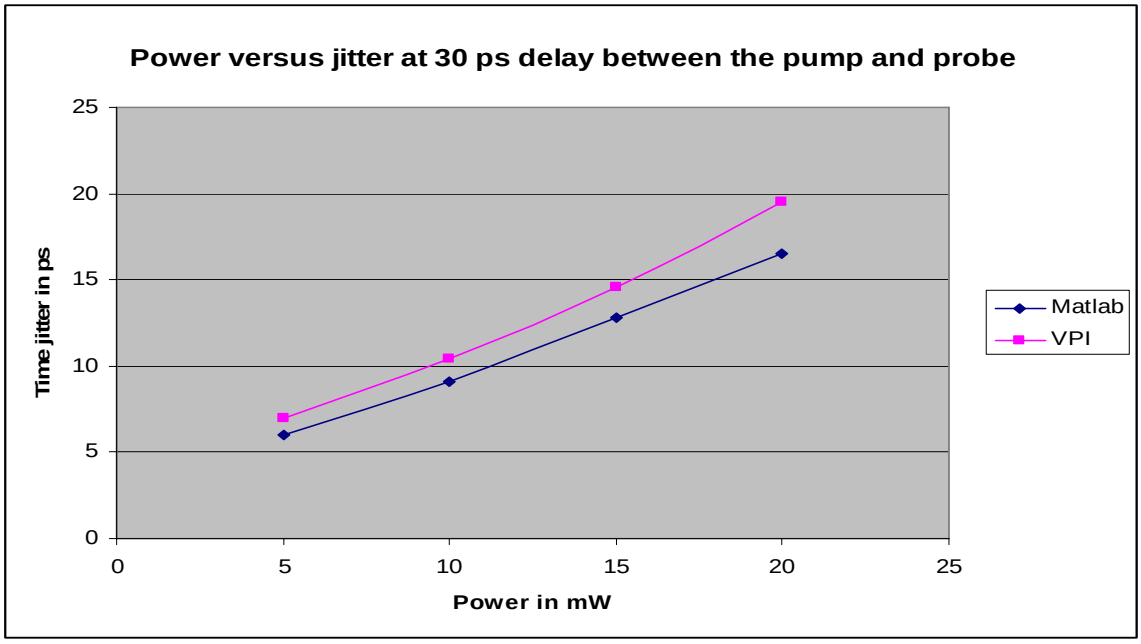

Figure 4.20 Power versus time jitter plot for VPI and analytical model at 30 ps delay

From figure 4.20, we see that the time jitter values of analytical model have a good match with the VPI model.

Power in mW	MATLAB time jitter in ps	VPI time jitter in ps
5	6	7
10	9.1	10.4
15	12.8	14.6
20	16.5	19.5

Table 4.7 Power versus time jitter values for both VPI and analytical model for 30 ps delay between the pump and probe

From table 4.7, we see the time jitter values of both analytical model and VPI models.

The same experiment is carried out with different delay between the probe and pump data bit patterns and the results are tabulated below:

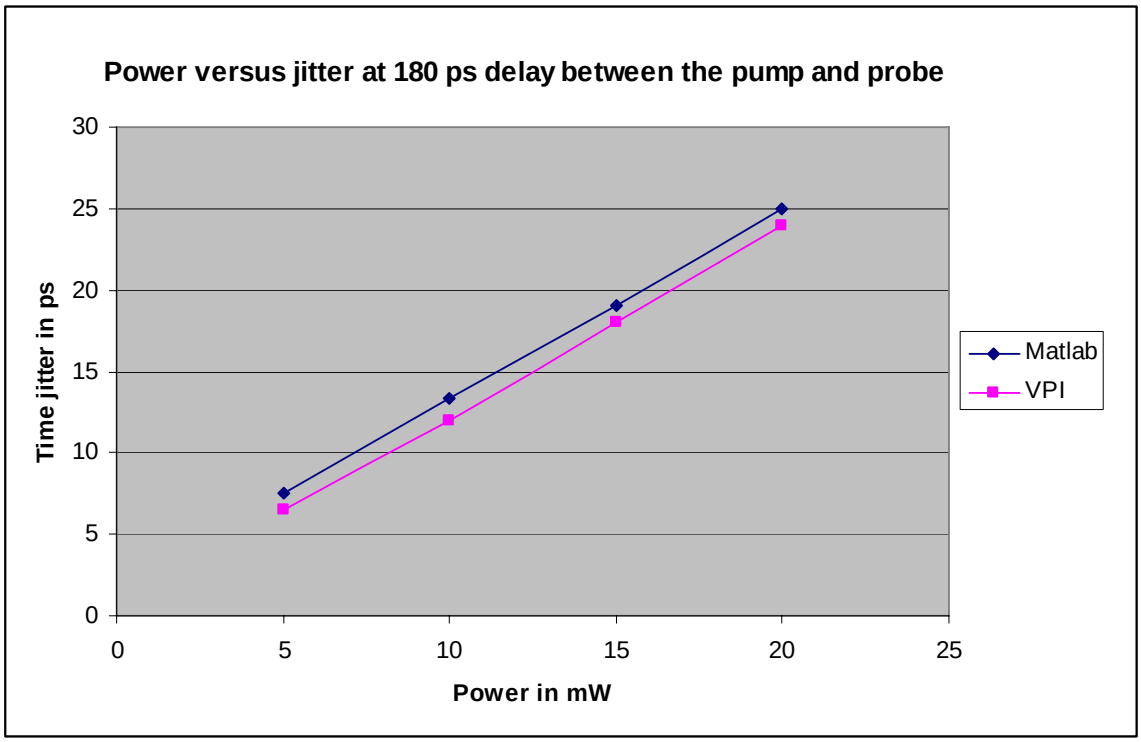

Figure 4.21 Power versus time jitter plot for VPI and analytical models at 180 ps delay

From figure 4.21, we see that the time jitter values form a better match due to the bit pattern alignments. Thus delay plays a very important role in measuring the time jitter values. But this effect is attributed towards the gradual walk off effect discussed in previous section.

Power in mW	MATLAB time jitter in ps	VPI time jitter in ps
5	7.5	6.5
10	13.3	12
15	19	18
20	25	24

Table 4.8 Power versus time jitter values for both VPI and analytical model for 180 ps delay between the pump and probe

Table 4.8, we see the time jitter values of both analytical model and VPI models.

4.5 RZ 1 span analysis

Up till now, the thesis concentrated on NRZ modulation format. NRZ holds good for lower bit rate systems. When it comes to higher bit rates in case of terrestrial [18] and transoceanic [19] systems that require higher spectral efficiency and better distance bit-rate products, RZ modulation is considered to be better than the NRZ modulation format. Earlier research on cross phase modulation was carried out in NRZ modulation format, but due to the higher bit rate advantage, RZ modulation is considered in this thesis. Both the VPI and the analytical model block diagrams remain the same except for the coder component in the block diagram. The NRZ coder component is simply replaced by RZ coder component and the cut off frequency of the filter is set at 15 GHz as RZ requires twice the bandwidth of the NRZ format. Also average powers at the amplifiers will change which will be explained under the section 4.6. RZ eye diagrams are different than the NRZ diagrams. They do not have the eye crossing as NRZ does.

The various parameters and their values are tabulated below:

Parameter	Value
Launch power	5mW - 20 mW
Number of spans	One
Dispersion	17 ps/nm/Km
Fiber length	80 Km single span
Modulation format	RZ waveform

Table 4.9 Parameters used for RZ modulated waveform in a single span system

The table 4.9 holds the values that would be used for simulation in both VPI and in analytical model. The following sections shows the various eye diagrams generated for different power levels. A comparison is made between the time jitter values of both VPI and the analytical model.

4.5.1 Eye diagram for 5 mW pump power

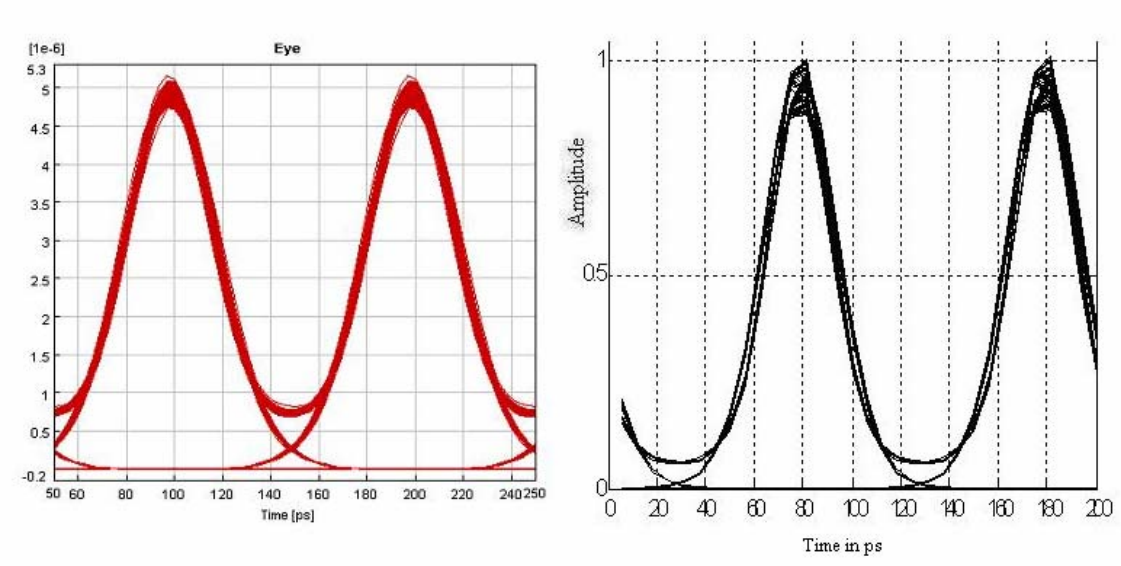

Figure 4.22 RZ eye diagram for 5 mW of pump power

From figure 4.22, we see that the time jitter for analytical model is 3.25 ps and for VPI it is 3.75 ps.

4.5.2 Eye diagram for 10 mW pump power

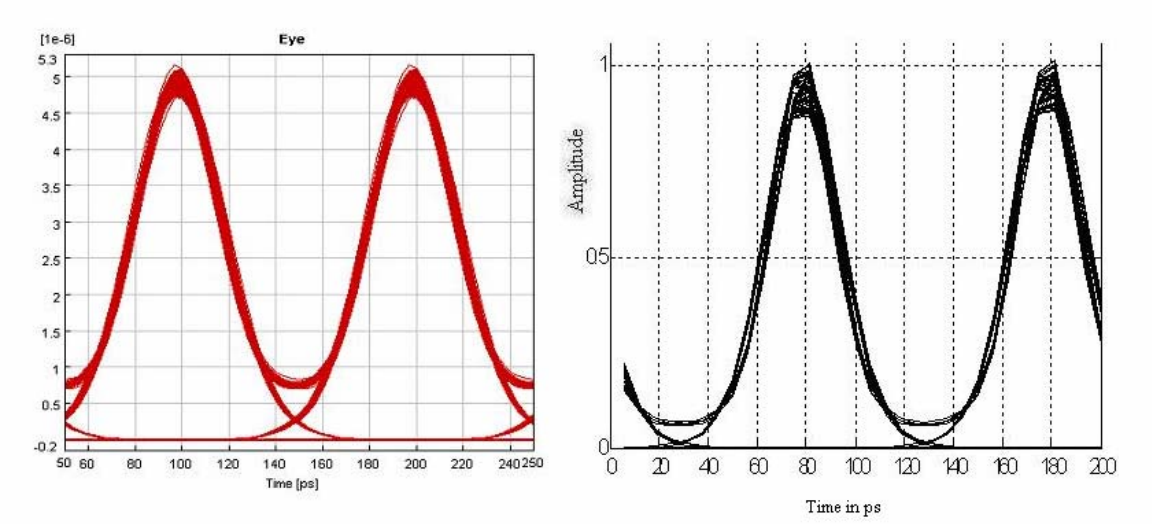

Figure 4.23 RZ eye diagram for 10 mW of pump power

From figure 4.23, we see that the time jitter for analytical model is 3.5 ps and VPI it is 3.85 ps.

4.5.3 Eye diagram for 15 mW pump power

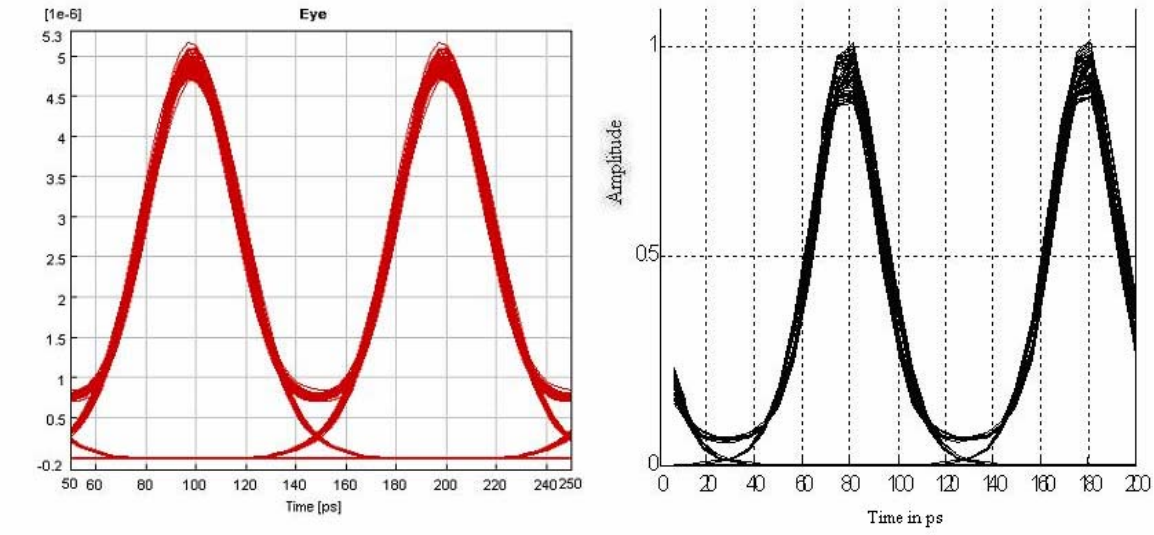

Figure 4.24 RZ eye diagram for 15 mW of pump power

From figure 4.24, we see that the time jitter is 3.75 ps for analytical model and 3.95 ps for VPI

4.5.4 Eye diagram for 20 mW pump power

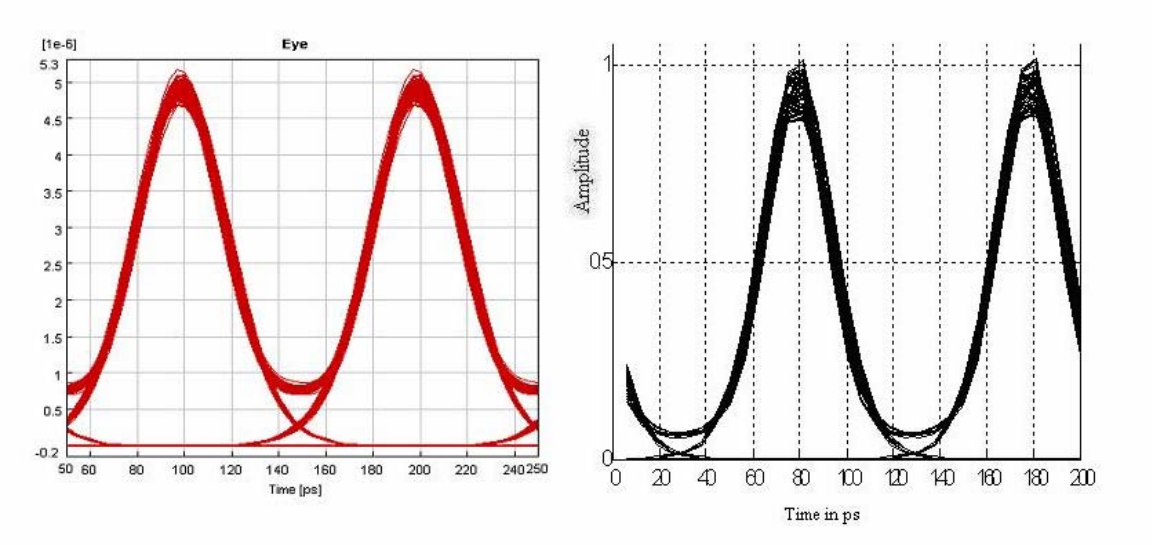

Figure 4.25 RZ eye diagram for 15 mW of pump power

From figure 4.25, we see that the time jitter is 4.1 ps for analytical model and 4.2 ps for VPI

4.5.5 Analytic model and VPI comparison

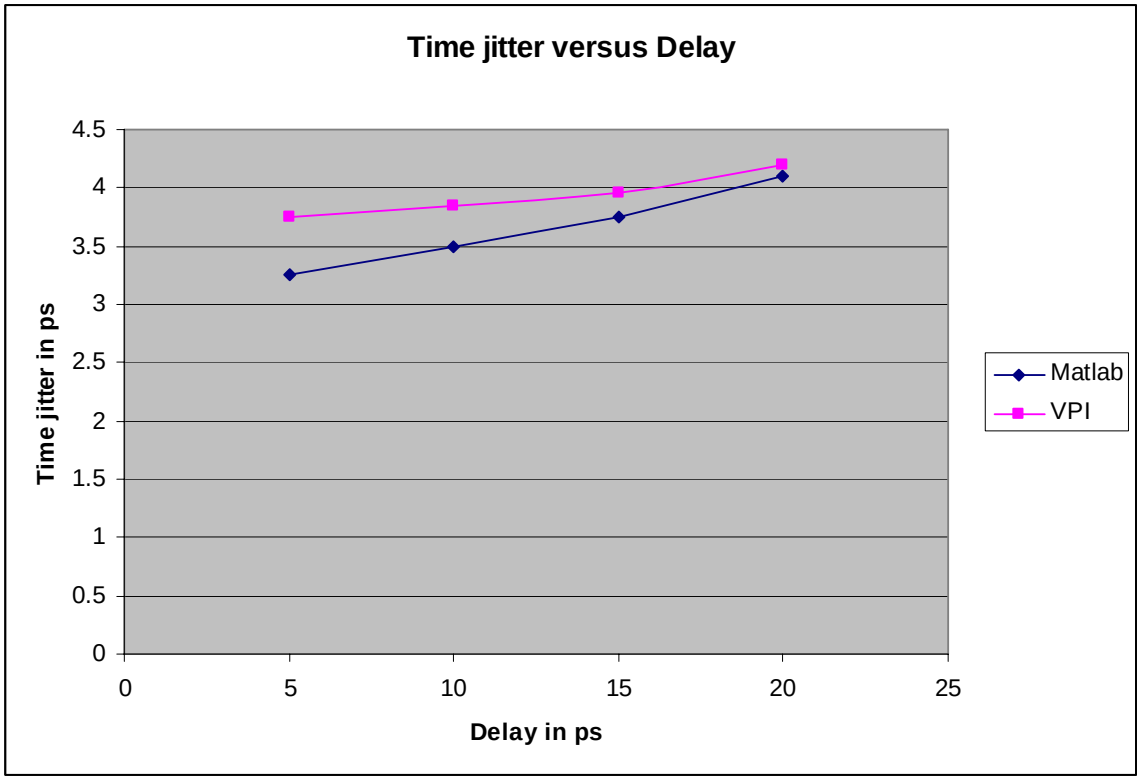

Figure 4.26 Power versus time jitter values for RZ single span system with 270 ps delay

From figure 4.26, we see that the time jitter values of analytical model and VPI do not vary by a very huge difference. The small differences once again are attributed to the gradual walk off effect in VPI.

Power in mW	MATLAB time jitter in ps	VPI time jitter in ps
5	3.25	3.75
10	3.5	3.85
15	3.75	3.95
20	4.1	4.2

Table 4.10 Comparison of analytical model and VPI time jitter values

Table 4.10 gives the different time jitter values for both VPI and analytical model for different power levels.

The figure below shows the delay versus time jitter values for various delays between the probe and the pump channel.

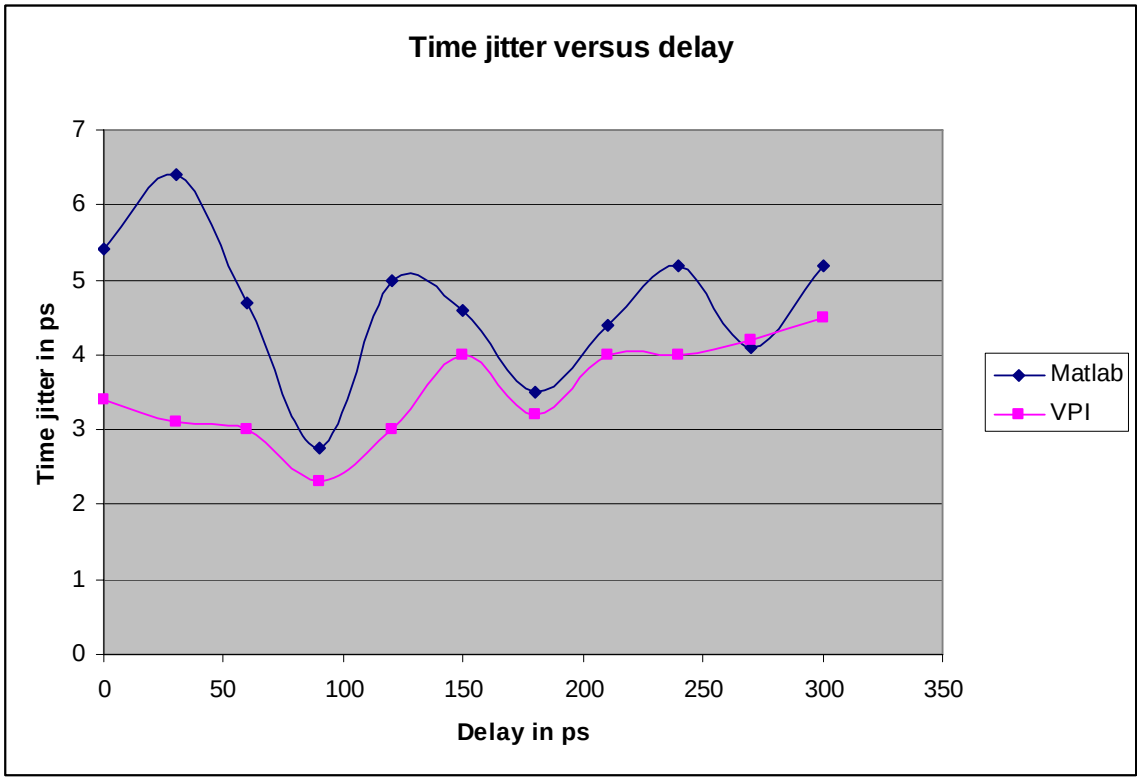

Figure 4.27 Time jitter versus delay between the probe and pump channels

4.6 RZ 3 span analysis

In case of 3 span analysis, the block diagram for both VPI and analytical model are the same as the RZ 1 span system except for the number of spans and the amplifiers used. This also includes dispersion compensation in order to reduce the effects of dispersion in the system. The amplifiers are fed with a power one eighth of the peak

power at the laser diode, the explanation of which is given in section 3.5. The parameters and their values are tabulated below:

Parameter	Value
Launch power	5mW - 20 mW
Number of spans	3
Dispersion	17 ps/nm/Km
Fiber length	80 Km
Modulation format	RZ waveform

Table 4.11 Parameters and their values used for RZ modulated waveform in a three span system

Similar experiments are carried out in case of the 3 span system and a comparison is made between the VPI and analytical model time jitter values. The eye diagrams for various power levels and delays are analyzed and a plot is obtained for the time jitter as a function of power in the optical system's pump channel. The following sections describe the eye diagram comparison for various power levels.

4.6.1 Eye diagram comparison for 5 mW pump power

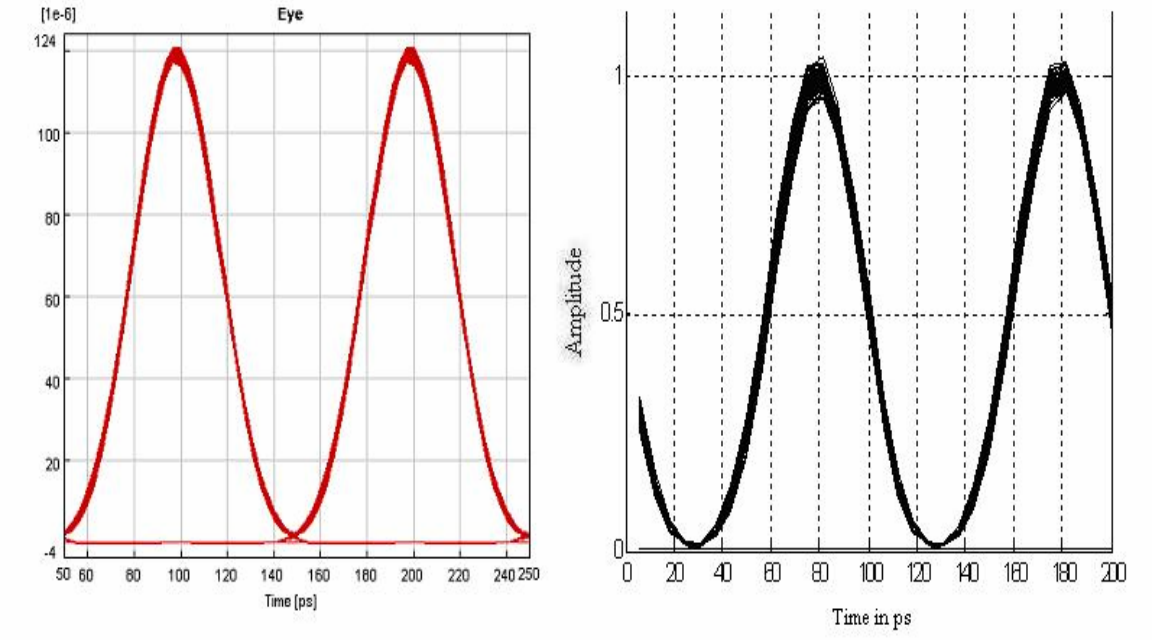

Figure 4.28 Eye diagram comparison for 5 mW pump power for 270 ps delay

From figure 4.28, we see that the time jitter is 3 ps for analytical model and 1.3 ps for VPI.

4.6.2 Eye diagram comparison for 10 mW pump power

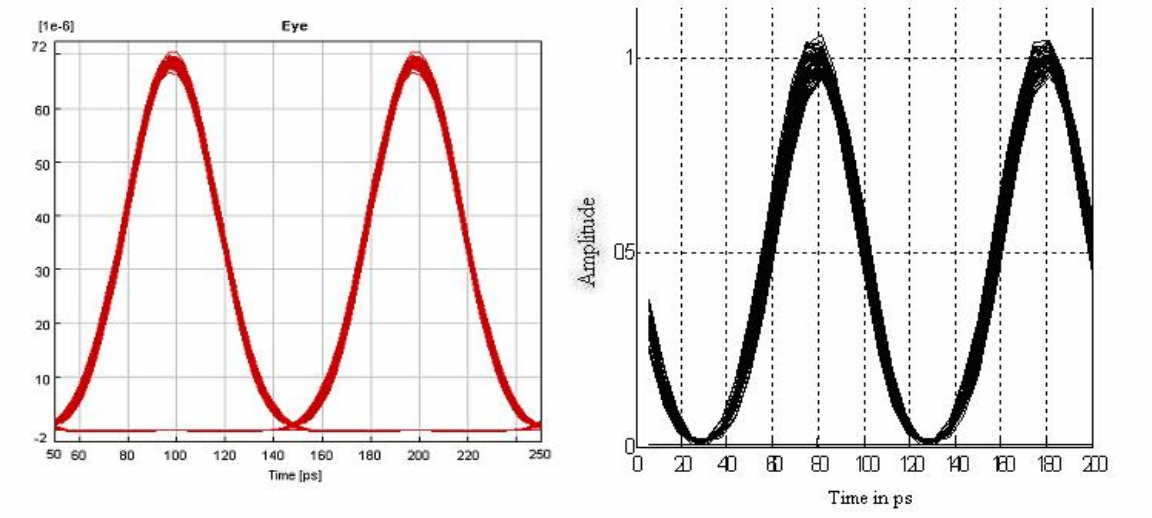

Figure 4.29 Eye diagram comparison for 10 mW pump power for 270 ps delay

From figure 4.29, we see that the time jitter is 5.8 ps for analytical model and 2.5 ps for VPI.

4.6.3 Eye diagram comparison for 15 mW pump power

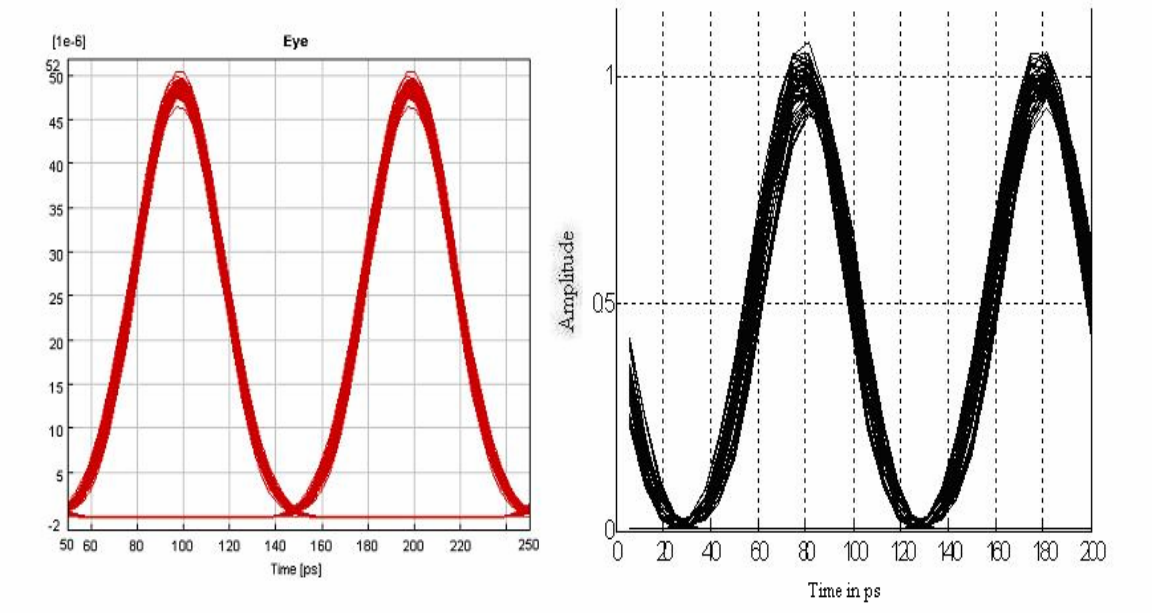

Figure 4.30 Eye diagram comparison for 15 mW pump power for 270 ps delay

From figure 4.30, we see that the time jitter is 8 ps for analytical model and 3.8 ps for VPI.

4.6.4 Eye diagram comparison for 20 mW pump power

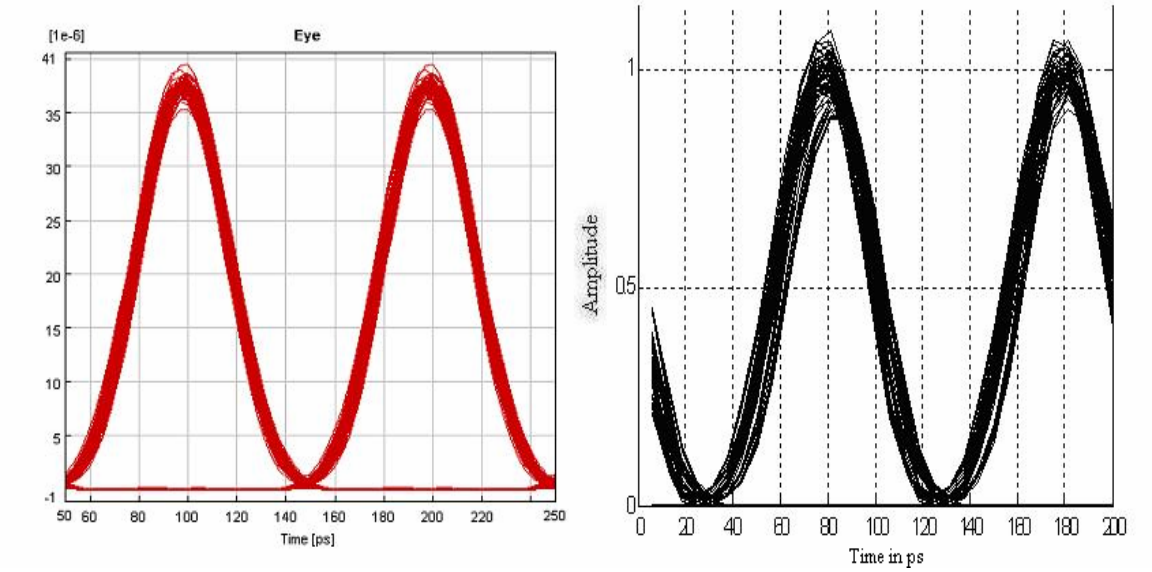

Figure 4.31 Eye diagram comparison for 20 mW pump power for 270 ps delay

From figure 4.31, we see that the time jitter is 12 ps for analytical model and 5.6 ps for VPI.

The results clearly state that there is a 3 dB difference between analytical model and VPI time jitter values. This can be confirmed by the following plot between analytical model and VPI time jitter values.

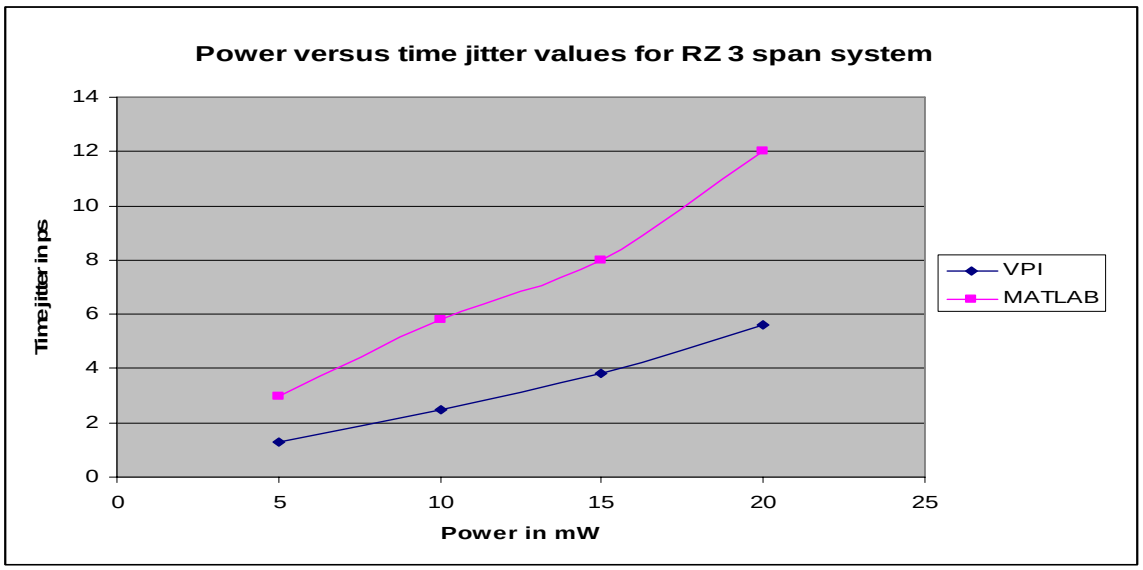

Figure 4.32 Power versus time jitter for analytical model and VPI with a 3 dB difference

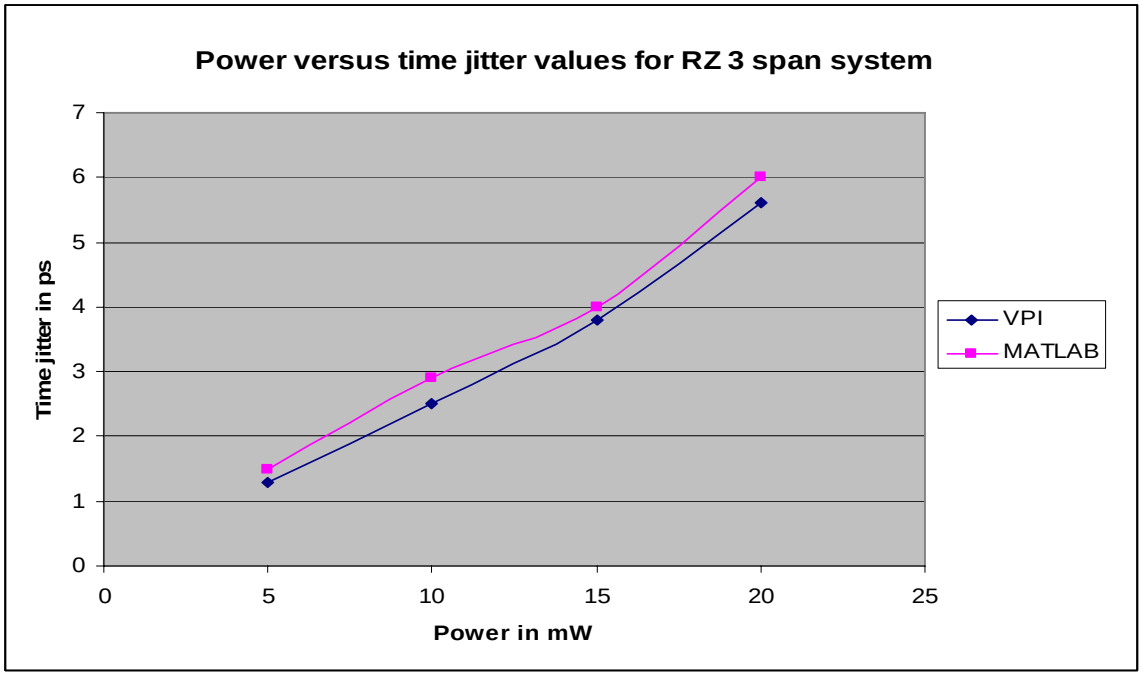

Figure 4.33 Power versus time jitter for analytical and VPI models without a 3 dB difference

Thus from figure 4.32 and figure 4.33, it is seen that the time jitter values exhibit a 3 dB difference between their values for VPI and the analytical model. The gradual walk off effect has considerable effect on this 3 span RZ system.

For 180 ps delay between the data bit patterns of the pump and the probe, we see the same 3 dB difference which is plotted below:

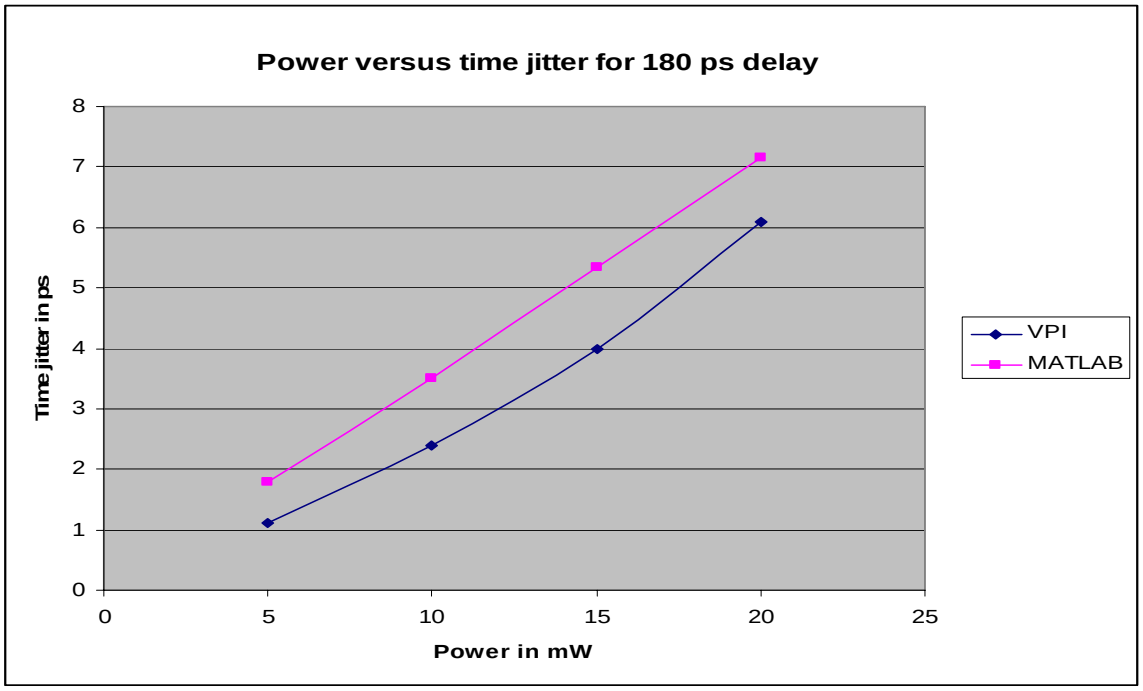

Figure 4.34 Power versus time jitter for analytical model and VPI without a 3 dB difference for 180 ps delay

Thus from the above results, we see that the analytical model compares favorably to the VPI model to use it for the RWA systems. The difference in VPI and analytical model time jitter values is attributed towards the gradual walk off effect in VPI.

4.6.5 Program execution timings

Number of spans	VPI execution time in s	MATLAB execution time in s
1	~ 12	1.4
3	~ 38	2.5

Table 4.12 Execution times of both VPI and analytical model

From table 4.12, we see that our analytical model performs the calculations at a faster rate than the VPI models. Thus RWA algorithms could efficiently make use of this analytical model.

5. CONCLUSION AND FUTURE WORK

In this thesis, an analytical model is developed to evaluate the impact of cross phase modulation on high bit rate WDM optical networks. Chapter 1 provided a brief introduction about optical communication systems, WDM concepts, modulation formats, and simulation tools used. The purpose and application of this thesis were also discussed. Chapter 2 provided information about the fiber characteristics, non linear effects such as SPM, FWM, SBS, SRS, and XPM which is the main topic of this thesis. Chapter 3 dealt with the analytical modeling developed to model the cross phase modulation, and effects of intensity modulation along with other concepts relating to cross phase modulation such as conversion of phase to intensity modulation, dispersion and non linear effects that contribute to cross phase modulation were discussed. Chapter 4 dealt with comparison with a previous work done to verify the analytical model developed. Various comparisons were made with VPI and analytical model for NRZ and RZ modulation formats and resulting eye diagrams and comparison plots were generated to evaluate the impact of cross phase modulation. RZ modulation formats are discussed as future high bit rate systems require higher spectral efficiency and distance bit rate products for efficient transmission. A system model is built in both MATLAB and in the VPI simulation software. This analytical model is implemented in MATLAB and numerous comparisons were made with the VPI models for various power levels and delay values between the channels propagating in the WDM links. It was seen that there

was always a difference between the VPI and analytical model time jitter values which is due to the gradual walk off effect in VPI. Since VPI has the walk off gradually throughout the length of the fiber, the XPM builds up gradually. But in the analytical model, the walk off is seen only at the end of the fiber while superimposing the time jitter on the probe wave. Thus our analytical model might have the higher jitter values at some delay values and lower values at other delay values. This also explains the delay curve between VPI and the analytical model.

Future work includes finding a solution to implement this gradual walk off effect in the analytical model and comparing the eye diagrams again to get a better match between the values. In this thesis, even though the time jitter values are not exactly equal, a fair enough match has been obtained which was evident in the results obtained in the comparison plots in the results section. Also the computation time was greatly reduced with the analytical model developed in this thesis. Hence this work could serve as the basis for future models that will be developed which includes the gradual walk off effect for the analytical model.

6. REFERENCES

[1] F. P. Kapron, D. B. Keck, and R. D. Maurer, *Appl. Phys. Lett.* 17, 423 (1970)

[2] G.E.Kaiser, *Optical Fiber Communications*, 3rd edition, McGraw Hill, New York.

[3] Special issue on "Undersea Communications Technology", *AT&T Tech. J.,* vol. 74, Jan./Feb. 1995

[4] Govind P. Agrawal, *Fiber-optic communication system*, Wiley series.

[5] http://www.vpiphotonics.com/photonics_home.php

[6] M. Born and E. Wolf, *Principles of optics,* 7th ed, Cambridge University Press, New York, 1999

[7] G.P.Agarwal*, Nonlinear Fiber optics,* 3rd ed, Academic Press, San Diego, CA, 2001.

[8] N. Kikuchi and S. Sasaki, "Analytical evaluation technique of self-phase modulation effect on the performance of cascaded optical amplifier systems," J. Lightwave Tech., vol. 13, pp. 868-878, May 1995

[9] G. Goeger, M. Wrage, and W. Fischler, "Cross-Phase Modulation in Multispan WDM systems with Arbitrary Modulation Fromats", IEEE photonics technology letters, Vol 16, No 8, August 2004.

[10] J. Wang and K. Petermann, "Small signal analysis for dispersive optical fiber communication systems," J.Lightwave Technol., vol 10, pp.99-100, Jan 1992

[11] M. Shtaif, "Impact of cross phase modulation in WDM systems," in Proceedings of the Optical Fiber Communication Conference, Baltimore, 2000, Paper ThM1 (invited)

[12] F. Forghieri, R.W. Tkach, and A.R. Chraplyvy, "Fiber nonlinearities and their impact on transmission systems," in *Optical Fiber telecommunications IIIA,* Eds 1.P.Kaminow and T.L.Koch, Academic Press, *San* Diego, 1997.

[13] M. Eiselt, M. Shtaif, R.W. Tkach, F. A. Flood, S. Ten, D. L. Butler, *Tech. Dig.* OFC '99, San Diego, paper ThCl

[14] Rongqing Hui, Kenneth R. Demarest, and Christopher Allen, "Cross phase modulation in multispan WDM optical fiber systems", J of Lightwave Tech., Vol 17, No. 6, June 1999

[15] R. A. Saunders, B. L. Patel, H. J. Harvey, and A. Robinson, "Impact of cross-phase modulation seeded modulation instability in 10Gb/s WDM systems and methods for its suppression," in *Proc. Optic. Fiber Comrnun. Conf. OFC'97,* Dallas, TX, Feb. 1997, paper WC4, p. 116.

[16] Micheal Eiselt, Mark Shtaif, and Lara D. Garrett, "Contribution of timing jitter and amplitude distortion to XPM system penalty in WDM systems", IEEE photonics tech letters, vol 11, no 6, June 1999.

[17] Biswanath Mukherjee, Yurong (Grace) Huang, and Jonathan P. Heritage, "Impairment aware routing in wavelength routed optical networks", TuCC4(Invited)

[18] D. Le Guen, S. Del Burgo, M.L. Moulinard, D. Grott, M. Henry, F.Favre, and T.Georges,"Narrow band 1.02 Tb/s soliton DWDM transmission over 1000 Km of standard fiber with 100 km amplifier spans," in proc. Optical fiber communication conf., 1999 OSA Tech. Dig.ser., postdeadline papers, Washington, D.C.,1999,postdeadline paper PD4

[19] N.S. Bergano, C.R. Davidson, C.J.Chen, B. Pederson, M.A. Mills, N. Ramanujam, H.D. Kidorf, A.B. Puc, M.D. Levonas, and H. Abdelkader, "640 Gbps transmission of sixty-four 10 Gb/s WDM channels over 7200 km with 0.33(bits/s) spectral efficiency," in proc. Optical fiber communication conf., 1999 OSA Tech. Dig.ser., postdeadline papers, Washington, D.C.,1999,postdeadline paper PD2

[20]http://www.highfrequencyelectronics.com/Archives/Nov05/HFE1105_Tutorial.pdf